2018-05-22

Catalytic Upgrading Process of Ligno-cellulose Derived Heavy Crude Oil

Trujillo Vaccari, Marianna Isabel

UNIVERSITY OF CALGARY

Catalytic Upgrading Process of Ligno-cellulose Derived Heavy Crude Oil

by

Marianna Isabel Trujillo Vaccari

A THESIS

SUBMITTED TO THE FACULTY OF GRADUATE STUDIES

IN PARTIAL FULFILMENT OF THE REQUIREMENTS FOR THE

DEGREE OF MASTER OF SCIENCE

GRADUATE PROGRAM IN CHEMICAL ENGINEERING

CALGARY, ALBERTA

MAY, 2018

Abstract

The high oxygen content of lignocellulose-derived bio-crudes results in thermal instability, corrosiveness, and low energy density in comparison to petroleum fuels. A pioneer Catalytic Upgrading Process is investigated in this thesis through a first-of-a-kind combination of two hydrogen addition processes, namely a first hydrogenation step and a second steam-cracking step producing lighter fractions and hydrogen. The preliminary effect of operating conditions was evaluated for each process using a fixed-bed reactor configuration. First, a Hydrotreating process at 320ºC, $0.20h^{-1}$, and 1400-psig that achieved 59% hydro-deoxygenation, and >98% total-acid-number reduction was implemented. Complementarily, Catalytic Steam Cracking as secondary process completed desired conversion to petroleum equivalents of 5.6% Naphtha (IBP-190ºC), 12.8% Jet-fuel (190-260ºC) and 25.6% Diesel (260-343ºC) range hydrocarbons, supplying hydrogen by catalytic splitting of water, thus omitting the requirements for costly hydrogen sources or high-pressure equipment as in Hydrocracking processes. One novelty relies on the recycle of unconsumed hydrogen, at least partially sourcing the hydrotreater's hydrogen consumption.

Acknowledgements

First and foremost, I extend my most sincere gratitude to my supervisor, Dr. Pedro Pereira-Almao. It has been an honor to be a part of his team, whilst being guided by his expertise. Without his able guidance and encouragement, this thesis would not have been possible and I shall eternally be grateful to him. *Dr. Pereira, thank you for the opportunity of a lifetime in Canada, and thank you for allowing me to fulfill my potential and pursue my dream of a career in Chemical Engineering.*

I would like to acknowledge the financial support for this work provided by the Chemical and Petroleum Engineering Department, Schulich School of Engineering at the University of Calgary, and Steeper Energy Canada for providing the research topic opportunity and the resources to carry out this investigation.

Moreover, I am indebted to Dr. Monica Bartolini, Mr. Lante Carbognani, Dr. Gerardo Vitale, Dr. Josefina Scott, Dr. Azfar Hassan and Dr. Carlos Scott. I am grateful to them for their guidance and helpful suggestions, for tirelessly answering my many uncertainties, and for revising this manuscript providing valuable and constructive criticism.

Likewise, thanks to my colleagues with whom I have been privileged to work with at various stages of my research, engaged in thoughtful conversations, shared courses and study sessions, accompanied me in all-nighters in the laboratory, shared words of encouragement when experiments were not going my way, and enjoyed good laughs. Thank you, Violeta, Tatiana, Alejandro, Maysam, Erika, Christian, Sukhdeep, Jose Luis, Peter, Josune, Moein, Diego, Vahide, Maria, Dana, Ghada, Mina, and really to all former, and present members of the CAFE research group.

To my main supporters and biggest fans: my parents, Gustavo and Eleonora. Thank you for believing in me, for encouraging me, for your prayers, and for being the best versions of yourselves to provide endless opportunities to my brother and me. *Mami, Papi, ¡gracias por tanto!* To Gus, for being the best little brother I could have asked for. Your hugs make any day better. To my loving grandparents: Abuelita Maria, Abuelita Cirila, y Abuelito Toto. Thank you for inspiring me to never give up, and thank you for your strength and your prayers. To my parents-in-law, Gloria and Andres. It truly is a blessing to have you in my life, and to count on you and on your prayers. To my family in Venezuela, and to those now relocated to many different parts of the world. There is no distance long enough to separate our family, and I know we will continue encouraging each other to pursue our dreams and take every opportunity that comes our way. To our friends that have become our family in Canada and to my unconditional friends: you know who you are. Thank you for your love, understanding, and encouragement. Now, let's celebrate! Finally, my heartiest appreciation and love go to my husband and best friend, *Mauro*. Thank you for your continuous support, encouragement and unending patience during the many months I devoted to this experimental work, and to writing this manuscript. Thank you for your love, and for knowing when I need an extra push, and when I simply need serenity and a good laugh. Gracias, Esposo. *¡Lo logramos!*

Dedication

Gracias a Dios

por quienes me acompañan en mis lindas aventuras:

Eleonora y Gustavo

Gus

María Griselda, Cirila Elena, Luis Guillermo

Y especialmente Andres Mauricio

Ustedes son mi motivación, mi fuerza y mi inspiración.

Para ustedes, y por ustedes.

Table of Contents

List of Tables

List of Figures

List of Symbols, Abbreviations, and Nomenclature

Symbol	Description	Units
ASTM	American Society for Testing and Materials	
C	Carbon	
CAFE	Catalysts and Adsorption for Fuels and Energy	
CSC	Catalytic steam cracking	
CSR	Catalytic steam reforming	
DOD	Degree of deoxygenation	%
FTIR	Fourier Transform Infrared	
g	grams	g
GC	Gas Chromatography	
GHG	Greenhouse Gas	
H	Hydrogen	
HBO	Hydrotreated Bio-oil	
H/C	Hydrogen to Carbon ratio	
HDT	Hydrotreating	
HDN	Hydro-denitrogenation	
HDO	Hydro-deoxygenation	
HDS	Hydro-desulphurization	
HHV	High Heating Value	MJ/kg
HTL	Hydrothermal liquefaction	
HTSD	High Temperature Simulated Distillation	
IBP	Initial boiling point	^{o}C
$\dot{m}_i$	Mass flow-rate	g/h
M	Mixer	
MCR	Micro Carbon Residue	%
MFC	Mass flow controller	
MW	Molecular weight	g/mol
N	Nitrogen	
ND	Not determined	

O	Oxygen	
P	Pump	
rWGSR	Reverse Water Gas Shift Reaction	
S	Sulphur, Separator	
T	Tank	
TAN	Total acid number	mg KOH/g
V	Valve	
$\dot{v}_i$	Volume flow-rate	cc/h
w_i	Mass fraction	
WHSV	Weight Hourly Space Velocity	h^{-1}
x_i	Mole fraction in liquid	
y_i	Mole fraction of gas	

Greek Letters

μ	Viscosity	cP
ρ_i	Density	g/mL, kg/m^3

Subscripts

G	Gas
H	Hydrogen
H/i	Hydrogen fraction over component i
i	Component, initial
W	Water

Chapter One: Introduction

1.1. Overview of Bio-Crude Oil Production and Upgrading

The 19th century discovery of crude oil created an inexpensive liquid fuel source that allowed to industrialize the world. However, prior to the discovery of inexpensive fossil fuels, our society was dependent on plant biomass to meet its energy demands. Nowadays, declining petroleum resources, combined with an increasing demand for petroleum by emerging economies, and political and environmental concerns about fossil fuels, in general, have become apprehensive for academia, industry, and governments. The 2015 Paris agreement, signed by 193 countries, addressed the urgent and potentially irreversible threat of climate change and the necessity to reduce greenhouse gas (GHG) emissions from the energy sector (United-Nations, 2015). Therefore, it is imperative to explore and develop economical and energy-efficient processes for producing a diversification by incorporating other sources of energy.

One feasible alternative equivalent to the conventional fuels, and thus compatible with the infrastructure as we know it, but also a fuel that is sustainable and will decrease the environmental man-made footprint is the use of bio-mass to generate liquid fuels (Pachauri, et al., 2014). Renewable biomass has the ability to directly produce hydrocarbon-based liquid fuels that could approach carbon neutrality. Therefore, re-discovering plant biomass is a current sustainable source of organic carbon; and biofuels, as fuels derived from plant biomass, appear to be the only current sustainable source of liquid fuels, since other known alternatives like the Fischer-Tropsch conversion of syn-gas to alkanes (Lillebø, et al., 2013) has proven very expensive.

Steeper Energy Canada Ltd, a Danish-Canadian clean-fuel company, is in the process of commercializing their proprietary hydrothermal liquefaction (HTL) technology, Hydrofaction™.

This facilitates production of bio-crude from lignocellulosic biomass residues, such as agricultural, industrial, and forest wastes. Biomass derived fuels could become prospective fuels as these can be produced within relatively short cycles and are considered benign for the environment (Balat, 2011; Roedl, 2010).

The most significant problems of bio-crudes as a fuel are poor volatility, high viscosity, coking by thermally unstable components, corrosiveness, and cold flow problems. Furthermore, bio-oils polymerize and condense with time, and this process is accelerated by increasing temperature, oxygen exposure, and UV light exposure. Therefore, bio-crudes must be upgraded if they are intended to be used as transportation fuels. And thus, the upgrading of Hydrofaction^{TM} Renewable Crude Oil is crucial before these may be used as transportation fuels, either in neat form or as fuel blends.

A pathway of choice for upgrading technology developments relies on hydrogen addition processes to produce an increase of the H/C ratio of heavy molecules by a reaction between them and an external source of hydrogen. Hydroprocessing such as hydrotreating, and specifically hydro-deoxygenation, becomes a process of interest to treat highly acidic and oxygenated bio-crudes, as these impart a number of undesirable qualities to the oil product, such as lower energy content, poor thermal stability, lower volatility, higher corrosivity, and a tendency to polymerize (Grange, et al., 1996; Furimsky, 2000). Hydrotreating processes address concerning issues regarding the instability of bio-crude. Furthermore, hydrotreating is done to prevent catalyst deactivation in further processing, to minimize coking, and to enhance fuel characteristics by improving the oil's heating value (Alfke, et al., 2008). Depending on the severity of hydroprocessing, the treated oil is free of heteroatoms, but it has non-polar, high-molecular weight organic compounds in the oil phase (Patel & Kumar, 2016). Consequently, the oil requires further

processing. Also, it has been determined that hydroprocessing alone consumes large amounts of expensive high-pressure hydrogen (Robinson & Dolbear, 2007). Therefore, an alternative offered for development to Steeper Energy by Dr. Pereira-Almao's group, starting with this thesis, is the tandem Catalytic Hydrotreating and Catalytic Steam Cracking that has the features to be considered for bio crude upgrading. Similar to a process developed by Dr. Pereira-Almao, AquaConversion (Pereira, et al., 2001), it follows the same hydroprocessing principles but uses water to supply hydrogen by the catalytic splitting of the water molecule in the Catalytic Steam Cracking process (Banerjee, 2012), while cracking large molecules in the feedstock. Therefore, this process, now configured in a single bed, allows for further processing of the hydrotreated bio-crude with water as a source of hydrogen, where the unconsumed hydrogen becomes an onward source of hydrogen. Consequently, a complete bio-crude upgrading process is proposed, implementing mild hydrotreating to lower the bio-oil's acidity, followed by the catalytic steam cracking of the high molecular weight fibers to produce a lighter oil anticipated to be functionally indistinguishable from their petroleum counterparts and thus compatible with refinery streams. Since the unconsumed hydrogen is to be recycled back into the high-pressure hydrotreating process, along with the hydrogen generated on the steam cracking section where all hydrocarbons gases can be steam reformed to hydrogen (and CO_2), the preceding bio-crude upgrading process becomes an alternative to tackle the costly hydrogen demand of the process.

1.2. Proposed Bio-crude Upgrading Scheme

A major 21st century goal for academia, industry, and government should be the development of efficient and economical utilization of biomass resources, bio-crude production, and upgrading; as these appear to hold the key for participating in supplying the basic needs for our societies by the sustainable production of liquid transportation fuels. Bio-crude upgrading faces the challenges of high oxygen content, high acidity, high viscosity, and the presence of thermally unstable components that lead to polymerization and thus gum formation. Herein, a novel catalytic upgrading approach is proposed where a mild Hydrotreating (HDT) process, followed by Catalytic Steam Cracking (CSC) are the pathways of choice for this investigation.

The objective of HDT is to hydrogenate oxygenates present by producing either water or CO_2 via hydro-decarboxylation, thus reducing the acidity of the bio-crude; then, the CSC process improves the quality of the bio-oil through the conversion of the oil via thermal cracking and hydrogen addition from catalytic steam dissociation reactions. In CSC, hydrogen radicals are catalytically formed from the dissociation of water molecules. As a consequence, the produced hydrogen radicals are involved in the saturation of hydrocarbon radicals generated during molecular cracking, and also act in the prevention of condensation reactions, which otherwise result in the production of carbonaceous residues.

One novelty of the proposed scheme relies on the fact that the unconsumed hydrogen produced in CSC may be recovered and recycled back to the HDT unit, thus reducing the fresh hydrogen make-up otherwise required for this unit. Figure 1-1 illustrates the overview of the herein proposed scheme. The processes are to be evaluated separately first, at least for this pioneer research.

First, the HDT process is investigated through the operation of an up-flow fixed bed reactor containing a catalyst developed for this purpose. This HDT catalyst, non-disclosed in this

document, has been found to be very active in hydrogenation-related reactions, having a strong hydrogenating function. Then, the produced HDT bio-oil is to be processed through the CSC process. Therein, the HDT-bio-oil is fed up-flow a fixed bed reactor containing a previously assessed catalyst, also non-disclosed in this document, composed of a combination of transition and rare earth metals which favour both, water dissociation and hydrogenation reactions.

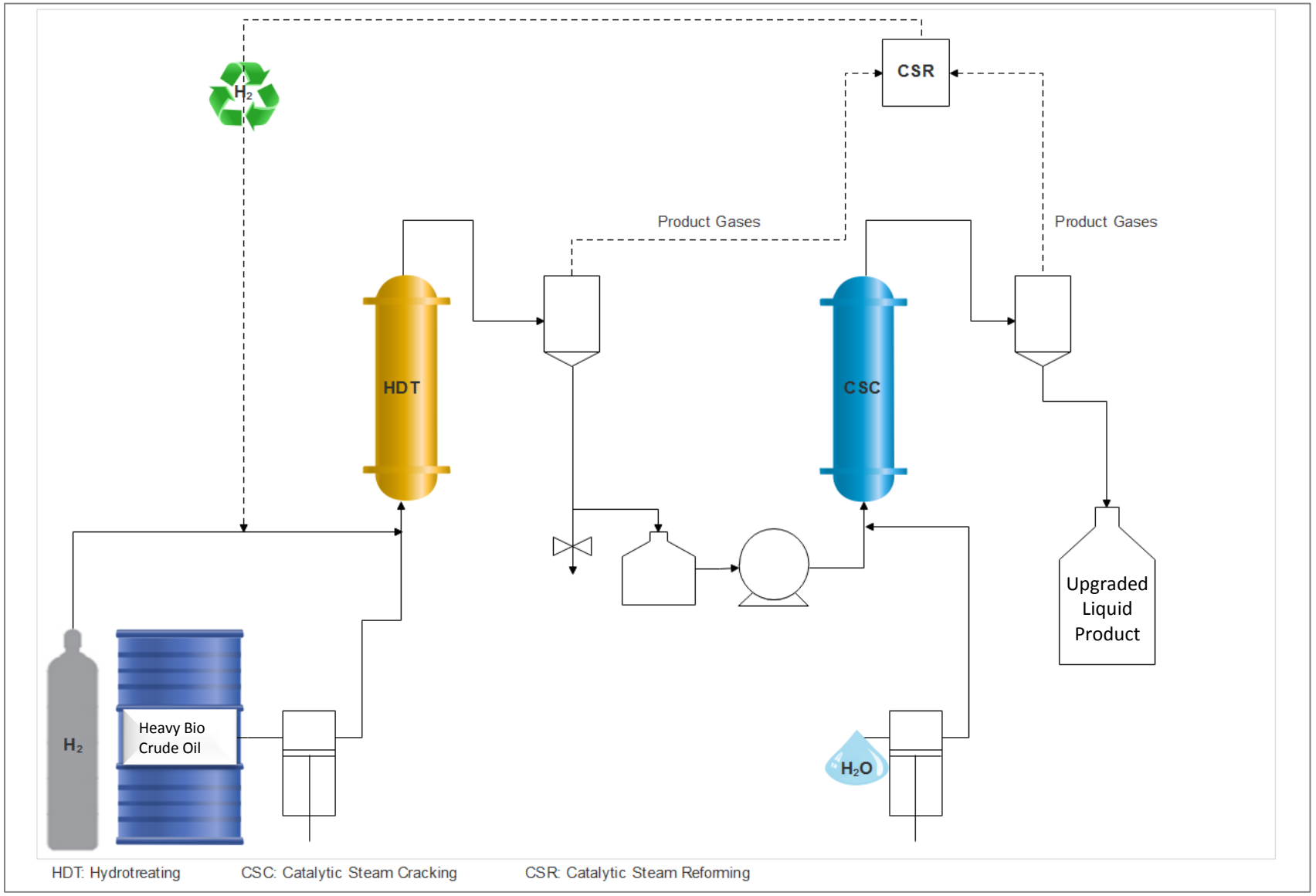

Figure 1-1 Proposed bio-crude upgrading scheme via HDT and CSC

The main advantage of this upgrading process, compared to most common hydrogen addition processes (i.e. hydrocracking), lies in the fact that there is no need for hydrogen to be fed into the CSC stage of the process. Therefore, the economy of processing feedstock derived from renewable organic material may be considerably enhanced, given that neither the need for hydrogen generation units nor the use of special materials to operate at high pressures, are required by the CSC process, and particularly because the catalyst for CSC is also an adequate catalyst for steam reforming of the light hydrocarbon gases produced in both HDT and CSC.

1.3. Objectives

In order to assess the viability of processing Steeper Energy Hydrofaction^{TM} Renewable Crude Oil (bio-crude) via the scheme proposed above with Hydrotreating followed by Catalytic Steam Cracking, both evaluated separately in fixed-bed reactors as conversion units, the exploration of different variables and their effect on the produced oil was investigated for each process.

Therefore, the general goal of the present research project is to explore the overall upgrading process for lignocellulose derived bio-crude, and whether the required hydrogen make-up level may be reduced by the hydrogen recycle proposed in the catalytic upgrading scheme.

To accomplish the general goal, the following specific objectives were established:

- Explore the HDT by performing a screening of operating conditions varying temperature, space velocity, catalyst participation, hydrogen-to-oil ratio, and pressure in order to determine preliminary favourable conditions for the hydrogenation of lignocellulose derived bio-crude;

- Explore the CSC process for the produced HDT-bio-oil, evaluate the dependence of the CSC on the feedstock, investigate preliminary effects of varying temperature and space velocity, and define the requirements for preventing rapid catalyst deactivation;
- Perform a complete characterization of the produced HDT-bio-oil and CSC-bio-oil through a series of analytical methods;
- Calculate the global mass balance in hydrogen to assess the feasibility of the hydrogen recycling to reduce fresh hydrogen make-up in the proposed scheme, and determine whether further processing of the gaseous stream is required to meet the hydrogen requirements.

Chapter Two: Literature Review

The concepts and background knowledge required for a proper understanding of the present thesis project are presented in this chapter. The literature review begins with the description of lignocellulosic biomass and its components to understand the nature of the biomass producing the bio-crude herein investigated. Then, the conversion of lignocellulosic biomass to bio-crude via thermochemical processes is reviewed, depicting Steeper Energy's Hydrofaction™ as well as the chemistry behind these reactions. Subsequently, an overview of the produced bio-crude and its characteristics is presented, followed by the upgrading technologies currently in use. The final focus of interest reviews the upgrading processes herein investigated, their fundamentals, backgrounds and previous findings.

2.1. Lignocellulosic Biomass

There is a renewed interest worldwide in the production of biofuels from a range of biomass feedstocks, and lignocellulosic biomass presents an attractive advantage to the biofuel industry. Lignocellulosic biomass derived transport fuels differ from other well-established biofuel sources such as hydrotreated vegetable oils and animal fats, as well as ethanol and biodiesel; lignocellulosic biomass-derived transport fuels present the advantage that these do not compete with food end uses, and have the potential of being energy-dense biofuels indistinguishable to fossil equivalent (Karatzos, et al., 2014). Furthermore, lignocellulosic biomass is readily and commercially available in large aggregated volumes; it is derived from forest wood harvest and from wood processing residue that includes tree branches, bark, leaves, wood pulp wastes, and sawdust (Eisentraut, 2010).

As shown in Figure 2-1, lignocellulose is a complex structural material located in the cell walls of woody biomass, and it is composed of three primary components: cellulose, hemicellulose polysaccharides, and lignin aromatic polymers. The exact proportions of each of the main components may vary significantly amongst different plant genotypes, and even amongst phenotypes (ECN, 2012).

Garrote *et al.* (1999) present typical cellulose, hemicellulose, and lignin fractions of various hard-woods, softwoods, and agricultural residues. A summary of these biomass compositions is presented in Table 2-1; and as a general trend, cellulose appears as the predominant component throughout the different lignocellulosic materials; cellulose is followed by lignin, which for forest residues (i.e. bark, pine) is a major component; and lastly, hemicellulose is generally found to contribute the least to lignocellulosic materials.

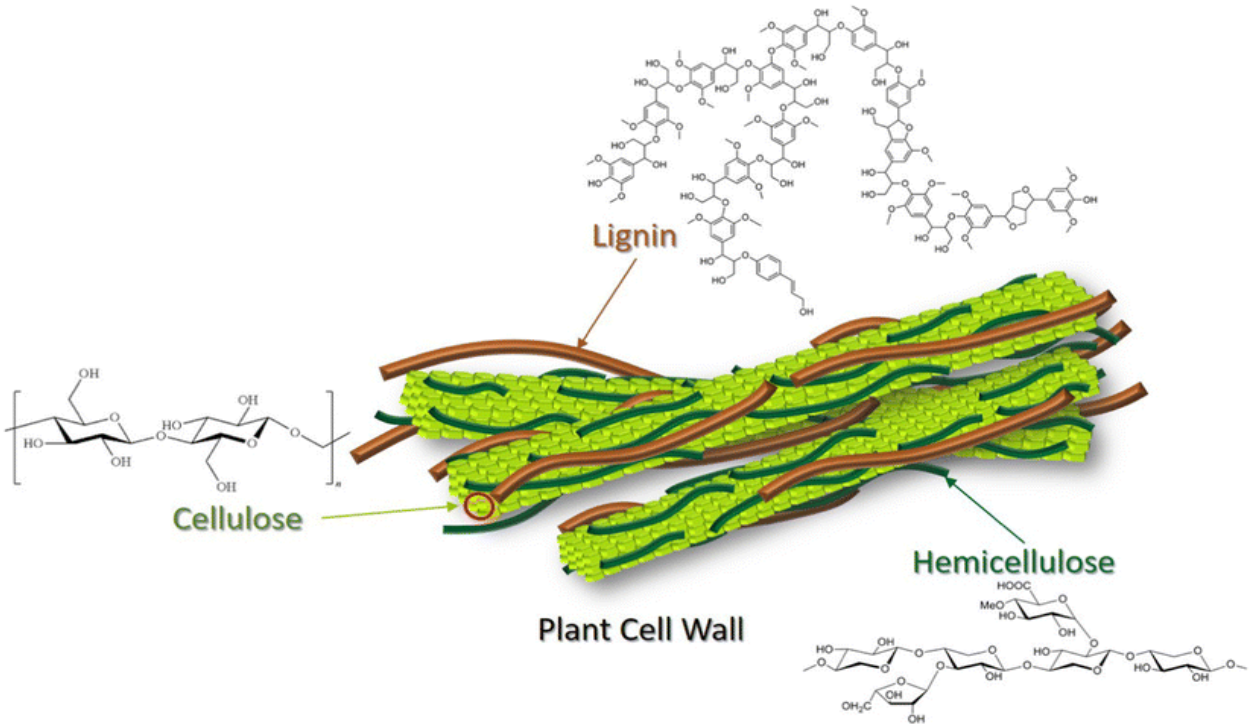

Figure 2-1 Structure of lignocellulosic biomass **(Jensen, et al., 2017)**

Table 2-1 Cellulose, hemicellulose and lignin contents as weight percent of dry biomass for representative lignocellulosic materials, adapted from Garrote *et al.* 1999.

Lignocellulosic materials	Cellulose	Hemicellulose	Lignin
Hard woods			
Poplar	46.2	24.4	24.5
Birch	40.6	29.6	20.2
Willow	60.5	29.9	25.6
Eucalyptus	43.2	22.5	25
Soft woods			
Spruce	44.1	21.2	26.9
Pine	43.6	24.9	25.6
Coniferous wood	57.5	22.5	30
Douglas fir	45.4	20.9	26.1
Forest residues			
Bark, pine	23.7	24.9	50.0
Wood stems	42.6	22.3	37.7
General residues	45.5	21	27.3

Cellulose is a polysaccharide composed of units of glucose monomers connected via β (1 → 4) glycosidic bonds aligned in parallel to each other, allowing a very tight network of strong intra and inter molecular hydrogen bonds to form (Okuda, et al., 2004). This arrangement makes them crystalline and thus resistant to swelling in water, and chemical or biological decomposition (Peterson, et al., 2008). Nevertheless, biomass decomposition at supercritical conditions is possible, as demonstrated in a work by Deguchi that reported how cellulose undergoes a transformation from crystalline to amorphous form in water at temperature and pressure conditions of 320^{o}C and 250 bar, respectively (Deguchi, et al., 2006). Furthermore, alkaline aqueous solutions have been reported to interfere with cellulose crystallinity (Bali, et al., 2015), providing another route for cellulose degradation. Therefore, a hydrothermal process operating at supercritical conditions and in the presence of alkaline aqueous solutions would be considered capable of

decomposing lignocellulosic biomass, where cellulose is a primary component. Such process is reviewed in Section 2.2.

Hemicellulose is a heteropolymer composed of a collection of amorphous, branched sugar monomers that can have side chains. Opposed to cellulose, hemicellulose does not form a crystalline and resistant structure due to the lack of repeating β (1 → 4) glycosidic bonds arrangement, thus providing random nature to the hemicellulose polymer. Therefore, compared to cellulose, hemicellulose is much more susceptible to hydrothermal processes; according to Bobleter, hemicellulose is easily dissolved in water at temperatures above 180 ºC (Bobleter, 1994). Finally, **Lignin** is a complex non-linear high molecular weight macromolecule with an even more random structure than hemicellulose. Lignin results from the polymerization and C-C, and C-O-C ether bonds cross-linking of the most prevalent monomers in lignin: p-coumaryl alcohol, coniferyl alcohol, and sinapyl alcohol (Sjöström, 1993), as shown from left to right in Table 2-2.

Table 2-2 Representative lignocellulosic biomass feedstock chemical compounds, adapted from Peterson *et al.* (2008)

Substance	Chemical formula	Structural information
Cellulose	$[C_6H_{10}O_5]_n$	n ≈ 500–10,000; β (1 → 4) linkages between glucose residues
Hemicellulose	Typical monomers: $[C_5H_8O_4]$, $[C_6H_{10}O_5]$	Branched with variable monosaccharide residues; degree of polymerization ~500–3000
Lignin	Typical monomers: 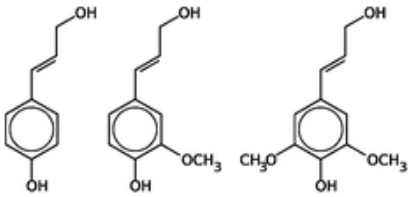	Polymer of aromatic subunits in random structure; molecular weight: >10,000 Da

Research carried out by Quitain *et al.* (2003) and Okuda *et al.* (2004) have explored using hydrothermal processes to extract potentially valuable chemicals from lignin, and Karagöz *et al.* (2005) have taken it a step further to investigate hydrothermal processes for oil production from lignin. The density of water within the hydrothermal media has been found to be a key parameter (Quitain, et al., 2003; Okuda, et al., 2004; Karagöz, et al., 2005). Many studies agree that higher water densities increase the breakdown of lignin for the production of oils and gases, presumably by enhanced hydrolysis with the higher water density (Funazukuri, et al., 1990; Saisu, et al., 2003). Therefore, thermochemical processes employing such supercritical conditions and high water density would be suitable for the conversion of lignin in lignocellulosic biomass to produce bio-crude; this is further reviewed in Section 2.2.

It has also been determined from elemental composition that lignocellulosic biomass is mainly composed of carbon, hydrogen, and oxygen at average values of 50 wt. %, 6 wt. %, and 43 wt. %, respectively (Jensen, et al., 2017). The remaining <1 wt. % is composed of nitrogen and very little chloride. Sulphur is rarely present as an elemental component of lignocellulosic biomass. The high oxygen content in lignocellulosic biomass is undesirable for the production of transportation biofuels anticipated to be functionally indistinguishable to their petroleum counterparts. Therefore, lignocellulosic originated bio-crude relies fundamentally on the deoxygenating of the lignocellulosic biomass; the produced bio-crude then requires upgrading processes capable of further increasing H/C ratios before the bio-oil is considered as transportation fuel.

2.2. Lignocellulosic Biomass to Bio-crude

In the first half of the 20th century, motivated by arguments regarding the biological origins of petroleum for fossil fuel production, researchers started proposing that renewable petroleum could be produced from biomass. In fact, dating back to 1944, Berl proposed that a variety of biomass sourced from cornstalks, corn cobs, seaweed, algae, sawdust, and grass could be turned into a petroleum-like crude; he reported that said crude contained 60% of the starting material's carbon, and 75% of the starting material's heating value (Berl, 1944). Scattered research continued since then. Most recently, in the search for alternative energy sources, lignocellulosic biomass conversion to bio-crude gained interest, particularly as lignocellulosic biomass-derived transport fuels do not compete with food end uses. In the past few years, research on the conversion of biomass to liquid fuels has grown, ranging from studies of thermochemical biomass conversion technologies such as pyrolysis, and hydrothermal liquefaction (HTL) processes (Ragauskas, et al., 2006) all the way to upgrading processes (Ramirez, et al., 2015). The common objective is to produce biofuels that are functionally indistinguishable from the fossil equivalents and are fully

compatible with existing petroleum infrastructure. These biofuels are also defined in the literature as “drop-in” oil (Jensen, et al., 2017).

2.2.1. Thermochemical biomass conversion technologies.

In this section, the production of liquid bio-crudes by thermochemical treatment of biomass is reviewed. Pyrolysis and Hydrothermal Liquefaction (HTL) are two major thermochemical biomass conversion technologies being developed to produce drop-in biofuel blend stock from non-edible and lower cost lignocellulosic biomass.

Pyrolysis was initially investigated for the production of chemicals from wood (Paul de Wild, 2011); nowadays, pyrolysis has been widely researched and developed to industrial-scale processes for the production of oils from biomass (Bridgwater & Peacocke, 2000). Among different pyrolysis processes, fast pyrolysis has been determined to maximize liquid products (Bridgwater, et al., 2002). Fast pyrolysis occurs at atmospheric pressure, under high temperatures (~500 ^{o}C) with very short residence times (< 2 s). Compared to other thermochemical biomass conversion processes, fast pyrolysis oils have the advantage of lower capital costs compared to liquefaction, and short residence times. However, fast pyrolysis is limited by its requirements for low moisture content feedstock, rapid heating and quenching rate, and high temperature requirements (Mohan, et al., 2006).

On the other hand, **HTL** has been acknowledged with the potential of becoming a competitive and resource effective pathway for the production of lignocellulosic biomass-derived transport fuels. HTL is often considered to take place near or below the critical point of water, at temperatures of approximately 280 – 374 ^{o}C and at a pressure of at least the saturation pressure of water to avoid boiling (Jensen, et al., 2017). HTL’s high efficiency has been demonstrated in a study by Tews *et al.* (2014), where hydrotreated HTL biofuel was found to be less expensive in terms of mass and

energy balances compared to the fast pyrolysis equivalent. Furthermore, it was also estimated that wood-derived HTL biofuel allows for a 70% GHG emission savings compared to the 2005 petroleum baseline (Tews, et al., 2014). Lignocellulosic biomass feedstock contains large amounts of water; in conventional processing, the water is typically thermally separated by vaporization during pyrolysis. These separation steps lead to large parasitic energy loses that consume much of the energy content in the biomass (Peterson, et al., 2008). However, in the case of HTL, reactions are carried out under pressure, and thus the phase change is avoided providing possible efficiency advantages in hydrothermal processing. Therefore, HTL technologies can largely avoid energetic sinks associated with the evaporation of water and can thus result in more efficient processing of biomass.

Further advantages presented by HTL, compared to pyrolysis, are found in the quality of the produced oils. Table 2-3 presents typical properties of wood-biomass HTL-produced and pyrolysis-produced oils; the moisture content, elemental composition, high heating values (HHV), and viscosity of sample oils from the two methods are compared. Oils produced from HTL typically have more desirable properties than fast pyrolysis oils and can be made with higher energetic efficiency by avoiding evaporating water (Elliott & Schiefelbein, 1989). Although bio-crudes produced by HTL processes are typically more viscous and higher in oxygen content than petroleum crude oil, these are lower in oxygen content compared to pyrolysis bio-crudes (Elliott, et al., 1991).

Table 2-3 Typical properties of wood HTL oil, wood pyrolysis oil, and heavy fuel oil

	HTL oil[a]	Pyrolysis oil[a]	Heavy oil[b]
Moisture content, wt.%	5	15-30	0.1
Elemental composition, wt.%			
C	73	54 – 58	85
H	8	5.5 – 7.0	11
O	16	35 – 40	1.0
N	-	0 – 0.2	0.3
Ash		0 – 0.2	0.1
HHV, MJ/kg	34	16 – 19	40
Viscosity at 50°C, cP	15,000 (at 61°C)	40 – 100	180

[a] adapted from Elliot and Schiefelbein (1989), [b] adapted from Czernik and Bridgwater (2004)

As a reference, typical properties of petroleum heavy oil are also included in Table 2-3. Such properties evidence the requirement of further treatment of the bio-crudes before these may be used as transportation fuels, either in neat form or as fuel blends; upgrading of the crude-oil is an alternative and such processes are reviewed in Section 2.4.

2.2.1.1. Lignocellulosic biomass HTL via Steeper Energy's Hydrofaction™.

Steeper Energy is commercializing its proprietary HTL technology as a potential path to sustainable lignocellulosic-derived transportation fuels. Steeper Energy's Hydrofaction™ utilizes a unique combination of high-density, supercritical water chemistry and homogeneous catalysts at distinctively higher pressure and temperatures than most literature on HTL. Contrary to most HTL processes, Hydrofaction™ takes place above the critical point of water at temperatures between 390 – 420°C and at pressures ranging between 250 – 350 bar, in the presence of homogenous alkaline metal catalysts at alkaline conditions with a recycling of aqueous and oil products (Jensen, et al., 2017). Figure 2-2 is adapted from Jensen *et al.* (2017), and it illustrates the phase diagram

of water to picture the different operating regimes, and thus visualize the difference between traditional HTL processes and Hydrofaction™.

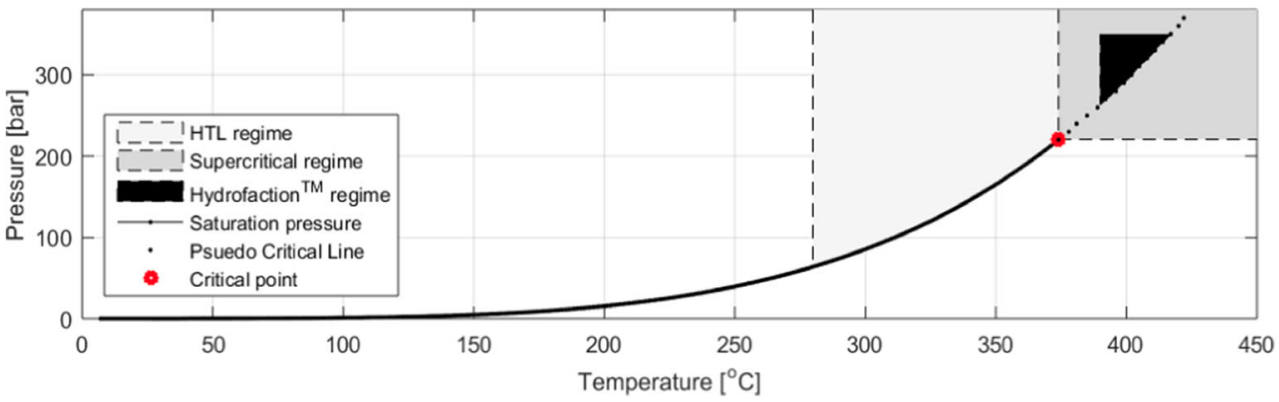

Figure 2-2 Phase diagram of water showing the typical HTL and Hydrofaction™ operating regimes, adapted from Jensen *et al.* (2017).

Jensen *et al.* (2017) state that the higher operating pressures of Hydrofaction™, compared to other HTL processes, allows for key thermodynamic properties of water such as density to be maintained at the same order of magnitude as for the sub-critical conditions; and at the same time, higher temperatures favour the process in the sense of faster kinetics.

Generalities of HTL processes have evolved in this area of research since the early 1980s when many researchers expected that altered or even enhanced rates of chemical reactions would occur near the critical point of solvents such as carbon dioxide or water (Peterson, et al., 2008). However, it has been commonly accepted that no such enhancement takes place regarding water as a solvent (Narayan & Antal Jr., 1990); nevertheless, observed rates have been found to be significantly enhanced by the loss of mass transfer limitations given that most organic species become miscible with supercritical water. Also, observed rates can be enhanced by the ability of supercritical water to sustain both ionic and free radical reactions (Antal Jr., et al., 1987).

Therefore, the fundamentals of Hydrofaction™ rely on taking advantage of supercritical water chemistry (Iversen, 2015). The polarity of water diminishes as supercritical conditions are reached, allowing water to dissolve biomass molecules including phenolic and polyaromatic hydrocarbons derived from lignin, which are hydrophobic at ambient conditions. The accelerated lignocellulosic biomass conversion takes place through hydrolysis and solvolysis reactions as mass transfer limitations are reduced under supercritical conditions. Such ionic reactions are further promoted by water dissociation, which is maintained high in relatively high-density supercritical water (Jensen, et al., 2017). Overall, the reaction chemistry of HTL is complex; many chemical reactions are possible depending on the specific operating conditions. Jensen *et al.* (2017) have proposed a scheme for the major reactions occurring throughout the Hydrofaction™ process; this scheme is illustrated in Figure 2-3.

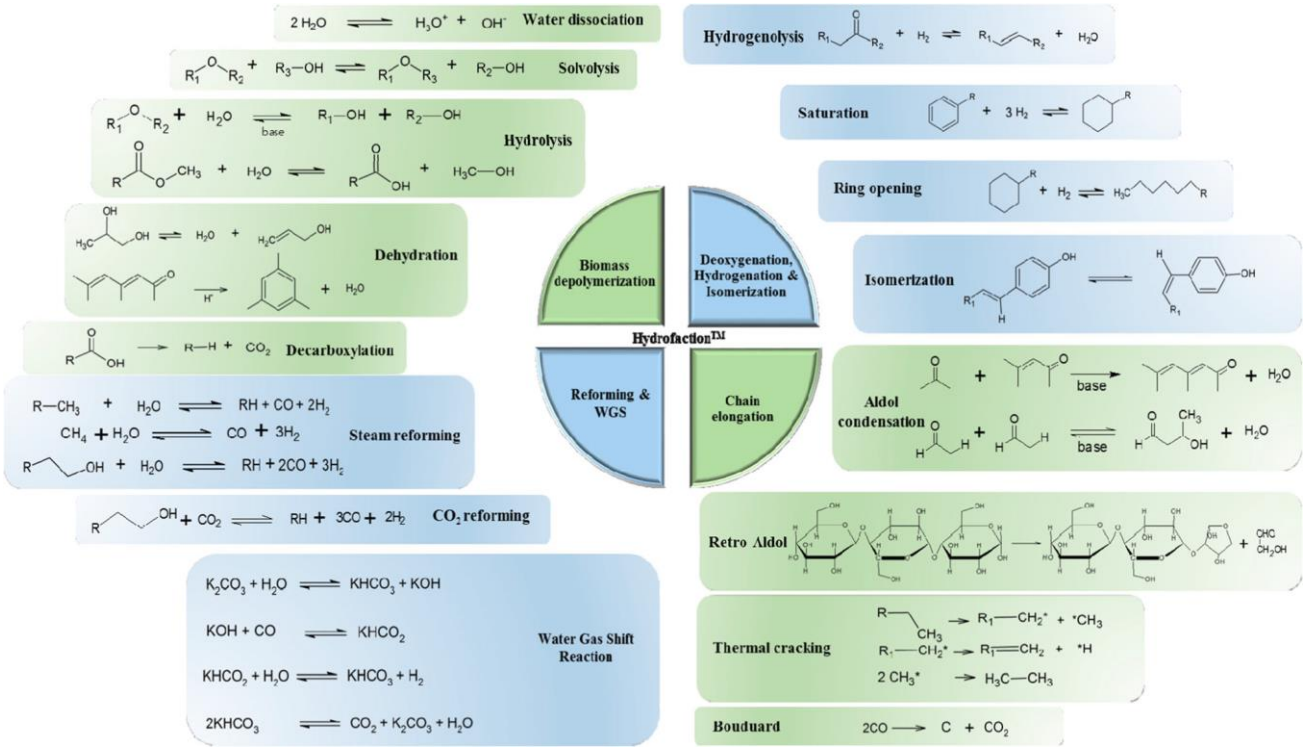

Figure 2-3 Major chemical reactions occurring during Hydrofaction™ **(Jensen, et al., 2017)**.

Hydrofaction™'s alkaline conditions facilitate the decomposition of the lignocellulosic feedstock to its major compounding macromolecules: hemicellulose, cellulose, and lignin; these are reviewed in Section 2.1. During the heat-up stage of this HTL process, the macromolecules depolymerize to oligomers and eventually monomers through alkaline hydrolysis and solvolysis type reactions. Oligomers and monomers formed from hydrolysis dehydrate and isomerize to form carboxylic acids, aldehydes, and enols. According to Jensen *et al.* (2017), lignin depolimerization may follow two reaction pathways; the first being an ionic one through the hydrolysis and solvolysis of intermolecular ether bonds – leading to the formation of low molecular weight phenolics; and the second being a radical pathway through the thermal cleavage of both ether and C–C bonds. As temperature increases and approaches the critical point of water, rapid dissolution of cellulose occurs and its hydrolysis is greatly accelerated by overcoming mass transfer limitations. Water dissociation catalyzes additional ionic reactions such as isomerization, saturation, and hydrogenolysis. Furthermore, a significant degree of biomass deoxygenation does take place during the Hydrofaction™ process, leading to a bio-crude with significantly lower oxygen content compared to other thermochemical processes. Nevertheless, the still high oxygen content (10 – 12 wt. %) can impart a number of undesirable qualities to the oil product, such as lower energy content, poor thermal stability, lower volatility, higher corrosivity, and a tendency to polymerize (Grange, et al., 1996; Furimsky, 2000).

The resulting compounds comprising the produced bio-crude are many, thus their analysis becomes very complex. Nevertheless, the reaction pathways for cellulose decomposition in supercritical water investigated by Kruse & Gawlik (2003) and Watanabe et al. (2005) give an idea of what compounds may be present in lignocellulosic derived bio-crude via Hydrofaction™.

The chemistry for the decomposition pathways of cellulose in supercritical water is shown in Figure 2-4, and hemicellulose has been found to undergo analogous reaction pathways.

The glucose monomer undergoes isomerization to form fructose, which then can undergo dehydration to form 5-Hydroxymethylfurfural (5-HMF) (Antal, et al., 1990). Further dehydration of 5-HMF yields a 1:1 mixture of levulinic and formic acids. Angelic lactone forms by dehydration of levulinic acid. Retro-aldol reactions produce glycolaldehyde, dihydroxyacetone, and erythrose from the original cellulose and hemicellulose components.

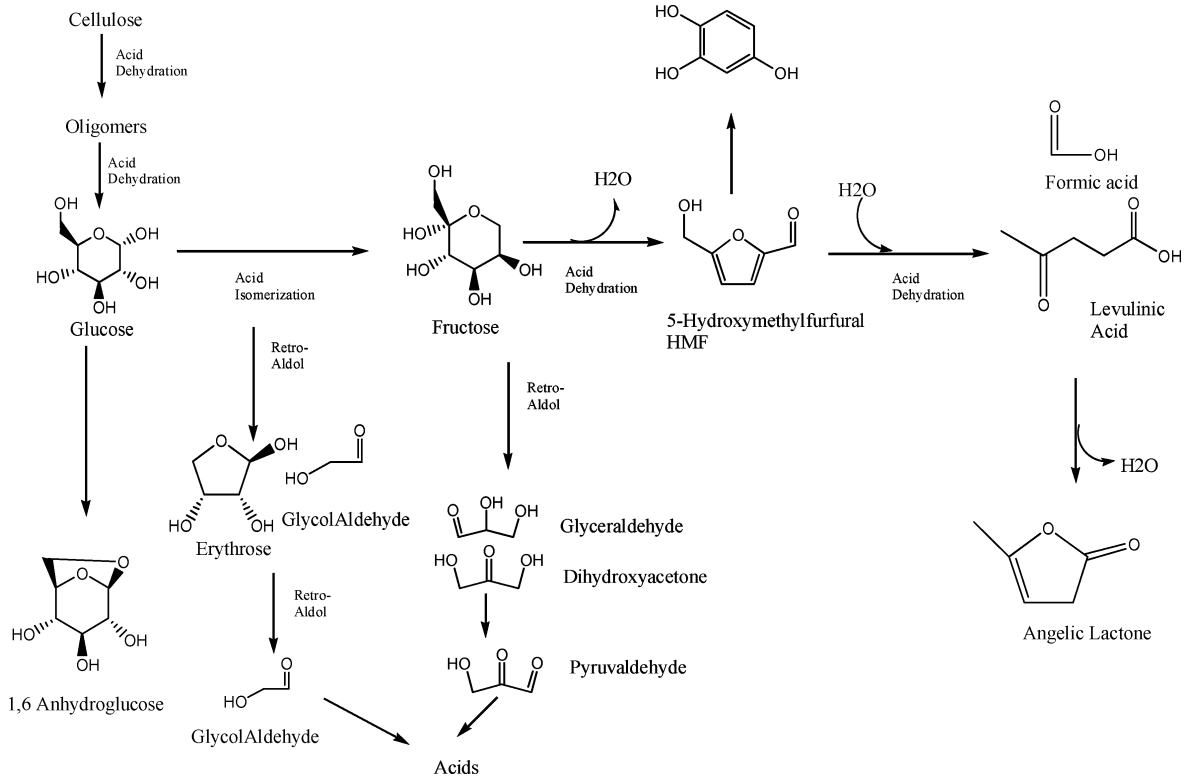

Figure 2-4 Cellulose decomposition pathways in supercritical water **(Kruse & Gawlik, 2003; Watanabe, et al., 2005)**.

A review of the representative chemistry, reactions, and produced molecules that have been found to be present in the thermo-chemically converted lignocellulosic biomass has been presented in this section. This provides some guidance regarding the nature of the produced bio-crude feedstock of interest for this thesis investigation and the path that this research may undertake in upgrading it. A review of such bio-crude's properties is depicted in the following section.

2.3. Lignocellulosic Biomass-derived Bio-crude

Bio-crudes are a dark brown liquid with a distinctive smoky odor. The exact composition of the bio-crude is dependent on the thermochemical process (i.e. HTL, Hydofaction^{TM}) and the reaction conditions such as temperature, solvent, solvent density, reaction time, and gas used as reaction atmosphere (Ramirez, et al., 2015). Furthermore, the composition of the biomass fed into the liquefaction process has the most significant effect on the chemical composition of the bio-crude (Akhtar & Amin, 2011).

2.3.1. Bio-crude properties

An overview of the different physicochemical properties of bio-crude is presented in this section. Physical properties such as viscosity and chemical properties such as oxygen content and chemical compositions are presented. This allows for an understanding of the differences between lignocellulosic derived bio-crudes and petroleum crudes, and a look into the required upgrading pathways for bio-crudes.

Viscosity is a physical property defined as the measure of the flow behavior of a fluid. For an organic compound, its viscosity is related to its chemical structure. Previous studies by Bouelhouwer *et al.* (1951) have concluded that alcohols and acid groups have a stronger effect on viscosity compared to ester and ketone groups; aromatic structures are less viscous than their

corresponding hydrogenated forms; and straight chain hydrocarbons have higher viscosities compared to branched hydrocarbons (Boelhouwer, et al., 1951).

The **acidity** of bio-crude promotes condensation reactions, accelerating aging and a declination of bio-crude properties, and makes the bio-crude immiscible with petro-fuels. Therefore bio-crudes should be upgraded so that these can directly be used as a fuel or mixed with crude oil. Moreover, bio-oil is highly unstable because of the presence of unsaturated carbon, which is active during polymerization and condensation (Elliott & Neuenschwander, 1998). These findings suggest the criticality of an upgrading process capable of eliminating alcohols and acid groups through possible hydrotreating processes, cracking straight chain hydrocarbons, and treating aromatic compounds in ways which viscosity benefits.

The **heating value** is another physical property, and it is a quantitative representation of the bio-crude's energy content (Schaschke, 2014). This quantity also gives the energy density of the fuel, which dictates how much energy is released with each volume of fuel injected into the combustion chamber. The heating value of bio-crude is 20-30 MJ/kg (Huber, et al., 2006), which is significantly higher than that of raw biomass but lower than that of crude oil, whose value is around 40 MJ/kg (Czernik & Bridgwater, 2004). Correlations state that heating value is directly proportional to the elemental composition, with carbon and hydrogen increasing heating value and oxygen and nitrogen having a negative effect (Demirbas, et al., 1997). Therefore, the low heating value of bio-crude compared to petroleum crude oil is due to the presence of high molecular-weight oxygenated compounds, where nitrogen content is negligible. The highly unstable nature of bio-oil can be correlated to its deteriorating heating values. This deterioration occurs over time due to polymerization and condensation between the oxygen-containing compounds themselves. Therefore, by upgrading bio-crude though hydrotreating reactions, removal of oxygen would be

beneficial regarding the heating value of the produced bio-oil, and concomitantly, its improved storage stability.

Regarding chemical properties of bio-crude, as reviewed in Section 2.2, thermochemical conversion of woody biomass results in the depolymerisation of lignocellulosic material. This produces a viscous crude oil replacement, which has an important key difference from conventional crude oil: the oxygen content of the bio-crude is significantly higher; **oxygen content** in bio-crude is typically 10 – 30 wt. % compared to < 1% in conventional petroleum (Aitani, 2004). Therefore, the produced bio-crude has a significant oxygen content in the form of organic acids, alcohols, ketones, aldehydes, furans, phenols, guaiacols, amongst other oxygenates (Huber, et al., 2006). Such high oxygen content can impart a number of undesirable qualities to the oil product such as lower energy content; oxygenated compounds have been linked to poisoning of catalyst in crude-oil refining processes (Alfke, et al., 2008); a high tendency for corrosion by oxygenates present in the form of acids, and lastly polymerization of phenolic components present in the bio-crude has been observed (Huber, et al., 2006).

On the other hand, bio-crude from thermochemical conversion of lignocellulosic biomass has been found to have low levels of nitrogen content with a maximum of 1% (Demirbas, 2005). As well, lignocellulosic materials have very minimal sulphur content. Thus bio-crude has been produced with < 0.05 wt. % sulphur (Huber, et al., 2006). Table 2-4 reports the above-mentioned physicochemical properties of typical bio-crudes and compares these with petroleum crude oils. One crucial difference between the two is the elemental composition (Venderbosch, et al., 2010; Zhang, et al., 2007). This affects the homogeneity, polarity, heating value, viscosity, and acidity of the oil. Furthermore, the H/C ratio comparison between bio-crudes and petroleum crudes further emphasizes the requirements for bio-crude hydrotreating.

Table 2-4 Comparison between a wood derived bio-crude and crude oil.

	Bio-crude [a]	Alberta Bitumen [b]
Viscosity at 40°C, cP	6,000 – 30,000	12,000
HHV, MJ/kg	12 – 30	40 – 44
Elemental composition, wt.%		
C	65 – 75	82 – 83
H	5 – 8	10
O	10 – 30	<1
N	<0.5	<1
S	<0.05	4.5 – 6.0
H/C molar ratio	1.3 - 1.1	1.76

[a]Data is adapted from Huber et al. (2006), Zhang et al. (2007), Holmgren et al. (2008), Venderbosch et al. (2010), [b] *(Banerjee, 2012)*.

Regarding the chemical composition, bio-crude is a complex mixture of oxygenated organic material as previously discussed in Section 2.2. A study by Branca *et al.* (2003) summarizes the chemical composition of typical bio-crudes. More than 300 different organic compounds have been identified in bio-crudes, where the specific composition of the product depends on the feed and process conditions used (Zhang, et al., 2007). Figure 2-5 shows the range of compositions. The multicomponent mixtures are derived primarily from depolymerization and fragmentation reactions of the three key building blocks of lignocellulose: cellulose, hemicellulose, and lignin.

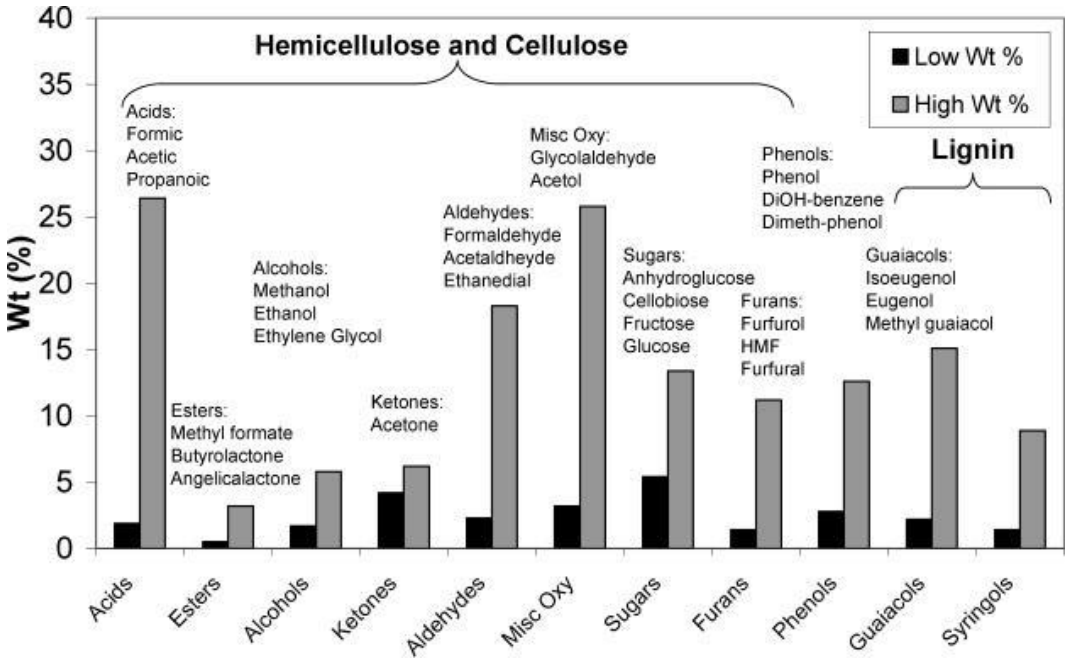

Figure 2-5 Chemical composition of bio-crudes showing the most abundant molecules of each of the components and the biomass fraction from which the components were derived **(Branca, et al., 2003)**

Physicochemical properties of this bio-crude such as density, viscosity, volatility, and polarity are affected by high oxygen content, thus compromising the bio-crude's compatibility with petroleum equivalents. Therefore, said crude oil requires further upgrading to meet fuel specifications, as any petroleum-crude would. An upgrading process of choice for highly oxygenated bio-crudes is hydrotreating (HDT); whereas hydro-desulfurization (HDS) and hydro-denitrogenation (HDN) would be dominating reactions in the hydrotreating of petroleum-crudes, hydro-deoxygenation (HDO) would be the reaction of interest in the hydrotreating of lignocellulosic derived HTL bio-crudes. Bio-crude upgrading technologies are reviewed in the following section.

2.4. Bio-crude Upgrading

Upgrading refers to processing oils, whether these are petroleum-crudes or bio-crudes, in order to improve their physical and chemical properties to meet values reported by existing fuel standards. Catalytic upgrading of bio-crude is a complex reaction network due to the high diversity of compounds present, as reviewed in Section 2.3. Nevertheless, technologies to upgrade biomass-derived oils have been investigated and thoroughly reviewed by many (Furimsky, 2000; Elliott, 2007; Ramirez, et al., 2015; Patel & Kumar, 2016; Mortensen, et al., 2011).

A pathway of choice for upgrading technology developments relies on hydrogen addition processes (i.e. hydroprocessing) to produce an increase of the H/C ratio of heavy molecules by a reaction between them and an external source of hydrogen. Figure 2-6 illustrates the general flow of hydroprocessing technologies.

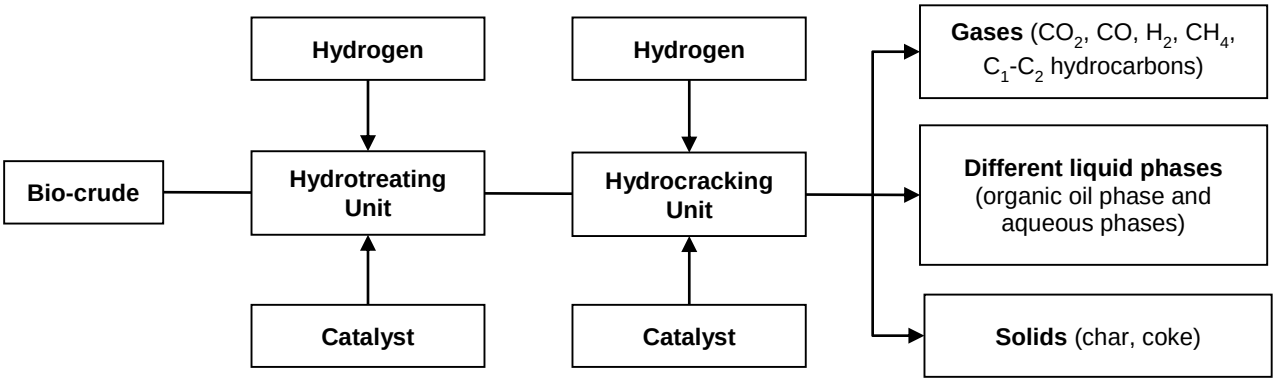

Figure 2-6 General flow diagram for a common bio-crude upgrading technology: hydroprocessing **(Patel & Kumar, 2016)**

Through hydrotreating (HDT), followed by hydrocracking (HDK), bio-crudes are upgraded into an oil product with properties similar to those of petroleum fuel (Ward, 1993). However, larger investments are necessary, requiring a hydrogen source and most of them involve a catalyst (Speight, 2013). Nevertheless, hydroprocessing such as hydro-deoxygenation technologies is a pathway of choice for bio-crude upgrading.

The HDT unit is a primary pre-treatment unit that hydrogenates unsaturated hydrocarbons and removes heteroatoms from the feedstock. Depending on the molecule targeted, HDT reactions can be classified as hydro-desulfurization (HDS), hydro-denitrogenation (HDN), hydro-demetallization (HDM), aromatic/olefin saturation, or hydro-deoxygenation (HDO) (Banerjee, 2012). In the case of bio-crude, such HDT reactions are analogous to but certainly not identical to HDT reactions for converting petroleum crude oil to fuels. Petroleum-crude oil processing techniques typically focus on the removal of nitrogen and sulfur, as well as molecular weight reduction. In contrast, treatment of bio-crude will typically be more focused on oxygen removal and molecular weight reduction. In lignocellulosic biomass-derived oil, oxygenates are the main components, sulfur and nitrogen compounds are found in insignificant quantities. Therefore, HDO is critical in the removal of the oxygen heteroatom from the feedstock.

On the other hand, hydro-dealkylation, hydrocracking, isomerization of alkanes, and hydro-decyclization are key reactions that occur simultaneously in the hydrocracking unit. Therefore, hydrocracking reactions crack big molecules, forming free radicals. These free radicals react with the hydrogen avoiding the formation of coke. Hydrocracking operates at high pressures, and the use of high pressure of hydrogen implies a high capital expenditure and high operation costs.

Other technologies based on similar principles have been developed since 1980. Among the technologies in development, two of them (GenOil Upgrader and Aquaconversion) are based on the same hydroprocessing principles but use water to supply hydrogen by the catalytic splitting of the water molecule (Banerjee, 2012; Pereira, et al., 2001). These processes are often referred to as Catalytic Steam Cracking (CSC). A bio-crude upgrading process via HDT followed by CSC is investigated in this thesis.

2.4.1. Hydrotreating.

Hydrotreating (HDT) is a conventional form of petroleum hydroprocessing technology, and it is a well-established process in petroleum refining with the purpose of increasing saturation of hydrocarbons, and remove heteroatoms present in the feedstock. Heteroatoms such as oxygen, nitrogen, and sulphur are removed via HDT reactions in the form of water, ammonia, and hydrogen sulphide, respectively.

Undesirable reactions of aldehydes and organic acids, and an increase in the amount of higher molecular weight compounds due to polymerization and condensation reactions have been reported in bio-crudes (Diebold, 2000). Nevertheless, Tang *et al.* (2009) reported that HDT is an efficient way to convert such aldehydes and unsaturated compounds into more stable compounds by removing its oxygen atoms (Tang, et al., 2009). Thus, HDT processes address concerning issues regarding the instability of bio-crude due to polymerization or degradation of components. Furthermore, HDT is done to prevent catalyst deactivation in further processing, to minimize coking, and to enhance fuel characteristics by improving the oil's heating value (Alfke, et al., 2008).

Examples of common HDT reactions adapted from previously reported chemical reactions (Wildschut, et al., 2009) are presented in Table 2-5. In bio-crudes, oxygenates are the main components, whereas sulphur, and nitrogen compounds are found in insignificant quantities (Elliott & Schiefelbein, 1989). Therefore, hydro-deoxygenation (HDO) reactions are critical in the removal of the oxygen heteroatom from the feedstock. A few more reactions may occur under HDT conditions without hydrogen: decarboxylation, and decarbonylation; these also participate in the removal of the oxygen heteroatom from the bio-crude. Decarboxylation and decarbonylation reactions remove oxygen in the form of carbon dioxide and carbon monoxide, respectively.

In the presence of hydrogen and a catalyst, hydro-decarboxylation and hydro-decarbonilation reactions occur. Furthermore, reverse water-gas-shift reactions (rWGSR) as well as methane formation through CO hydrogenation (i.e. methanation), and coke formation reactions take place as side reactions.

Table 2-5 Reactions occurring in HDT processes.

Hydrotreating Reaction	
Hydro-deoxygenation (HDO)	$R-OH\ +\ H_2 \rightarrow R-H\ +\ H_2O$
Hydro-desulfurization (HDS)	$R-SH\ +\ H_2 \rightarrow R-H\ +\ H_2S$
Hydro-denitrogenation (HDN)	$Pyridine\ +\ H_2 \rightarrow Pentane\ +\ NH_3$
Hydrogenation	$RH-C=C-R'H'\ +\ H_2 \rightarrow R-CH_2CH_2-R'$
Other simultaneous reactions	
Hydro-decarboxylation	$R-COOH \overset{H_2}{\rightarrow} R-H\ +\ CO_2$
Hydro-decarbonylation	$R-COH \overset{H_2}{\rightarrow} R-H\ +\ CO$
Reverse water gas shift (rWGS)	$CO_2\ +\ H_2 \rightarrow CO\ +\ H_2O$
Methanation	$CO\ +\ 3H_2 \rightarrow CH_4\ +\ H_2O$
Coke formation	$Poly-oxygenated\ aromatics\ \rightarrow Coke$

HDT reactions take place in the presence of hydrogen and a catalyst. The main component of a HDT unit is the reactor, which consists of a high-pressure vessel, the proprietary catalyst, and other internal technology (Mortensen, et al., 2011). The most common obstacle in HDT processes is that the yield of hydrotreated-upgraded bio-oil is relatively low, and the problem of catalyst deactivation and reactor clogging arises due to the production of a large amount of coke and tar by the thermally unstable components (Junming, et al., 2008). The coking can be so severe that it plugs fixed-bed reactor systems resulting in termination of experimentation (Baker & Elliot, 1988). Typical operating pressure ranges between 50–200 bar, and the temperature varies from high 200's to low 400's °C (Elliott & Neuenschwander, 1998; Gandarias, et al., 2008). Depending on the

temperature, the hydrotreating process is considered to be high severity or low severity (Elliott & NG, 1996). High-severity hydrotreating is considered to be complete hydro-deoxygenation and low-severity hydrotreating is considered as partial hydro-deoxygenation.

An important aspect of HDO reactions is the consumption of hydrogen. Venderbosch *et al.* (2010) investigated hydrogen consumption for bio-crude upgrading as a function of deoxygenation rate over a Ru/C catalyst in a fixed bed reactor. The results are summarized in Figure 2-7. The stoichiometric requirement was calculated on the basis of an organic bound oxygen content of 31 wt. % in the bio-crude and a hydrogen consumption of 1 mol H_2 per mol of oxygen; the experiments were performed with a Ru/C catalyst at 175 – 400 ^oC and 200 – 250 bar in a fixed bed reactor fed with bio-crude. The high temperatures were used in order to achieve high degrees of deoxygenation. It was reported that the hydrogen consumption becomes increasingly steep as a function of the degree of deoxygenation (Venderbosch, et al., 2010).

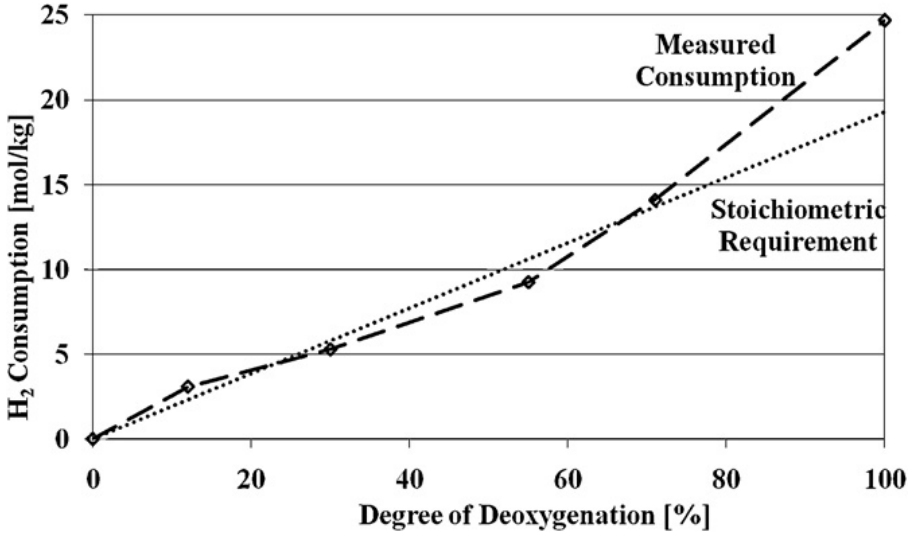

Figure 2-7 Consumption of hydrogen for HDO as a function of degree of the deoxygenation compared to the stoichiometric requirement. Data are from Venderbosch *et al.* (2010)

Venderbosch's reaction trends could be explained by the different reactivity values of the compounds in the bio-crude. Highly reactive oxygenates, like ketones, are easily converted with low hydrogen consumption, but some oxygen is bound in the more stable compounds. Thus, the more complex molecules are accompanied by an initial hydrogenation and/or saturation of the molecule and therefore the hydrogen consumption exceeds the stoichiometric prediction at the high degrees of deoxygenation (Furimsky, 2000). Furthermore, for increased complexity of the bound or sterically hindered oxygen, as in furans or ortho substituted phenols, it has been found that significantly higher temperature is required for HDO reactions to proceed (Mortensen, et al., 2011). On this basis, the apparent reactivity of different oxygenated compounds has been summarized by Furimsky (2000):

$$alcohol > ketone > alkylether > carboxylic\ acid \approx M\text{-}/P\text{-}phenol \approx naphtol > phenol >$$

$$diarylether \approx O\text{-}phenol \approx alkylfuran > benzofuran > dibenzofuran$$

Also, the effect of temperature was investigated by Elliot *et al.* (2009) for HDO of wood based bio-crude over a Pd/C catalyst, in a fixed bed reactor at 140 bar. It was found that the oil yield decreased from 75% to 56% when increasing the temperature from 310^{o}C to 360^{o}C; this was accompanied by an increase in the gas yield by a factor of 3; and the degree of deoxygenation increased from 65% at 310^{o}C to 70% at 340^{o}C where above 340^{o}C the degree of deoxygenation did not increase further, but instead extensive cracking took place rather than deoxygenation (Elliott, et al., 2009).

Depending on the severity of HDT, the treated oil is free of heteroatoms, but it has non-polar, high-molecular weight organic compounds in the oil phase (Patel & Kumar, 2016). Consequently, the oil requires further processing. Also, it has been determined that HDT consumes large amounts of expensive high-pressure hydrogen (Fathi et al., 2011). Therefore, an alternative that has been

explored in recent years, and is herein implemented as a co-process for bio crude upgrading is catalytic steam cracking (CSC). This allows for further processing of the hydrotreated bio-crude with water as a source of hydrogen, where the unconsumed hydrogen becomes an onward source of hydrogen.

2.4.2. Catalytic Steam Cracking.

This process has been defined as a moderate-conversion process for unconventional oil or heavy cuts, that catalytically produces hydrogen through steam dissociation while, in parallel, cracks heavy molecules both thermally and catalytically (Trujillo-Ferrer, 2008). Catalytic Steam Cracking (CSC) is considered an alternative process for heavy oils and bitumen upgraders due to its low investment cost (Marzin, et al., 1998; Pereira, et al., 2001), given that there is no requirement for hydrogen production or high-pressure equipment compared to Hydrocracking (Speight, 2014). Furthermore, an appealing advantage of this process is that not only hydrogen is substituted by water, but also hydrogen is produced in the reaction as a by-product.

In this hydrogen addition upgrading process water is added as the source for hydrogen; thus hydrogen radicals are formed catalytically from the dissociation of water molecules. As a consequence, the formed hydrogen and oxygen radicals participate in saturation of present hydrocarbon radicals, which are generated through the thermal cracking; also in the prevention of undesirable condensation reactions, and thus avoid the production of carbonaceous residue. Furthermore, the steam processing stage is a new path that may be considered at lower costs, and thus an appealing upgrading technology for further processing of feedstock such as the above mentioned hydrotreated bio-crude.

2.4.2.1. CSC reaction mechanism.

A mechanism describing the reactions occurring via CSC has been proposed by Pereira-Almao, *et al.* (2013). The mechanism appears to be similar to what has been proposed to describe hydroprocessing reactions (i.e. hydrocracking), with the difference that in CSC the catalyst dissociates the water molecule, instead of the hydrogen molecule. The CSC reaction mechanism is presented in Table 2-6 (US Patent No. 2013/0015100 A1, 2013). According to Pereira-Almao *et al.* (2013), the CSC reaction mechanism proceeds via the unique interaction between two non-noble metal catalysts. The first catalyst enhances the dissociation of water into hydrogen and oxygen free radicals; the highly reactive hydrogen free radicals that are formed accelerate the thermal cracking rates of the paraffinic components of the feedstock and stabilize the resulting thermal products by saturating olefinic free radicals. Then, the second catalyst minimizes possible condensation reactions by promoting the addition of hydrogen to the hydrocarbon free radical; this results in the formation of smaller hydrocarbon components as well as additional hydrogen free radicals and carbon dioxide (Trujillo-Ferrer, 2008).

Table 2-6 Reactions occurring in CSC processes

Catalytic Steam Cracking Reaction Mechanism *(Pereira-Almao, et al., 2013)*		
1. Thermal Cracking	$R - R_n' \rightarrow R^{\bullet} + R_n'^{\bullet}$	**Eq. 2-1**
2. Catalytic dissociation of Water	$H_2O \xrightarrow{cat} H^{\bullet} + OH^{\bullet}$	**Eq. 2-2**
3. Saturation of organic free radicals by hydrogen free radicals	$R^{\bullet} + R_n'^{\bullet} + 2H^{\bullet} \xrightarrow{cat} R - H \ + \ R_n' - H$	**Eq. 2-3**
4. Oxidation	$R_n'^{\bullet} + 2OH^{\bullet} + H^{\bullet} \xrightarrow{cat} R_{n-1}' - H + CO_2 + H_2$	**Eq. 2-4**
5. Condensation	$R_n'^{\bullet} + R^{\bullet} \rightarrow R_n' - R_n', R - R, R - R_n'$	**Eq. 2-5**

Equations 2.1 and 2.2 show the hydrocarbon thermal cracking and the water splitting of the water molecule, respectively. When using a catalyst able to perform water splitting, hydrogen is produced in the reactor and used to hydrogenate heavy molecules. At the same time, cracking reactions take place. Catalytic steam cracking can be considered as a combination of steam reforming and thermal, or catalytic, cracking (Righi, 2016). Equation 2.3 represents the saturation of the organic free radicals reaction with the hydrogen free radicals. Equation 2.4 shows the reaction between the hydroxyl free radical with the hydrocarbon free radical to produce carbon dioxide, a smaller hydrocarbon, and hydrogen as a by-product. Equation 2.5 shows the undesirable though likely occurring condensation reactions between two hydrocarbon free radicals. This entire reaction sequence effectively reduces the formation of coke precursors and the undesirable aromatic-condensation reactions. The highest activation energy value in the previous reactions has been found in the range of 40-60 kcal/mol and corresponds to thermal cracking reaction (Trujillo-Ferrer, 2008). For this reason, Equation 2-1 is considered the rate-limiting step in this mechanism, and both Equations 2-1 and 2-2 are initiation reactions.

Therefore, in order to favour the occurrence of the catalytic steam cracking process, two main reactions must be favoured: the hydrocarbon cracking following either catalytically or thermally, and the catalytic water dissociation. The hydrocarbon cracking via thermal cracking is an endothermic reaction and it follows a free radical mechanism; it is thus favoured by an increase of the temperature. However, it can be improved by the incorporation of an acidic material, such as those in hydrocracking type of catalysts where the reaction follows the carbonium-ion mechanism like in conventional catalytic cracking. This kind of mechanism leads to the production of a large amount of branched paraffins. In the case of aromatic reactants, the carboniun-ion mechanism in the presence of hydrogen leads to the de-alkylation or saturation of the aromatic rings into

naphthene molecules (Flinn, et al., 1960).

On the other hand, the dissociation of water molecules is a key step in the production of the hydrogen required to avoid the undesirable condensation reactions. Therefore, it is important to understand the chemistry involved in the adsorption and dissociation of the water elements. The water molecule can be adsorbed on the catalyst surface creating a variety of species. The simplest pathways for water dissociation are adsorption and splitting into hydroxyl and atomic hydrogen or further splitting into atomic oxygen and atomic hydrogen (Thiel & Madey, 1987). This is illustrated in Figure 2-8.

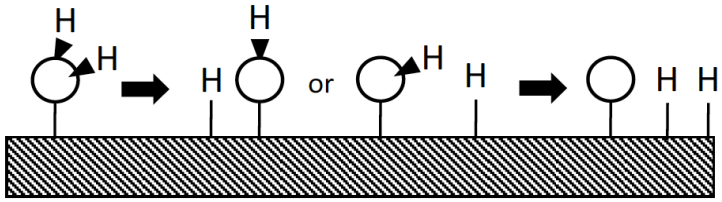

Figure 2-8 Pathway for dissociation reactions of adsorbed water **(Thiel & Madey, 1987)**.

The products and the stability of the products on the surface of the metal are controlled thermodynamically, which controls the products to either recombine to reversible liberate water or to stay stable as individual entities on the surface, leading to irreversible dissociation (Garcia-Hubner, 2015). Reversible water dissociation is typically observed on oxide surfaces, while irreversible dissociation is observed on metals and semiconductors (Henderson, 2002).

Overall, the CSC reaction mechanism depends on the type of material used as catalyst. Nevertheless, it has been reported that catalytic cracking reactions and water dissociation reactions do not compete for the same sites (Praharso, et al., 2004). Furthermore, the steam processing stage is original and has not been previously investigated for bio-crude feedstock processing to the best of the author's knowledge. And regarding catalyst formulations, for this specific application, it becomes original because they are a first of a kind for such application of bio-crude upgrading.

Chapter Three: Experimental Section

In this section, a description of materials, experimental set-ups, characterization methods, and procedures applied throughout this project are presented. The characterization of the Hydrofaction™ Renewable Crude Oil (bio-crude) provided by Steeper Energy for this investigation is presented in section 3.1. The description of the experimental set-up is given in section 3.2, and the description and methodology applied to run the experiments is given in section 3.3. The analytical methodologies employed for the samples characterization are presented in section 3.4.

3.1. Bio-crude Feedstock

The bio-crude-upgrading investigation performed throughout this thesis research project was carried out with the use of Hydrofaction™ Renewable Crude Oil. This is produced from Steeper Energy's lignocellulosic biomass conversion, via their proprietary supercritical hydrothermal liquefaction technology: Hydrofaction™. Information regarding the variability of biomass feedstock handled by Steeper Energy is not provided for this investigation, and thus the scope of this thesis work focuses on treating the bio-crude "as provided" by Steeper Energy. The bio-crude herein tested is described in Table 3-1, following the analytical methods described in section 3.4. The values are presented as ranges due to the biomass composition variability entering the Hydrofaction™ process, as discussed in section 2.2. Thus Steeper Energy does not guarantee that there is no variability in the composition of the produced and herein tested bio-crude, though they do guarantee to meet certain properties (i.e. oxygen content).

Table 3-1 Bio-crude feedstock properties.

Property	Bio-crude
Viscosity at 40°C, cP	6,500 – 23,150
TAN, mg KOH/g	51.0 – 52.6
Water content, wt.%	< 1
MCR, wt.%	20.49 – 20.96
Oxygen content*, wt.%	12.5
H/C molar ratio	1.34
O/C molar ratio	0.12
HHV^{+}, MJ kg^{-1}	36.9
Distillation Cuts, wt.%	
Naphtha, (IBP-190 °C)	2.4
Kerosene (190-260 °C)	6.9
Diesel (260-343 °C)	13.0
VGO (343-550 °C)	33.5
Residue (550+ °C)	44.2

*By difference from CHN analysis.
$^{+}$Calculated by the Dulong Formula, with the elemental composition from the CHN analysis.

To differentiate between the feedstock and the products throughout this thesis, the Hydrofaction™ Renewable Crude Oil feedstock is herein referred to as “bio-crude”, the product from the HDT process is named “HDT-bio-oil”, and finally, the product from the CSC process is named “CSC-bio-oil”. The term “bio-oil” may refer to the upgraded product, either HDT-bio-oil or the CSC-bio-oil.

3.2. The Continuous Bench Pilot-Plant Description

The bio-crude upgrading experiments performed to achieve the goals of the thesis were done on a bench scale pilot-plant unit. This unit was previously designed, constructed and placed in the laboratories of the Catalysts and Adsorption for Fuels and Energy (CAFE) research group at University of Calgary. This pilot-plant, named Catalyst Testing Unit 1 (CTU-1), was designed to evaluate small amounts of solid catalysts (between 1-10g) in a fixed bed reactor, under catalytic steam cracking conditions for a hydrocarbon feedstock. Catalytic steam cracking and thermal cracking reactions were performed in this unit prior to the beginning of the present investigation. Experiments at a temperature of 370 °C and a constant pressure of 400 psig with De-Asphalted Oil (DAO) produced from processing Athabasca Bitumen were performed by Garcia-Hubner (2015), and a thorough description of the design and construction of the CTU-1 was also reported. Upon the appointing of this pilot-plant to the present bio-crude upgrading investigation, an assessment of the unit was performed and modifications were made to accommodate this unit for the needs of the thermally unstable bio-crude oil to be treated. An overview of the modifications performed is found in Appendix I.

The Process and Instrumentation Diagram (P&ID) is presented in Figure 3.1; this pilot-plant unit can be divided into three main sections: Feed section, Reaction section, and Products Sampling section.

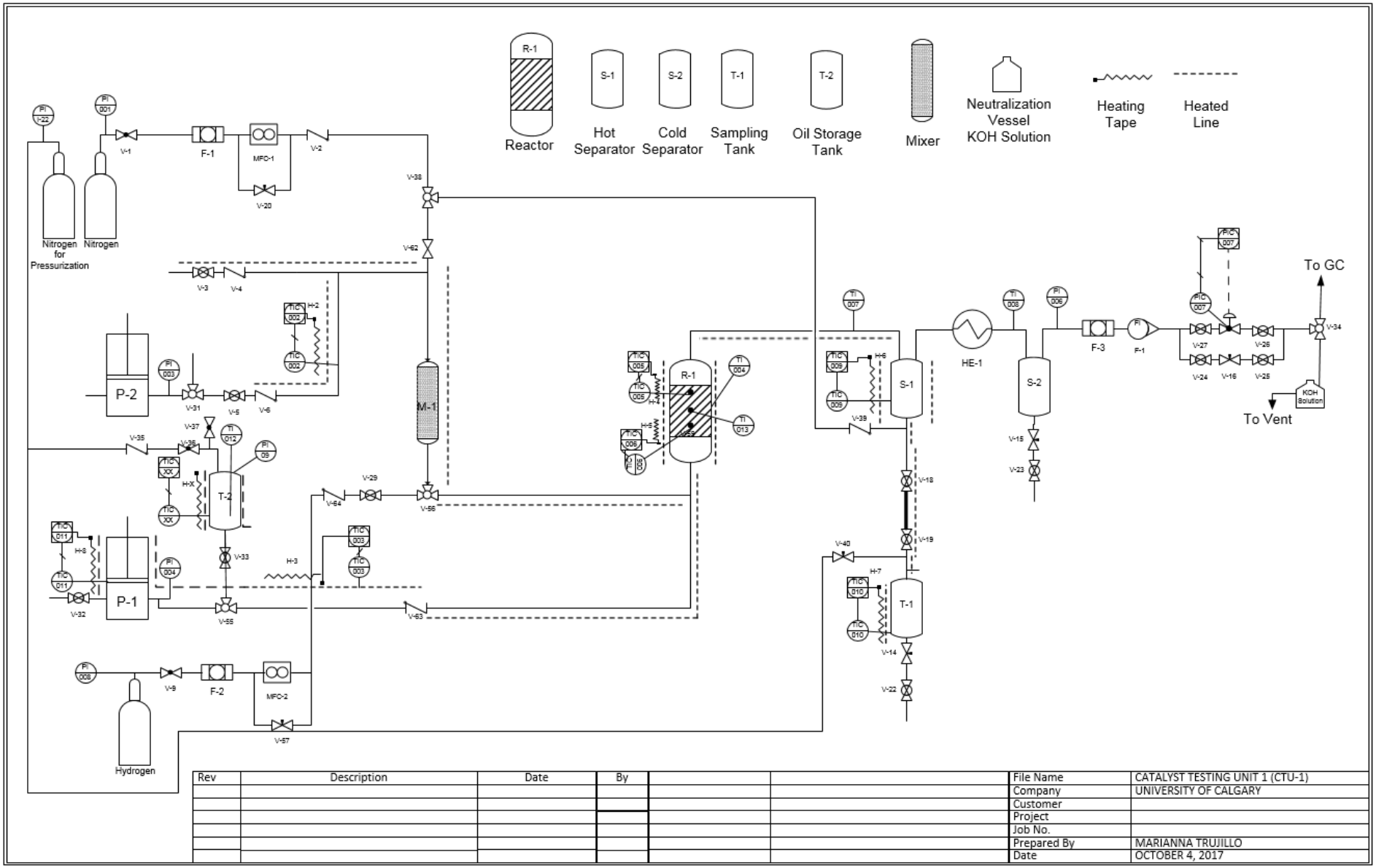

Figure 3-1 P&ID for CTU-1 pilot plant.

The Feed section prepares and handles the reactants such as the bio-crude for the HDT reaction, and/or the HDT-bio-oil and the water for the CSC reaction; this section contains two inlets for liquids and two inlets for gases. One of the two liquid inlets is used to flow the bio-crude oil, or any other type of hydrocarbon, by means of a pump named P-1 (500D Syringe Pump-Teledyne Isco) that is constantly heated and it is supplied with the content in the storage tank T-2. The heating of T-2 is controlled, monitored, and carried out in the presence of nitrogen. T-2 is heated only when required for filling up the pump, and a variable autotransformer (Staco Energy) is employed for controlling the current sent to the heating tape. The second liquid inlet is used for water as a reactant only required for CSC reactions; water is pumped into the system with P-2 (500D Syringe Pump-Teledyne Isco). The water pumped into the system by P-2 is initially heated up to its respective saturation temperature, in order to obtain the required phase change. The saturated vapour then passes through a steam generator or mixer (M-1); this consists of a 5 cm long tube of 0.95 cm (3/8'') diameter filled with glass beads that generate tortuosity and surface area, thus ensuring uniform steam generation. The resulting steam is then blended with the bio-crude oil at the desired ratio of 5 wt. % water and the blend enters the reaction section. The gas inlet is modified to accommodate each experiment's requirements. For HDT, hydrogen is required as a reactant whereas, for CSC, nitrogen is used as carrier gas. Furthermore, both hydrogen and nitrogen are used during catalyst activation operations mentioned in section 3.3 below. The required gas is introduced into the plant by means of two SLA5850 Brooks Mass Flow Controllers (MFC-1 of 30 Std. ml/min for nitrogen, and MFC-2 of 200 Std. ml/min for hydrogen).

The Reaction section consists of an up-flow stainless steel tubular reactor with 1.27 cm (1/2'') of external diameter and with 0.089 cm (0.035'') wall thickness. Regarding the temperature controls of the reactor, and based on previous empirical assessments of the system, it was determined that

two heating tapes of 1.27x5.08 cm (0.5x2.0'') were required to develop a 12.7 cm isothermal zone suitable to accommodate a catalytic bed, as illustrated in Figure 3-2 below. Each heating tape is controlled with wall thermocouples located alongside the thermocouple points 1 and 3, respectively. The internal temperature at these points was measured with a profile Omega probe of 0.32 cm (1/8'') diameter, placed inside the reactor with three measurement points separated by 6.35 cm. The three points along the length of the reactor allow for controlling and monitoring the temperature profile of the catalytic bed. Furthermore, a homogeneous temperature profile has been possible for every experiment with some physical manipulation and adjustments of the two heating tapes.

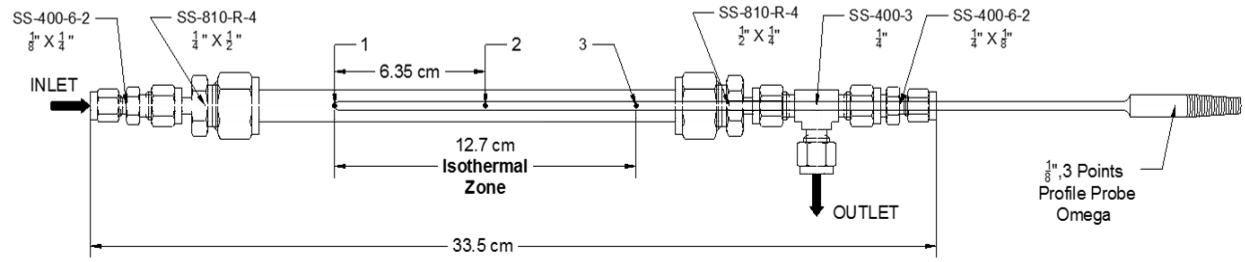

Figure 3-2 Reactor assembly, adapted from Garcia-Hubner (2015).

Depending on the experiment, whether it is to be a catalytic reaction or a thermal one as described in Chapter 4, the packing of the reactor will vary with either the presence of a catalyst or an inert material (i.e. carborundum), respectively. Nevertheless, the packing at the bottom of the reactor, from the inlet to the isothermal zone, and at the top of the reactor, from the end of the isothermal zone to the upper fittings, is consistent for both thermal and catalytic reactions. Therefore, the zones prior to and after the isothermal zone are filled with carborundum to hold the packed-bed; prior to the isothermal zone, the carborundum favours the preheating of the reactants and the development of a uniform flow pattern; after the isothermal zone, the carborundum avoids the

upward movement of the bed due to the pressure of the system. Furthermore, a layer of quartz wool is placed at the beginning and at the end of the reactor tube. The quartz wool helps to avoid any solids from the reactor packing to travel along the pilot plant's lines; also, to keep the catalytic bed in place, a layer of quartz wool is added between the carborundum and the catalyst.

The Product Sampling section manages the products of the reaction, allowing for the collection of produced bio-oil samples without interrupting the continuous operation of the pilot-plant system. The reaction's products are in the form of liquid and gas products. Upon exiting the reactor, the products go to a hot separator (S-1), therein the water and light hydrocarbons in the gas phase are separated (boiling < 225°C at 400 psig) and removed from the heavier hydrocarbons liquid fraction. Bubbling of nitrogen as a carrier gas through the bottom of S-1 assists in this phase separation. Gases and light hydrocarbons are bubbled up and out of S-1 through to a cold separator (S-2). A shell and tube heat exchanger fed with water at 5 °C acts in the line between S-1 and S-2 to favor the condensation of light hydrocarbons and water in the stream. The condensed product is accumulated in S-2, whereas the gas passes through the backpressure system, working with a Swagelok manual backpressure valve. Finally, product gases (i.e. gases produced in the reaction, and the carrier gas fed into the S-1 system) flow through to a three-way valve, where the flow can follow through to either a Ritter wet flow meter for quantification, followed by the vent, or a line connected to the GC for composition analysis. The remaining heavy product fraction in S-1 is transferred into a sampling tank (T-1) through two consecutive automatic valves (V-18 and V-19) working alternatively with a designed volume between them. This valve system prevents a significant pressure drop to occur and avoids any alteration to the continuously operating experiment. At a determined time, the top valve V-18 opens and the sample drops to fill the volume between V-18 and V-19, after certain time V-18 closes, and then the bottom valve V-19 opens to

allow the liquid product to flow into the sampling tank T-1 at operating pressure. After a determined time, this bottom valve V-19 closes and the cycle is repeated after a specified period of time. Every operation of this system generates a pressure drop typically of about 3 psig, which is quickly recovered by generated product gases and the bubbling nitrogen gas. Once the product is in the sampling tank, it can be easily collected through the valves V-14 and V-22. The time selected for the automatic operation of the double valve system is assigned depending on the bio-crude feedstock flow rate. The light condensed fraction (i.e. light hydrocarbons and water) is collected from the cold separator by means of two manual valves, V-15 and V-23, which are operated manually. This light fraction is collected at the same time as the end of the V-18-V-19 cycle depicted above for the heavy fraction; this allows for accurate mass balance calculations.

Therefore, the CTU-1 unit allows for measuring product flow and hydrogen gas flow as performance metrics; it also allows for the monitoring of parameters such as temperature and pressure in order to ensure overall process stability, and thus the collection of reliable data. Finally, and as described above, this bench scale pilot plant enables the collection of heavy and light liquid product samples during the continuous operating mode; this allows for the determination of mass balances to characterize the samples for oil quality, deemed a very important performance metric.

3.3. Operating Procedures

Depending on the process under investigation (i.e. HDT or CSC) in each experiment, the operating procedure varies slightly. However, prior to each process start-up, there are two previous steps that are common for both HDT, and CSC: reactor assembly, and catalyst activation.

Reactor assembly takes place prior to each experiment as a preparation step for the operating of the pilot-plant. The reactor assembly is a critical step and is performed carefully, given that reproducibly of results relies to some extent on the packing of the bed. Therefore, following the schematics presented in Figure 3-2, a small amount of quartz wool is inserted through the tube and placed at the end of the reactor arrangement (i.e. the end towards the exit of the reactor). Then, carborundum is added to the reactor until reaching the isothermal zone. At this point, a layer of quartz wool is incorporated before proceeding to fill the isothermal zone with the catalyst. In the case of thermal runs, the section depicted as "reaction zone" or "isothermal zone" is filled only with carborundum. Once a known mass of catalyst is added, another quartz wool layer is placed and the remaining void of the reactor is then filled with carborundum. A final layer of quartz wool is placed to ensure a successful packing of the bed, and finally, the reactor fittings are tightened up. The known mass of catalyst loaded into the reactor, together with the oil mass flow rate to be used for each specific experiment, allow for the determination of the Weight Hourly Space Velocity (WHSV) in h^{-1}. This is calculated by means of the Equation 3-1. The inverse of the WHSV provides the contact time between the oil and the catalyst in the reactor.

$$WHSV = \frac{oil\ mass\ flow\ rate}{mass\ of\ catalyst} \qquad Equation\ 3-1$$

Catalyst activation takes place upon the successful mounting of the assembled reactor onto the pilot plant, and leak tests are performed at 100 psig over the process operating pressure for 24

hours, constantly looking for leakages with Snoop Liquid Leak Detector from Swagelok, to guarantee that there are no leaks in any of the connections assembling the CTU-1. Depending on the process to be evaluated, whether it is HDT or CSC, different catalysts are employed. Nevertheless, these catalysts require some of their elements to be in metallic form; this is achieved by treating the catalysts with a flow of hydrogen under a temperature high enough to produce the reduction of the oxide species. These temperatures can vary from one catalyst to another; however, by previous testing of these solids, all of them proved to be reducible at 500°C (Vitale, et al., 2011). Therefore, a temperature of 500^{o}C along the reactor is selected to proceed with the activation. The complete explanation for the preparation and activation of the catalysts herein employed is well described by Vitale *et al.* (2011) and Moraes-Righi (2016), respectively. Dr. G. Vitale synthesized and prepared the catalysts for both HDT and CSC processes in this investigation.

3.3.1. HDT Operations.

Following the previously described reactor assembly and mounting, pilot plant leak test, and catalyst activation, the first stage of the Hydrofaction^{TM} Renewable Crude Oil upgrading process herein investigated is HDT. The pilot plant start up procedure for HDT begins with heating up the remaining cold sections of the pilot plant: the bio-crude line from P-1 to the reactor, which is heated to a temperature hot enough for the bio-crude to flow (< 100 ^{o}C) taking into consideration the oil's thermal instability and tendency to polymerization reactions; also the hot separator is heated by H-6, reaching a wall temperature of 290°C when operating at 900 psig, to allow for the water separation from the heavy products; lastly, the sampling tank (T-1) and pump P-1 are heated (90 ^{o}C) with H-7 and H-8 respectively, to keep the oil at low viscosity and guarantee the quality of the mass balances. After the pilot-plant has reached the established operating temperatures, the backpressure valve is set at the operating pressure and the system is pressurized by means of a

needle valve V-57 that bypasses MFC-2. Once the chosen pressure is established, MFC-2 is set to a hydrogen flow-rate depending on the operating H_2-to-oil ratio intended for the HDT process. The exploration of different variables' effect on the HDT process, including tests for different H_2-to-oil ratios, is presented in Chapter 4. Then, the system is left to stand at these conditions allowing it to reach stabilization of the gas flow rate, in order to measure the precise amount of hydrogen fed into the system. Finally, the bio-crude flows into the feed section lines through to the reactor and the hot separator S-1 at 25 ml/min to guarantee that the lines are flooded with the oil; and lastly, the intended operating bio-crude oil flow rate is adjusted.

3.3.2. CSC Operations.

The overall operation of the CTU-1 is very similar for CSC and HDT. However, the start-up procedure is different, given that in CSC water is introduced as a source of hydrogen.

Comparably to HDT, after the catalyst activation procedure is completed the remaining cold sections of the pilot plant are heated up to their respective temperatures. However, in CSC, the feed section containing the water line must be heated to a required temperature enough to guarantee the generation of steam (i.e. internal temperature of 225^{o}C when operating at 400 psig, calculated by the Clausius-Clapeyron relation). The oil-feedstock line is heated similarly to HDT; also the hot separator is heated externally up to 270°C when operating at 400 psig with H-6 to allow the water separation from the heavy products; also the sampling tank (T-1) and pump P-1 are heated (90 ^{o}C) with H-7 and H-8 respectively, to keep the oil at low viscosity and improve the quality of the mass balances in the case of T-1.

Once all the pilot plant's lines are heated as required for the experiment, the backpressure valve is set at the operating pressure and the system is pressurized by means of a needle valve that bypasses MFC-1. Once the chosen pressure is established, MFC-1 with a flow of nitrogen is set to the

selected flow rate to operate as bubbling and carrier gas in S-1. The system is left to stand at these conditions allowing it to reach stabilization of the gas flow rate, in order to measure the precise amount of nitrogen fed into the system. After the nitrogen flow rate is properly measured, the water pump is set to pump 25 ml/min for a period of time; the objective is to flood all the lines in the feed sections, reactor, and all the way to the sampling tank (T-1). Once the system is filled with the generated steam, the catalyst in the reactor is pre-treated with steam at reaction temperature with a water flow rate of 1 ml/min to initiate the water splitting reaction anticipated to occur in the CSC process. Finally, the HDT-bio-oil feedstock (i.e. bio-oil produced from the HDT process) flows through the feed section lines, to the reactor and finally T-1 at 25 ml/min to guarantee that all the lines are flooded with the oil, and lastly the operating feedstock flow rates are adjusted in P1 and P2, respectively.

Ultimately, in order to proceed with the continuous operation of the experiments, either HDT or CSC, both T-1 and S-2 are drained from any oil and or water that may have reached these sections by the previous flooding of the system. Once this is done, the cycle for the automatic operation of the two consecutive valves (V-18 and V-19) that transfer oil to the sampling tank T-1 is activated and this time is defined as “time-zero”, beginning of the experiment.

3.4. Analytical Methods

The liquid and gas products obtained during the experiments performed were analyzed to fully characterize their properties and allow for a thorough understanding of the effect of varying operating conditions in each experiment. In this section, the analytical methods employed to characterize and thus evaluate the produced bio-oil and gas properties are listed and explained.

3.4.1. Water Content by Coulometric Karl Fischer Titration.

Although the heavy products are separated from water and light material (boiling < 225°C at 400 psig, or < 270°C at 900 psig) in the hot separator, a small fraction of water remains in equilibrium with the heavy oil fraction. A successful water separation is achieved when the amount of water in the liquid oil product does not exceed 1 wt. %. Therefore, it is necessary to determine said water content in order to evaluate the separation process, and account for any water present during the characterization of the final bio-oil products. The water content analysis is performed with a Mettler Toledo C20 Coulometric KF Titrator. The analysis is carried out following the procedure proposed by Carbognani *et al.* (2014): three blank measures of a weighted aliquot of tetrahydrofuran (THF) are injected into the titrator containing Aqua Star® Coulomat A, provided by EMD – this step provides the blank value or the initial amount of water existing in the solvent (THF) which is used in the preparation of the samples. Subsequently, a solution of 0.4 g of oil sample diluted in 8 to 10 g of THF, both weighted to the nearest 0.0000 g, are prepared in a 20 mL vial, this is then manually shaken to promote the mixing. Finally, small weighted aliquots of the solution are injected into the titrator - this step is repeated three times per sample to test for reproducibility in the results. With the weight of the sample, the weight of the THF solvent, and

the initial amount of water in the THF solvent, the water content in the sample is calculated by material balance (Carbognani, et al., 2014)

3.4.2. Total Acid Number.

Total Acid Number (TAN) is a measure of the potential corrosivity of crude oils. It is defined by the amount of potassium hydroxide required to neutralize the acids in one gram of oil. Therefore, the TAN is expressed in terms of milligrams of potassium hydroxide per gram of oil (mg KOH/g) and it is not specific to a particular acid but it is supposed to refer to all possible acidic components in the oil (Speight, 2014). Oils with a TAN >1 mg KOH/g are considered corrosive and labeled as High-TAN oils (Schaschke, 2014). TAN is herein measured by following the titration methodology described by the norm ASTM D664. The titration was performed with a T70 Titration Excellence apparatus provided by Mettler Toledo, using a titrant solution of 0.1 M potassium hydroxide (KOH) in 2-propanol. Also, a solvent solution (50% v/v toluene, 45% v/v 2-propanol, 5% v/v water) is used for the dilution of oil samples. The solvent solution is also measured as a blank value; this is always measured prior to sample determination in order to set a baseline, and thus not have the solution acidity accounted for twice (ASTM-D664, 2011). The analysis is usually carried out with 1 gram of oil sample weighted in a titration vessel, then diluted with 60mL of solvent solution, and placed on an auto-sampler tray. The electrode, titrant solution dispenser, and mixer are placed inside the titration vessel. Sample amounts can vary from about 0.2 to 5.0 g, depending on the TAN values (i.e. > 30 to < 0.2 mg KOH/g). Once the system starts pumping titrant solution, the titration is potentiometrically monitored with the electrode and the inflection point determines the solution acidity. The final total acid number depends on the blank value and the mass of oil titrated. The TAN for a sample is determined using the titrant volumes used for sample and blank (V_s and V_b, in mL), the concentration of titrant solution (C_{KOH}, in

mol/L), and KOH molecular weight (MW_{KOH}, in g/mol), as shown in Equation 3-2. The TAN conversion (or reduction), expressed as X_{TAN}, can be calculated by Equation 3-3, using the TAN of the oil sample and feedstock. The relative error for this measurement is 20% for TAN <1 mg $_{KOH}$/g, with an improvement to 10% or better as higher TAN ranging 1 to 5 mg $_{KOH}$/g is measured, and further improvement to 3% or better for TAN for values as high as 50 mg $_{KOH}$/g.

$$TAN = \frac{(V_S - V_b)\ x\ C_{KOH}\ x\ MW_{KOH}}{W_S} \qquad Equation\ 3-2$$

$$X_{TAN} = 1 - \frac{TAN_S}{TAN_F} \qquad Equation\ 3-3$$

3.4.3. Viscosity.

Dynamic Viscosity is measured to determine the bio-crude and produced bio-oil's resistance to flow when an external force is applied. Therefore, the dynamic viscosity was determined using a Brookfield model RVDV-II+PRO viscometer with a relative error of ± 5%. Also, Brookfield TC-502 bath is used to set the temperature for the viscosity measurement. Due to the high viscosity of the bio-crude feedstock, and the herein produced bio-oil, a temperature of 40^{o}C was selected for all viscosity measurements. After temperature stabilization, a gap of 0.1 mm between the sample cup and the spindle is adjusted. The liquid sample is then placed in the viscometer cup and in contact with the spindle; once the desired temperature is reached, the spindle rotation is applied and manipulated until a torque value between the 40 to 70% range of the maximum 0.7187 milli N/m is achieved. To homogenize the sample film, the rule of thumb is allowing 5 revolutions to occur prior to taking the reading. The dynamic viscosity of these samples is then read in cP at 40^{o}C, and viscosity reduction was calculated throughout this thesis using Equation 3-4.

$$Viscosity\ Reduction = 1 - \frac{\mu_s}{\mu_f} \qquad Equation\ 3-4$$

3.4.4. Thermogravimetric Analysis (TGA).

Production of physical distillation cuts in laboratories is routinely performed through the use of systems able to mimic the performance of distillation towers found in refineries (ASTM-D2892, 2011). However, a faster, less labour intensive and less expensive technique is herein employed by the use of Thermogravimetry Analysis (TGA). Although TGA has been proposed as a feasible technique for determining evaporation rates (Zingjie, et al., 2006) and boiling range distributions (Huang, et al., 1996) (Schwartz, et al., 1987), TGA curves do not match the whole distillation curves provided by standard methods (ASTM-D5236, 2011; ASTM-D2892, 2011). Therefore, TGA is herein used to obtain an approximation of the different cuts composing the liquid bio-oil produced and thus, it represents an idea of the characteristics of the product. Nevertheless, a more reliable technique capable of matching said distillation curves provided by standard methods is also employed, and it is presented in subsection 3.4.5 below. However, the use of the latter is restricted to specific samples of certain characteristics (i.e. TAN < 9 mg $_{KOH}$/g $_{oil}$, oxygen content < 4 wt. %), whereas TGA may be used to analyze any sample of bio-oil produced.

TGA consists of analyzing the weight and heat changes experienced by a solid or liquid sample when it is submitted to an increase in temperature under the flow of a gas. The equipment used was a DT Q600 system from Thermal Analysis Instruments Company. The oil sample (25 mg) is heated at 10°C/min up to 800 °C in the presence of nitrogen flow at 100 Std. mL/min. The results produce a curve plotting Sample Remaining Weight % vs. Temperature. Also, differential mass loss, heat flow, and differential heat flow can be simultaneously determined.

3.4.5. High Temperature Simulated Distillation.

The High Temperature Simulated Distillation (HTSD), also referred to as SimDist, is another alternative method to the time-consuming, laboratory-scale physical distillation (ASTM-D2892, 2011; ASTM-D5236, 2011) previously mentioned. The SimDist methodology herein employed proceeds as described by Carbognani *et al.* (2013): 1µl of a solution containing 0.15 g of oil sample in 20 ml of CS_2 is injected into a nonpolar chromatography column placed inside a temperature-programmed oven; Hydrocarbons in the column are separated by boiling points, detected, and quantified at the exit of the column by a flame ionization detector (Carbognani, et al., 2013). By running reference n-alkanes, the chromatographic response was calibrated to obtain a result equivalent to the atmospheric boiling point of the sample aliquots. According to the literature, it has been found that HTSD is able to determine fraction boiling points up to 3 ^{o}C errors and is able to reproduce fraction yields with standard deviations around 0.5% (Raia et al., 2000). Alternatively, errors of 1% have been reported for samples with a boiling point below 550 ^{o}C and of 4% for heavier fractions (Rodriguez-DeVecchis et al., 2015). Lastly, a crude oil can be analyzed to temperatures up to 720 °C equivalent, with a weight standard deviation below 2% (Raia, et al., 2000). Through a SimDist curve, the cut composition of an oil can be determined and, throughout this thesis, the oil fractions and respective boiling point followed the ranges previously shown in Table 3-1, where the bio-crude feedstock's properties used are represented. The calculations for residue conversions (X_R) are also based on SimDist data and follow Equation 3-5, in which R is the residue content in the sample, i.e. the oil fraction with a boiling point above 550 ^{o}C.

$$X_R = 1 - \frac{R_s}{R_f} \qquad Equation\ 3-5$$

The equipment herein employed for the HTSD analysis of liquid samples is an Agilent Technologies Gas Chromatograph, model 7890-A working under conditions described in ASTM-D7169-2005. Chromatograms were analyzed with the software SimDist Expert, from the company Separation Systems Inc.

3.4.6. CHN Elemental analysis.

The elemental analysis for carbon, hydrogen, and nitrogen is conducted at the University of Calgary, by Mr. Johnson Li in the Department of Chemistry Instrumentation Facility. The instrument employed is a Perkin Elmer 2400 CHN Analyzer. In the CHN instrument, the sample drops into a high temperature (1,000 ^{o}C) combustion tube loaded with an oxidation catalyst. The sample combusts fully into CO_2, H_2O and NO_X gases. Then, these gases go through a reduction tube where NO_X is reduced to N_2, and this continues passing through a separation column where it is finally detected by a TCD detector. With a standard chemical as the reference, all three elements content (i.e. carbon, hydrogen, and nitrogen wt. %) can be determined. The oxygen content is calculated by difference of the former three elements, since the sulfur content for bio-crudes is negligible.

The HHV of the bio-crude and the HDT-bio-oil was determined using the Dulong formula presented in Equation 3-6.

$$HHV = 0.3383C + 1.443\left(H - \left(\frac{O}{8}\right)\right) + 0.0942S \ \ (MJ\ kg^{-1}) \qquad Equation\ 3-6$$

3.4.7. Micro-Carbon Residue.

Micro carbon residue (MCR) is a laboratory test used to provide some indication of a material's coke-forming tendencies. Herein, the remaining material after the bio-oil has been thermally treated is an indication of the tendency of said oil to form coke. Three well-known standard methods are commonly used to evaluate a material's coke-forming tendency: the Conradson method (ASTM-189); the Ramsbotton method (ASTM-524); and the Micro-carbon residue method (ASTM-4530). These methods differ on their experimental setup, conditions, and amount of sample, but they share the same principle: the difference between the final and initial mass of sample after heating under controlled conditions indicates the amount of residue present. The advantage of the modified Micro-carbon residue method (ASTM-4530) used in our laboratory, against the other methods, is the small amount of sample required to perform the test (Hassan, et al., 2008). This method employs a Barnstead Muffle furnace with a temperature controller. Inside the furnace, a metal tray with a diameter 10.12 cm is placed, and this contains 26-sorted vertical openings measuring 1/8'' in outside diameter and 3/4'' in length. Said vertical openings allow gas (i.e. nitrogen) to flow through. A glass cover is placed on top of the tray to create a nitrogen chamber when said gas flows through the openings of the tray, and the initial oxygen in the environment is purged via a 1/8" orifice located on top of the glass cover.

The procedure consists of weighting approximately 20 mg of sample into a 2 mL glass vial and placing it on the surface of the metal plate. Each sample is analyzed in duplicate. A standard oil sample of a known MCR value is included amongst the samples analyzed in order to evaluate for the reliability of the analysis. Once the samples are placed in the metal tray, the system is covered with the glass lid and the nitrogen flow is set at a flow rate of 900 ml/min, at room temperature and atmospheric pressure conditions. After 45 min of purging the oxygen from the system, the

furnace is turned on to reach a temperature of 500 °C at 10°C/min, then kept at this temperature for 20 minutes. Once the system has reached the desired temperature, it goes through a natural cooling in a nitrogen environment. After reaching room temperature, the vials are removed from the furnace to determine the final weight. Finally, the determination of the amount of residue or coke formed is done by calculating the weight difference with a relative error of 2%.

3.4.8. Gas analysis.

The gases generated during reaction tests were analyzed in a Gas Chromatograph (GC) to identify their volumetric/molar compositions. Connected to the exit of the CTU-1, an SRI multiple gas analyzer model 8610C with Multiple Gas #3 configuration was used. To separate the gas mixture by components, the chromatograph uses a packed molecular sieve 13X column (MS13X) of 183 cm (6'), one fused silica (HAYESEP-D) column of 183 cm (6') and a capillary column (MXT®-1) of 60 m. The system was calibrated using standard calibration gases with known and certified compositions. The relative errors between the certified composition and the composition obtained are presented in Table 3-2. For this project, hydrogen, CO, CO_2, and hydrocarbon from C1 to C5 were analyzed using the TCD at low gain for the amplifier and helium as a carrier gas.

Table 3-2 Relative error for gas composition determination

Component	Relative Error (%)	Component	Relative Error (%)
H_2	3.6	Propene	0.6
Methane	0.9	Propane	0.9
CO	0.4	iso-butane	3.7
CO_2	0.3	1-butene	3.0
Ethylene	0.4	n-butane	1.5
Ethane	0.3	iso-pentane	5.7

3.4.9. Fourier-transform Infrared spectroscopy.

Fourier-transform Infrared (FTIR) analysis is used to determine the chemical footprint and main functional groups present in both, the bio-crude and the produced bio-oils. IR spectra were run with an IRAffinity-1S spectrometer from Shimadzu. A CaF_2 cell was used for spectra acquisition of liquid samples. A total of 20 scans per run were acquired at a resolution of 4 cm^{-1}. General IR band assignment was based on well-known monograph (Silverstein, et al., 2005).

The sample preparation method was designed in-house to achieve the quantification of the functional groups of interest present in the samples. 150 mg of oil sample are dissolved in carbon tetrachloride (i.e. CCl_4) to the mark in a 20 mL Erlenmeyer flask. CCl_4 is selected as solvent because it is transparent in the 1000 to 4000 wavelength range, so it does not interfere with peaks of interest, also the solvent provides better signal resolution for diluted samples resulting in lesser overlaps. A CaF_2 liquid cell is filled with the prepared solution, and the sample is ready for spectra acquisition.

Chapter Four: HDT – CSC Upgrading Process Evaluation

This chapter presents the investigative process developed throughout the exploration of HDT and CSC as bio-crude upgrading processes. Each process is evaluated separately, beginning with HDT presented in Section 4.1. A screening of HDT variables was performed in order to acquire an essence of the HDT effect on the bio-crude. The quality of the hydrotreated bio-oil was evaluated in terms of total acid number (TAN), viscosity, micro-carbon residue (MCR), and oxygen content. Consequently, suitable operating conditions were defined for the production of HDT-bio-oil to be further processed following the second stage of this investigation: the CSC of the hydrotreated bio-crude oil. This is presented in the second half of this chapter, Section 4.2. Again, the exploration of main variables was evaluated, depicting the dependence of this process on the previously hydrotreated feedstock.

4.1. Hydrotreating (HDT) Process

Throughout this section, the investigation pertaining the first stage of the overall HDT-CSC upgrading process applied to Steeper Energy Hydrofaction^{TM} Renewable Crude Oil is presented. The pilot plant, operating procedures, and analytical methods described in Chapter 3 of this thesis were employed throughout the evaluation of catalytic and thermal HDT reactions of bio-crude. Herein, the main process variables exploration is described, and the results obtained during the course of this research are presented.

The catalytic experiments were performed using an original hydroprocessing catalyst. Along the experimental development, the catalyst formulation was progressively modified to enhance the catalyst's hydrogenating function. The HDT catalyst is synthesized by and provided for this investigation by Dr. G. Vitale, a specialist from the CAFE research group. The catalyst for HDT

is deemed original, not only in the manufacturing of highly hydrogenating active phases containing highly dispersed molybdenum carbide but also in the combination of two original hydrotreating and acidic-hydrogenating solid formulas. Further details on the catalyst cannot be provided to secure patentability of the formulas.

The produced HDT bio-oil was fully characterized in order to identify suitable operating conditions able to hydrotreat the high oxygen containing bio-crude, reducing the acidity the most, counterpartying with the oxygen content reduction via hydro-deoxygenation reactions. Furthermore, a thermal reaction was carried out in order to compare and assess the effect of catalytic behaviour on product quality. The main reactions that are expected to take place thermally or catalytically in the reactor during the HDT process were discussed in Section 2.4.1; the reactions occurring throughout the hydro-deoxygenation process of interest are presented in Figure 4-1 below. In addition, reverse water gas shift and methanation reactions are expected to take place, though these are considered undesirable side reactions.

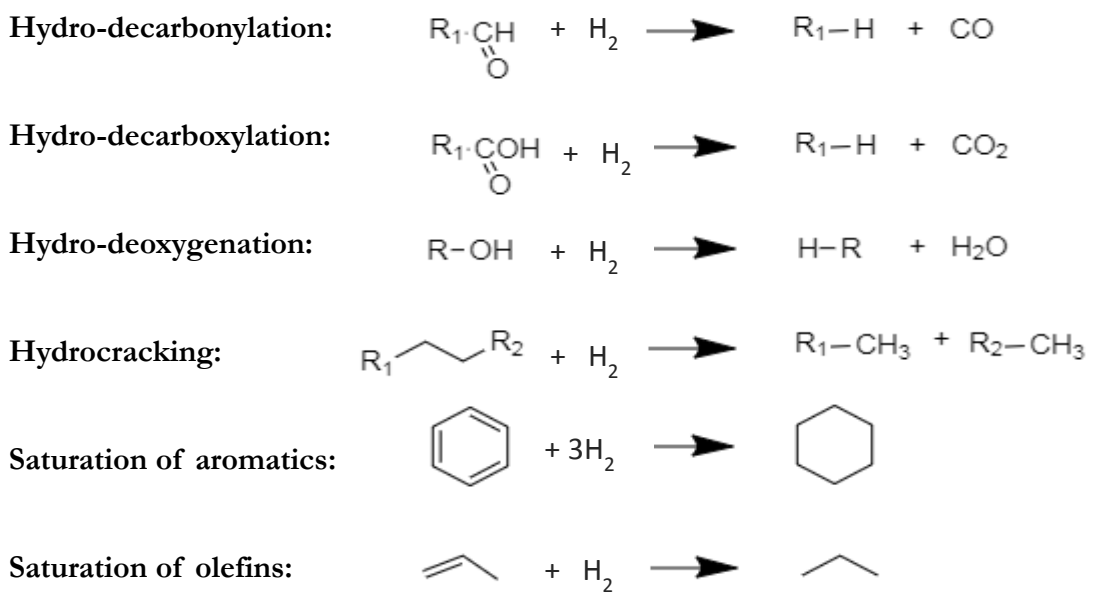

Figure 4-1 Common reactions occurring in HDT processes, adapted from Wildschut et al. (2009).

Though the desired reactions are known, due to the molecular complexity of the bio-crude and the products, the effectiveness of the HDT process is evaluated by the physical and chemical properties of the produced hydrotreated bio-oil. For instance, the hydrotreating of the bio-crude via hydro-decarboxylation of carboxylic acids present in the feedstock can be tracked by measuring the TAN reduction on the products in relation to the feedstock, and MCR indicates changes in the tendency to form carbonaceous material when products are submitted to further processing. In addition, tracking viscosity reductions can assess cracking reactions of any heavy molecule, and this is crucial information as cracking reactions are not the objective in this first stage of the overall upgrading process. Also, a comprehensive understanding of the products' properties on catalytic and thermal reactions is imperative to understand the benefits of using a selected process and selected operating conditions.

4.1.1. Experimental Results.

A thorough screening of different variables operating the HDT process was performed to evaluate the effect that each operating condition had on the HDO reactions desired for the highly oxygenated bio-crude feedstock. The parameters evaluated were Temperature, Weight Hourly Space Velocity (WHSV), Hydrogen-to-oil ratio, and Pressure. Each variable had a different effect on the quality of the produced oil, in terms of degree of hydro-deoxygenation monitored by water production, total acid number reduction by hydro-decarboxylation and carbon dioxide production, effects on viscosity and micro carbon residue. Overall, the study presented in this section allowed for an overview of HDT operating conditions to produce a HDT-bio-oil for the subsequent CSC upgrading process also investigated.

4.1.1.1. Temperature Effect.

Severe HDT via HDO reactions of biomass-derived oils have been previously investigated at temperatures between 250 and 450 ^{o}C (Venderbosch, et al., 2010); however mild HDT reactions are carried out at lower temperatures to prevent hydrocracking reactions. Therefore, the screening of temperatures herein performed covered a range between 180 and 310 ^{o}C. The primary objective discussed in this section has been to evaluate the effect of temperature on TAN reduction of the bio-crude, while monitoring viscosity and MCR to the extent of avoiding extensive cracking of the material.

The thermal instability of the highly oxygenated components in the bio-crude is a cause of continuous polymerization reactions if these are not hydrotreated as the bio-crude oil is heated. Thus, a temperature range between 180 and 200 ^{o}C became problematic as constant plugging prior to and in the reactor occurred. To proceed with the study, a pre-heating zone prior to the reactor with a temperature enough for the oil to flow (i.e. 100 ^{o}C) was implemented; this is the zone where the bio-crude flows upwards prior to entering the reactor. Then, an increase in the reaction temperature (i.e. above 200 ^{o}C) allowed for the continuous operation without plugging problems to proceed.

Stable operating conditions, where no plugging occurs, allowed proceeding with the investigation of the temperature effect on the TAN and viscosity of the bio-crude, in the presence of a catalyst. Results are presented in Figure 4-2.

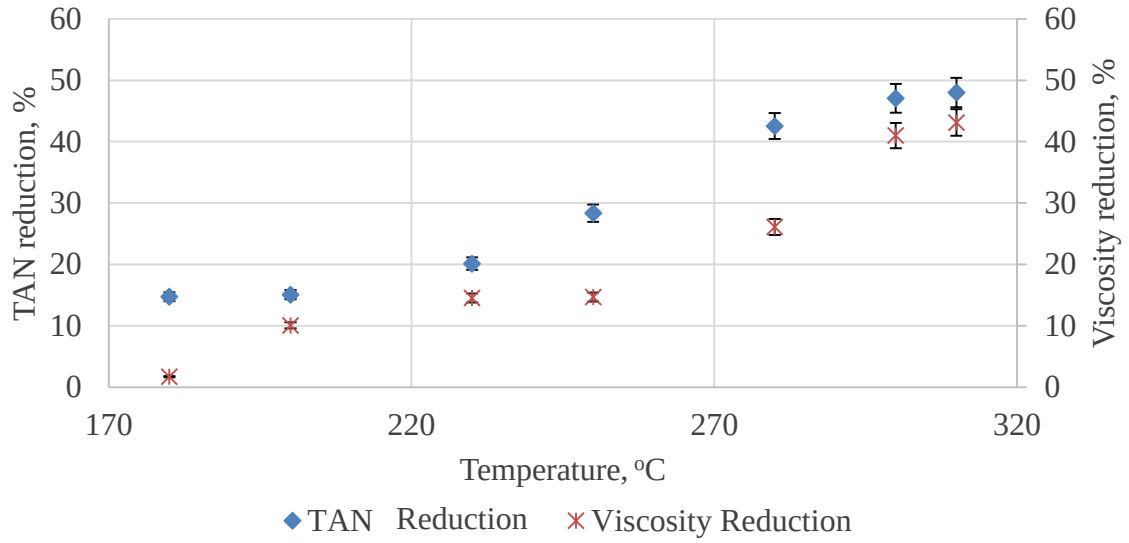

Figure 4-2 Effect of temperature on the quality of the hydrotreated oil (900 psig, 0.4 h^{-1}).

The viscosity reduction observed in Figure 4-2 is not significant in the lower temperature range between 180 and 230 ºC as cracking reactions are not expected to occur. However, as more severe conditions are tested, the possibility for cracking of the molecules increases and thus viscosity decreases. The reduction in viscosity becomes a route to achieve homogeneity of the hydrotreated oil, which is required for repeatability of analytics throughout the characterization of the produced oil and for consistency of product quality. Also, a reducing tendency of the oil to produce coke was observed as MCR values were found to decrease majorly as temperatures reach 300 ºC (20.9 % reduction relative to MCR of in bio-crude), and not as much at lower temperatures below 250 ºC (5.6 % reduction).

Furthermore, as seen in Figure 4-2, an increase in temperature to 310 ºC was found to contribute to TAN reduction of almost 50%. The correlation shows a minimum TAN reduction of 15% within the lower temperature range (i.e. 180 – 220 ºC); then, as temperature increased so did TAN conversion, until reaching temperatures around 300ºC where the increment in TAN conversion was not as pronounced, and remained close to 50% conversion.

The gas analysis provides valuable information regarding the level of HDO as well as undesirable side reactions and cracking reactions. The gas products distribution for the studied temperatures is presented in Figure 4-3.

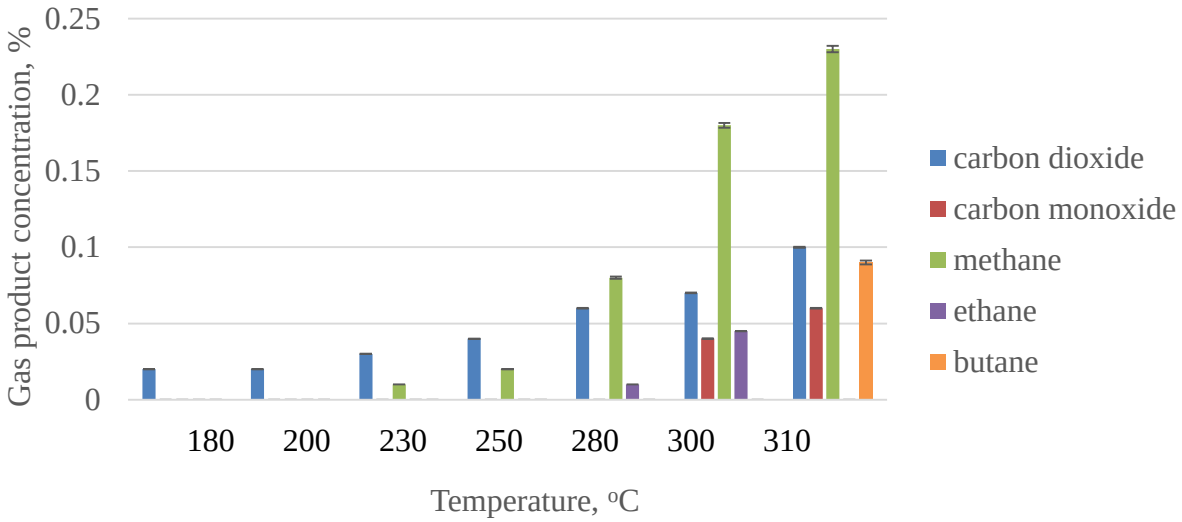

Figure 4-3 Gas products concentration at different HDT reaction temperatures.

Figure 4-3 shows an increase in carbon dioxide production as HDT reaction temperature increases probably due to the removal of the oxygen present in the bio-crude in the form of carboxylic acids, removed in the form of CO_2 via hydro-decarboxylation reactions (Egeberg, et al., 2009). This result is in accordance with the TAN reduction previously discussed. It is noteworthy that the standard method for TAN measures the acidity caused by carboxylic acids – phenolic acidity is not accounted for; this is further discussed in Section 4.2.2.

Figure 4-3 also shows that light hydrocarbons are produced in the range of 280 – 310 °C. However, no olefins are observed in the gas products, indicating that the catalyst is efficiently hydrotreating the oil. Furthermore, such evaluation of the produced gases allows for monitoring the production of thermodynamically favoured compounds such as CH_4. The presence of CH_4 begins after

230 ºC, from there on CH_4 only becomes significant over 300ºC. Also, ethane and butane are produced in the higher temperature range, resulting from the partial cracking of the material.

The observed production of carbon monoxide in the higher temperature range (i.e. 300 – 310 ºC) could evidence hydro-decarbonylation reactions, where HDO of aldehydes results in the production of carbon monoxide. The possibility of CO formation by considering another reaction normally occurring in the HDO process is the Reverse Water Gas Shift (rWGS) reaction. This takes place by reacting CO_2 with hydrogen, forming CO as presented in Equation 4-1.

$$CO_2 + H_2 \leftrightarrow H_2O + CO \qquad 41\ kJ/mol \qquad \text{Equation 4-1.}$$

The rWGS reaction is favoured with an increase in temperature. Carbon dioxide is not consumed at high temperatures. On the contrary, its production continues with increasing temperature. Thus, neither rWGS nor methanation reactions are taking place, and instead, CO and CH_4 are formed by hydro-decarbonylation and slight cracking reactions, respectively.

Based on information from the literature about the reactivity of oxygenated groups (Weisser & Landa, 1973) and the effect of temperature on the catalytic HDT process, a reactivity scale has been reported (Elliott, 2007) and it is shown in Figure 4-4.

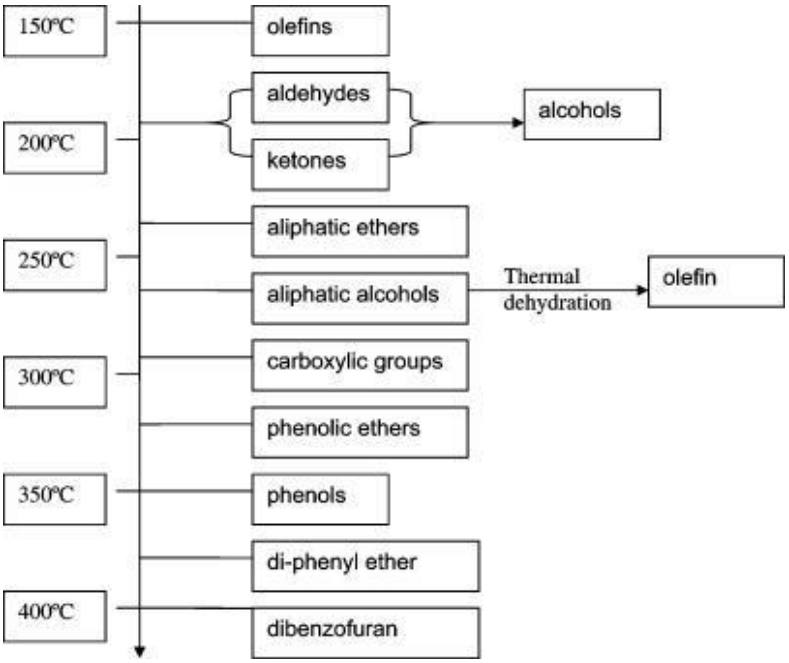

Figure 4-4 Reactivity scale of olefins and oxygenated groups via catalytic HDT, adapted from Elliott (2007)

As shown in Figure 4-4, at low temperatures, olefins, aldehydes, and ketones are readily reduced by hydrogen. These reactions stabilize the bio-crude by removing these reactive groups known to participate in polymerization reactions, as evidenced by the plug formation occurring at low operating temperatures (below 200 ºC). According to Elliot (2007), alcohols are reacted at 250-300 °C by catalytic hydrogenation but also by thermal dehydration to form olefins; and this olefin formation may lead to bio-oil polymerization at hydrotreatment conditions. Fortunately, no evidence of such polymerization was observed in the gas phase, although the olefin formation in the liquid product was not monitored. Carboxylic and phenolic ethers are expected to react at around 300 °C, and this was observed as TAN reduction, and CO_2 formation was enhanced with an increase in temperature to 300 ºC. Regarding the oxygenated groups reactive at temperatures beyond 350 ºC (i.e. Di-phenyl ethers and dibenzofurans), such families have not been found as significant components in bio-crude (Elliott, 2007).

Therefore, a temperature range between 280 and 310 ^{o}C is considered proficient for HDO of the bio-crude under the operating WHSV and pressure tested.

From the temperature screening, the maximum TAN conversion appears to have been achieved at the higher temperatures tested. At this point, the evaluation of other variables such as WHSV and pressure became relevant to identify their effect on the HDT process. The continuation of variables' screening proceeded with a high range of temperature between 280 and 310 ^{o}C, as this seems to assure the decarboxylation of the bio-crude and the reduction of the residue fraction.

4.1.1.2. Space Velocity Effect.

Residence time is defined as the inverse of space velocity and thus, residence time increases by decreasing the space velocity (Schaschke, 2014). An increase in residence time allows for a prolonged contact time between the bulk fluid (bio-crude) and the catalytic surface. This is expected to allow an increased time for deoxygenating and hydrogenation reactions to take place, as high degrees of deoxygenation are favoured by high residence times (Venderbosch, et al., 2010). In a continuous flow reactor, Elliott et al. (2009) showed that the oxygen content of the upgraded oil decreased from 21 wt.% to 10 wt.% when decreasing the LHSV from 0.70 h^{-1} to 0.25 h^{-1} over a Pd/C catalyst at 140 bar and 340 ^{o}C (Elliott, et al., 2009). Furthermore, aside from expecting high degrees of deoxygenation with higher residence times, the enhanced saturation with hydrogen of any cracked material is also possible following free radical saturation reactions and thus preventing undesired condensation reactions.

Therefore, two WHSV have been investigated to evaluate their effect on the HDT process at 300 ^{o}C. The results are presented in Table 4-1.

Table 4-1 Effect of WHSV on produced HDT-bio-oil and by-products.

Temperature	WHSV, h^{-1}	TAN Reduction, %	MCR Reduction, %	Viscosity Reduction, %	H_2O Yield, g_{H2O} / g_{oil}	CO_2, %	CO*, %
300 ºC	0.40	47.0 ± 2.3	20.9 ± 0.4	47.5 ± 2.4	0.037	0.07	0.04
	0.25	58.2 ± 2.9	45.0 ± 0.9	41.0 ± 2.1	0.043	0.08	0.10

*Gaseous product yield was consistent at 1.2% (0.40 h^{-1}) and 1.3% (0.25 h^{-1})

Upon comparison of two space velocities (i.e. 0.4 h^{-1} versus 0.25 h^{-1}), the lower space velocity is deemed a more adequate parameter to achieve hydro-decarboxylation reactions. This is evidenced by the enhanced TAN reduction as presented in Table 4-1. Also, a significant MCR reduction is observed with the lower WHSV, this explains the hydrogenation of the bio-crude whilst preventing condensation reactions. Furthermore, the observed lower reduction of viscosity points in the direction of reduction of aromaticity (i.e. aromatics hydrogenation). Lowering the aromaticity of the oil prevents a significant reduction in the viscosity as naphthenes are produced (Boelhouwer, et al., 1951). The disappearance of the π bonds in the aromatic compounds gives origin to hydrogenated products that loose rigidity, thus preventing significant reductions in the viscous forces. The aromaticity reduction is further discussed in Section 4.2.2.

Also, an increased yield of produced water corresponds to a favoured hydro-deoxygenation reaction as space velocity decreases and thus contact time increases. Furthermore, GC analysis shows that at lower space velocity, the formation of CO_2 accounted for in the gaseous products stream is lower with respect to the CO_2 production expected from the hydro-decarboxylation of carboxylic acids, contradicting the enhanced TAN reduction. However, this is evidence that part of the CO_2 formed via decarboxylation is consumed via the rWGS reaction ($CO_2 + H_2 \leftrightarrow CO + H_2O$). The slight increase in CO production also supports this idea.

4.1.1.3. Thermal Effect: The Absence of Catalyst.

In order to properly evaluate the effect of the catalyst on the bio-crude HDT reaction, the purely thermal effects of the reaction must be understood and used for comparison. The thermal effects are related to the capability of molecules to react without the use of a catalyst to promote the reaction. Expected improvements related to the use of a catalyst in this HDT study are: enhanced product quality (i.e. MCR and viscosity reduction), improved the degree of deoxygenation (i.e. TAN reduction) and hydrogenation (i.e. increased H_2O yield), and prevention of undesirable condensation reactions.

The thermal reaction was performed by entirely filling the reactor shown in Figure 3-2 with silicon carbide (carborundum). This material was pre-washed in an acid solution in order to dissolve any metals attached to it that could present catalytic activity during the reaction. The addition of carborundum was necessary to ensure that flow patterns were similar to the catalytic experiments. The thermal reaction followed the same pre-treatment procedure as in catalytic experiments described in Section 3.3. The selected WHSV of 0.25 h^{-1} was based on the enhanced TAN reduction discussed in Section 4.1.1.2. The thermal effect on the quality of the oil produced in the absence of catalyst was investigated at different temperatures and it is presented in Figure 4-5.

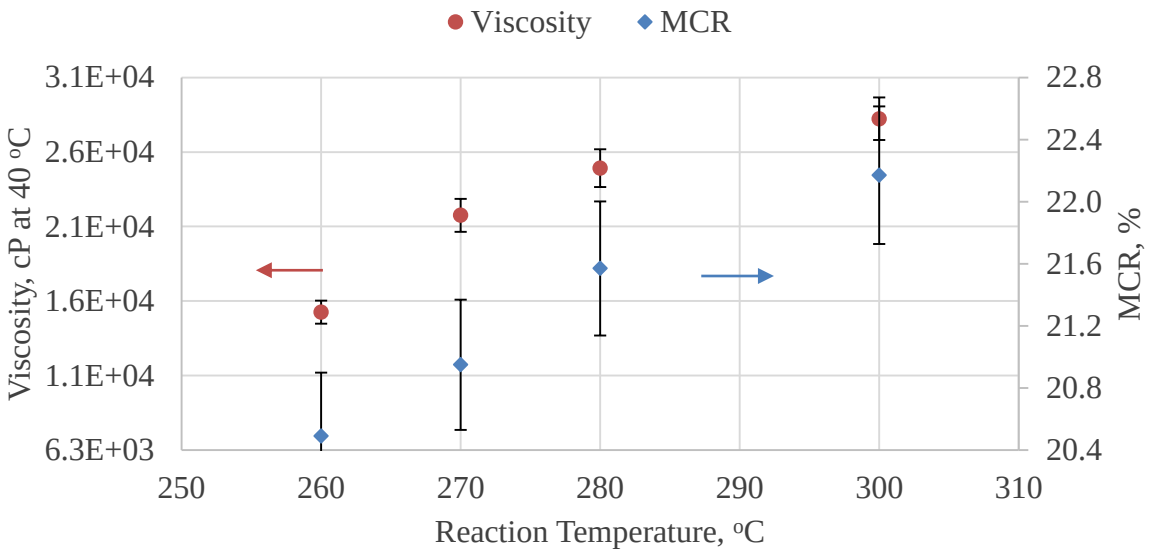

Figure 4-5 Effect of temperature on bio-oil viscosity and MCR in the absence of a catalyst.

In the absence of a catalyst, the active components in the bio-crude are prone to rapid polymerization and aggregation reactions when heated. This is evidenced by the increased viscosity and MCR presented in Figure 4-5; the initial feedstock's viscosity and MCR values are 6299 ± 300 cP at 40 °C and 20.1 ± 0.4 %, respectively. The thermal reactions result in a much more viscous oil with respect to the feedstock; thus, rather than a reduction in viscosity as seen in the catalytic tests, there is an increase in the viscosity of the oil, indicating that the condensation reactions of radicals are predominant. Therefore, in the absence of a catalyst, thermally produced radicals condense participating in polymerization and aggregation reactions. This is further supported by the observed increase in MCR, given that more residue accumulates as thermally formed radicals participate in condensation reactions promoted as reaction temperature increases.

On the other hand, thermal runs demonstrated that temperature alone, in the absence of a catalyst, contributes to TAN reduction as presented in Figure 4-6. However, the catalytic test shows further improvements on TAN reduction.

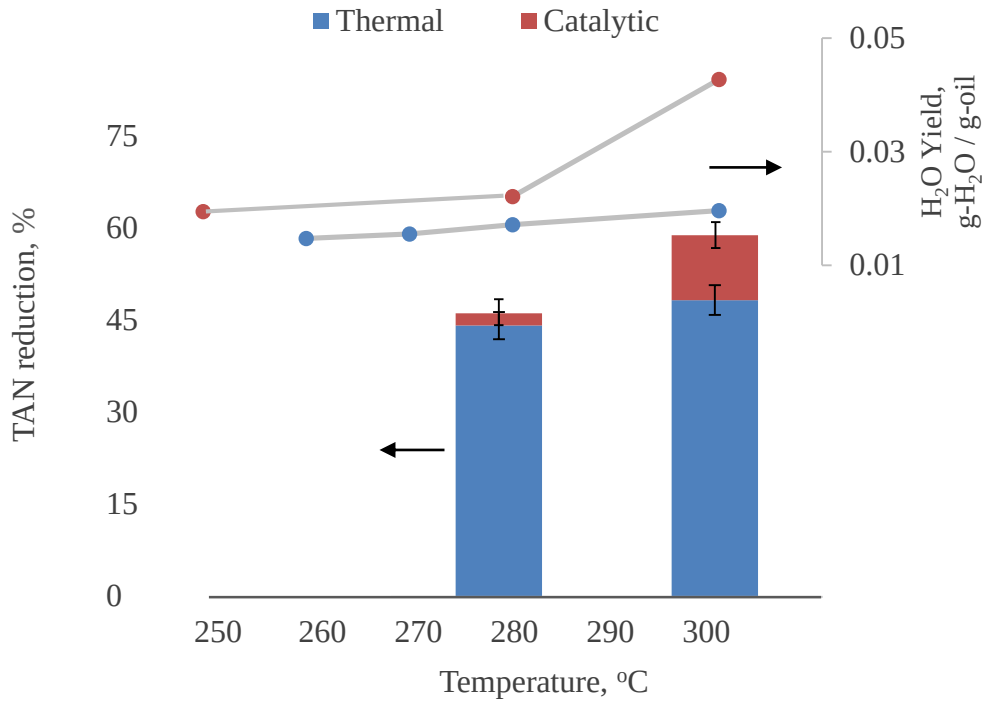

Figure 4-6 Comparison between thermal and catalytic effect on TAN reduction and water production.

Figure 4-6 shows how, compared to the thermal test, the catalytic test improves the TAN reduction the most by 11% at a temperature of 300 ºC. Therefore, both the catalyst and the temperature participate in the TAN reduction of the bio-crude via the HDT process.

Furthermore, Figure 4-6 presents evidence of hydro-deoxygenation reactions being greatly favoured in the presence of a catalyst, as the water product yield is higher, and even doubled as temperature increases from 280 to 300 ºC. These results demonstrate a clear participation of the catalyst.

4.1.1.4. Hydrogen-to-oil Ratio Effect.

The HDT process occurs in a hydrogen rich environment, and the effect of the hydrogen-to-oil (HTO) ratio has been investigated to assess how rich such environment is required to be to achieve the preferred hydro-deoxygenation and hydrogenation reactions. The HTO ratio is defined based on the volumetric flow rate of the bio-crude feedstock (i.e.$\dot{v}_f$), which depends on the mass flow rate calculated upon the WHSV and the mass of catalyst in the reactor, as presented in Equation 3-1. The HTO ratio is calculated following Equation 4-2.

$$HTO = \frac{\dot{v}_{H_2}}{\dot{v}_f} \qquad Equation\ 4-2$$

The effect of reducing the HTO ratio from 900 to 600, and to 300 was investigated by evaluating the quality of the HTD-bio-oil produced in terms of TAN reduction and viscosity as presented in Figure 4-7.

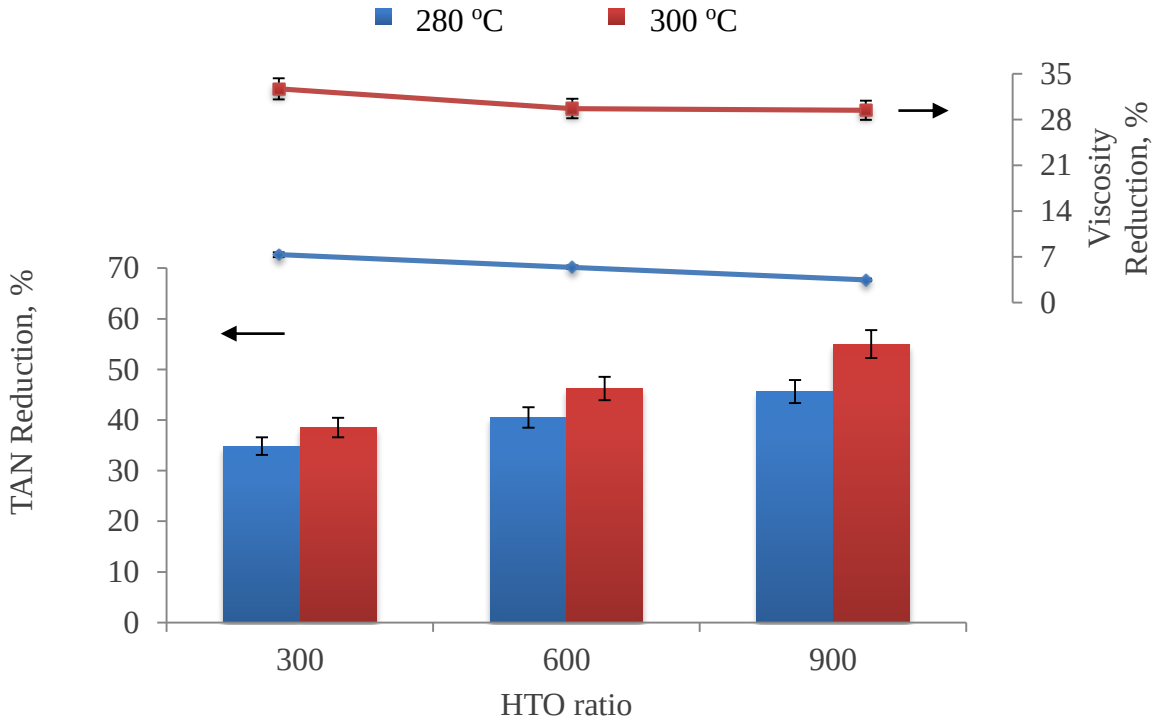

Figure 4-7 HTO effect on TAN and viscosity reduction for HDT operating at 280ºC and 300ºC

In addition to the enhanced TAN reduction by a temperature effect, as previously discussed in Section 4.1.1.3, the HTO ratio also participates in TAN reduction. The base case throughout the previous variable screenings was an HTO ratio of 900; Figure 4-7 shows that by decreasing this ratio to 600 and to 300, the TAN reduction declines by 5% and 16%, respectively, compared to the TAN reduction with an HTO ratio of 900. Therefore, the removal of oxygen present in the bio-crude by hydro-decarboxylation reactions appears to be dependent on the hydrogen rich environment. Thus, the higher the HTO ratio, the more significant the TAN reduction up to a value of 55%.

Furthermore, Figure 4-7 presents how the higher TAN reduction also participates in the viscosity reduction of the HDT-bio-oil produced. Also, when the HTO ratio is higher (i.e. 900) the aromatic compounds in the bio-oil are hydrogenated deeper by the catalyst. By saturating the π bonds in the aromatic compounds, the hydrogenated products lose their rigidity, increasing the viscous forces and thus counteracting the viscosity reduction caused by possible cracking of the material. Therefore, significant viscosity reductions are prevented, as the oil produced is further hydrotreated.

4.1.1.5. Pressure Effect.

The final exploratory phase of the bio-crude HDT investigation evaluated the pressure effect on the quality of the produced HDT-bio-oil. Hydrogenating catalysts usually require high pressures to perform hydrogenation reactions as discussed in section 2.4.1. High pressure in the range from 75 to 300 bar is generally used for HDT as reported in the literature (Venderbosch, et al., 2010; Elliott, et al., 2009; Mercader, et al., 2010). Patent literature describes HDT operating pressures in the range of 10–120 bar for bio-crude feedstock (Daudin, et al., 2013). The high pressure has been described as capable of ensuring a higher solubility of hydrogen in the oil and thereby a higher

availability of hydrogen in the vicinity of the catalyst. This increases the reaction rate and further decreases coking in the reactor (Kwon, et al., 2011).

An initial bio-crude HDT exploration was carried out at 450 psig (31.0 bar) and preliminary findings evidenced the occurrence of rapid polymerization reactions of thermally unstable components in the bio-crude; these must be counteracted by hydrogenation in order to prevent condensation reactions and the increased viscosity of the produced bio-oil. Consequently, an increase in pressure from 450 to 900 psig (31 to 62.1 bar) demonstrated this, as a higher hydrogen pressure allows for a reduction of mass transfer limitations of hydrogen between the bulk fluid (bio-crude) and the catalytic surface. Promising results at 900 psig provided a base variable for the exploration of temperature, WHSV, and HTO variables. Nonetheless, a further investigation regarding the pressure effect was deemed relevant and thus presented in this section.

The base operating conditions for the investigation of pressure effect on bio-crude HDT reactions were selected according to the screening presented throughout Section 4.1.1. Therefore, for the HDT process operating at 300 ^{o}C, WHSV of 0.25 h^{-1}, and HTO ratio of 900, the reaction pressure was investigated at 900 psig (62.1 bar) and compared with 1400 psig (96.5 bar).

In practice, it is difficult to evaluate the conversion of each individual component in the bio-oil. Instead, an important parameter was integrated to further evaluate the effect of pressure, this was the degree of deoxygenation (DOD), and it is calculated following Equation 4-3.

$$DOD = \left(1 - \frac{wt.\%_{O\ in\ prod}}{wt.\%_{O\ in\ feed}}\right) x\ 100 \qquad \text{Equation 4-3.}$$

DOD is calculated to provide a rough overview of the extent of the HDT reaction. The degree of deoxygenation describes how effective the oxygen removal has been and therefore indicates the quality of the produced oil. However, this parameter does not relate to the removal of specific troublesome species; these would have to be analyzed for in detail as presented in Section 4.2.2.

The DOD, TAN and viscosity reductions for the HDT-bio-oil produced at two comparative pressures are presented in Table 4-2.

Table 4-2 Characterization of HDT-bio-oil and H_2 consumption at 300ºC, 0.25h^{-1}, and two different operating pressures.

Reaction Pressure, psig	TAN Reduction, %	Viscosity Reduction, %	DOD	H_2 Consumption (mg H_2/ g oil)	H_2O Yield, g $_{H2O}$ / g $_{oil}$
900	55.7 ± 2.8	20.1 ± 1.0	32.1 ± 0.1	4.8	0.043
1400	67.9 ± 3.4	27.8 ± 1.4	37.1 ± 0.1	5.3	0.045

The results presented in Table 4-2 show a much more significant TAN reduction whilst operating at the higher-pressure range (1400 psig), evidencing further hydro-decarboxylation reactions taking place. Hytrotreating reactions are accounted for in the moderate viscosity reduction values, and the increased consumption of hydrogen at 1400 psig further provides evidence of higher HDT levels. Consequently, the DOD is in accordance with TAN reduction and hydrogen consumption; as the TAN reduction level increases, DOD increases, and thus hydrogen consumption also increases.

Regarding the gas products at different operating conditions, it must be considered that, according to Le Chatelier's principle, methanation reactions are favoured at elevated pressures (Stangeland, et al., 2017). Therefore, side reactions such as carbon monoxide and carbon dioxide methanation are thermodynamically favoured at higher pressure, and thus participate throughout the HDT process being much more possible at higher pressures. The overview of the gas products composition is presented in Figure 4-8.

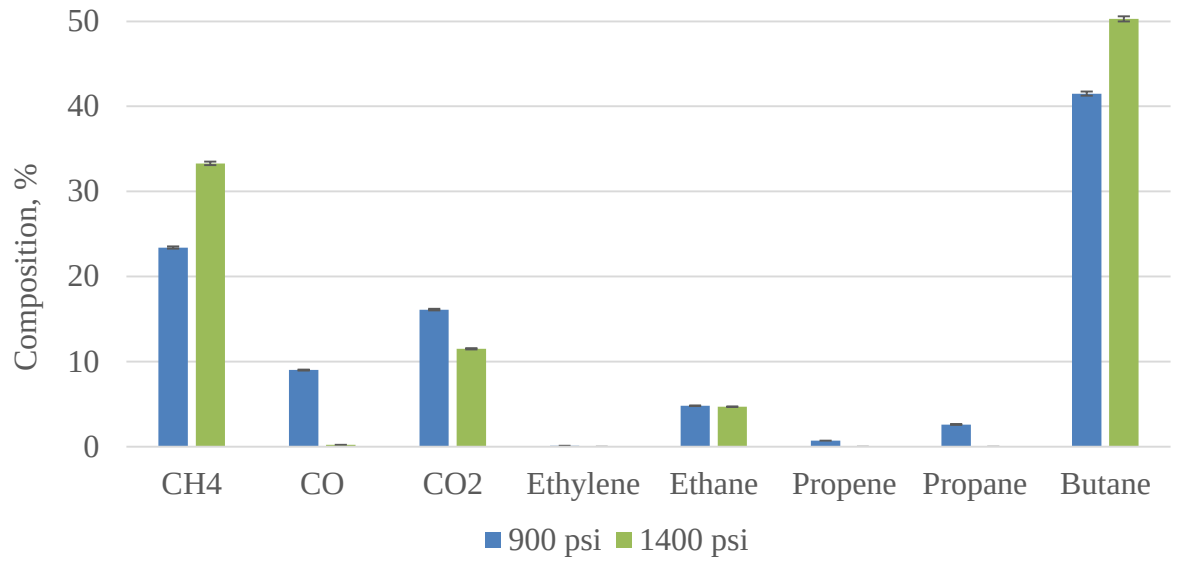

Figure 4-8 Pressure effect on product gas composition (free of hydrogen) for bio-crude HDT at 300ºC, and 0.25h^{-1}.

Figure 4-8 presents the gas products under two different operating pressures. The production of CO and CO_2 is due to the decomposition of oxygenated substituent groups in the bio-crude. This results in the production of carbon dioxide from hydro-decarboxylation of the carboxyl groups, water production from the hydroxyl groups, and carbon monoxide from the carbonyl in aldehyde groups. Some of the light hydrocarbons (i.e. C_1 – C_4) can result from the dealkylation of alkyl groups on alkyl phenol structures derived from lignin-produced bio-crudes (Egeberg, et al., 2009). The drastic reduction of carbon monoxide observed in Figure 4-8 at 1400 psig, as opposed to 900 psig, suggests the participation of methanation side reactions, which then correspond with the increase in methane produced at the higher pressure. Carbon dioxide may also be participating in such methanation reactions, given that both carbon monoxide and carbon dioxide react in the presence of hydrogen to form methane and water as presented in Equations 4-4, and 4-5.

$$CO + 3H_2 \leftrightarrow CH_4 + H_2O \qquad \text{Equation 4-4.}$$

$$CO_2 + 4H_2 \leftrightarrow CH_4 + 2H_2O \qquad \text{Equation 4-5.}$$

Therefore, the oxygen removed in the form of carbon monoxide and carbon dioxide from the bio-crude via hydro-decarbonylation and hydro-decarboxylation reactions, respectively, is consumed in-situ producing methane via methanation reactions.

Furthermore, the desirable hydro-decarboxylation and hydro-decarbonylation reactions also produce olefins and paraffins. Some may be present in the form of C_1-C_4 hydrocarbons as reported in the gas products in Figure 4-8. Additionally, the paraffin to olefin ratio favours the production of paraffins at the higher pressure, thus the possible production of olefins appears to be counteracted by hydrogenation reactions in the process.

Overall, the gas products reported are in accordance with the increased DOD, and further TAN reduction resulting from the bio-crude HDT at the higher operating pressure. Therefore, this indicates that the highest operating pressure secures a higher solubility of hydrogen in the oil and thereby a higher availability of hydrogen in the vicinity of the catalyst, resulting in a deeper HDT process.

4.1.1.6. Combined Variables Effect.

Moreover, based on the effect of the variables previously discussed, increasing the severity of all the HDT operating conditions was studied to further reduce the bio-crude's TAN. Therefore, provided that the intention of this bio-crude HDT investigation is to explore the effect of different variables, a final test was performed prior to the production of the HDT-bio-oil to be carried forward as feedstock for the CSC stage of the bio-crude upgrading process herein evaluated.

Section 4.1.1.1 explored the effect of temperature on the bio-crude HDT process, and it was determined that an increase in operating temperature resulted in significant TAN reductions; Section 4.1.1.2 evaluated the WHSV effect, and by allowing an increased oil residence time, the TAN reduction was found to be enhanced; Section 4.1.1.5 determined the requirement for high

operating pressure to ensure a higher solubility of hydrogen in the oil and thereby a higher availability of hydrogen in the vicinity of the catalyst, resulting in a deeper HDT process, improving TAN reduction.

Therefore, the final test herein explored implemented an increased severity combining temperature, and WHSV effects at the maximum operating pressure allowed within the pilot-plant system (i.e. 1400 psig). Table 4-3 tabulates the operating conditions investigated, and the results of this test are presented in Figure 4-9.

Table 4-3 HDT experimental parameters to investigate the increased severity effect

Temperature, ^{o}C	300	300	310	320^{+}
WHSV, h^{-1}	0.25	0.25	0.20	0.20^{+}
Pressure, psig	900	1400	1400	1400^{+}

$^{+}$ Experiment performed with an HDT catalyst of an increased hydrogenating agent composition, performed in parallel by another MSc student in this research group, and the complete evaluation will be reported in her thesis.

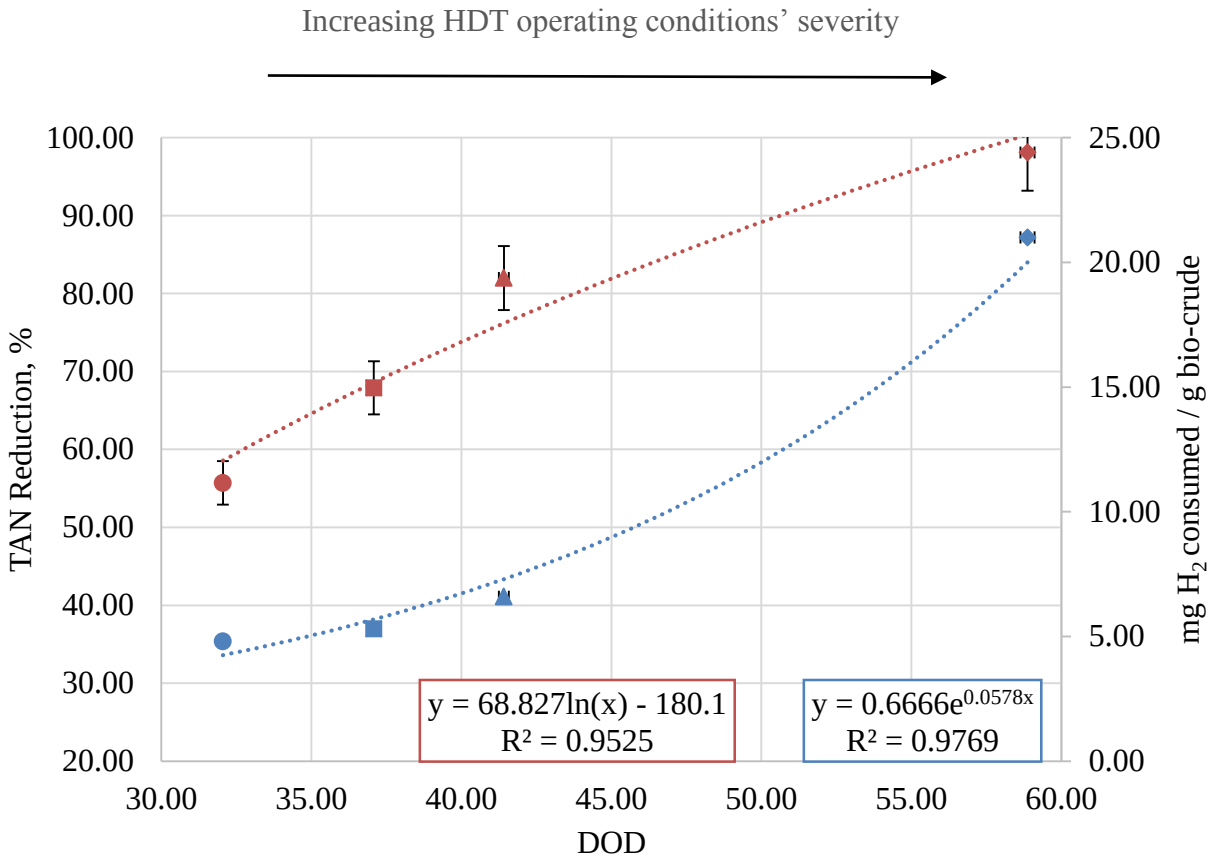

Figure 4-9 HDT severity effect on DOD, on the TAN reduction (in red) and hydrogen consumption (in blue) for bio-crude HDT at different operating conditions. ●: 300 ^{o}C, 0.25 h^{-1}, 900 psig; ■:300 ^{o}C, 0.25 h^{-1}, 1400 psig; ▲: 310 ^{o}C, 0.20 h^{-1}, 1400 psig; ♦: 320 ^{o}C, 0.20 h^{-1}, 1400 psig.

Figure 4-9 presents the TAN reduction and the hydrogen consumption as a function of the severity. DOD is also plotted showing how the oxygen content decreases as a function of HDT condition severity. TAN reduction appears to follow a logarithmic trend line. Therefore, with an increase in severity and thus DOD of the bio-crude, the rate of TAN reduction increases rapidly and then seems to reach the maximum TAN reduction > 98%. It was determined that, at the maximum TAN reduction, the oxygen content was not depleted from the oil, thus the TAN method herein applied accounts for carboxylic acidity alone, and phenolic acidity is not accounted for; this is further discussed in Section 4.2.2.

In accordance with the HDT severity and bio-crude's DOD, the hydrogen consumption also increases as the participation of hydro-deoxygenation reactions surges. The hydrogen consumption seems to best fit an exponential trend line in Figure 4-9, where the milligrams of hydrogen consumed per gram of bio-crude oil rise at increasingly higher rates as the DOD increases. Furthermore, the increased DOD is also complemented by an increase in H/C and a decrease in O/C ratios, as condition severity increases. This is sown in Figure 4-10.

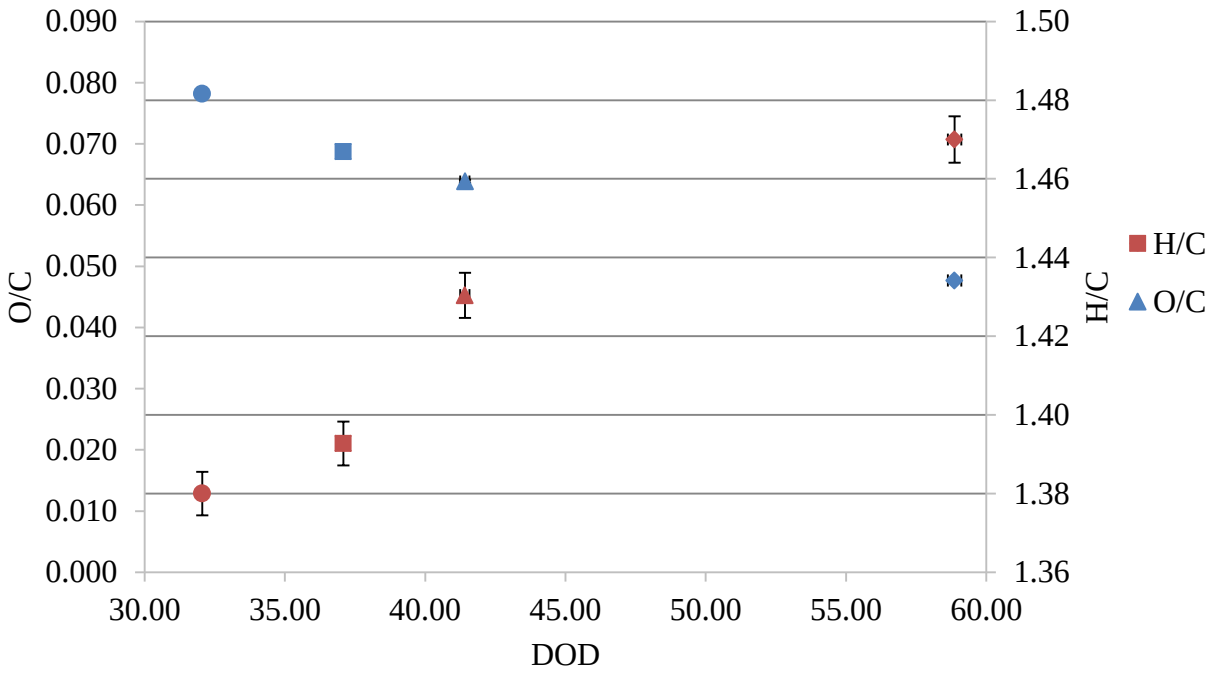

Figure 4-10 HDT severity effect on DOD, H/C ratio (in red) and O/C ratio (in blue) for bio-crude HDT at different operating conditions. ●: 300 ºC, 0.25 h^{-1}, 900 psig; ■:300 ºC, 0.25 h^{-1}, 1400 psig; ▲: 310 ºC, 0.20 h^{-1}, 1400 psig; ♦: 320 ºC, 0.20 h^{-1}, 1400 psig.

The studied bio-crude's initial H/C and O/C ratios are 1.34 and 0.12 respectively. The increase in H/C and the decrease in O/C ratios presented in Figure 4-10 are further indications of the deep HDT achieved at the most severe conditions tested, and in the presence of a higher hydrogenating metal composition in the improved HDT catalyst. Also, the increase in H/C and the decrease in O/C ratios both contribute to higher heating values. Consequentially, the requirement for high

severity conditions to achieve a deep HDT of the bio-crude is evidenced to achieve reducing the high bio-crude carboxylic acidity and oxygen content.

The first half of this chapter described the effect that different variables partake in the HDT process for Steeper Energy Hydrofaction^{TM} Renewable Crude Oil. The reaction conditions herein investigated do not reach severity values attributed to hydrocracking processes (Ramirez, et al., 2015). Therefore, the HDT-bio-oil produced qualifies as a product from a mild-to-deep HDT process. Further optimization of the HDT process is out of the scope of the present thesis, and the work is to be undertaken by another MSc student, also a member of the CAFE research group.

The overview of the different variables explored resulted in the selection of three HDT process conditions varying the severity of pressure, temperature, and WHSV for the production of three HDT-bio-oils, reaching different levels of HDT. The characterized produced HDT-bio-oils are described in Section 4.1.2. Furthermore, to proceed with the present research work, the produced HDT-bio-oils are carried forward as feedstocks for the co-upgrading CSC process herein proposed, where the dependence on the quality of the HDT-bio-oil is investigated. The complete exploration of the CSC process is discussed in the second half of this chapter, in Section 4.2.

4.1.2. Characterization of Produced Hydrotreated Bio-oil.

The exploration of the HDT process applied to Steeper Energy Hydrofaction^{TM} Renewable Crude Oil allowed for an understanding of the effect of different variables on TAN reduction, DOD, viscosity, as well as hydrogen consumption and water production. Three sets of HDT operating conditions were selected which resulted in the production of varying qualities of hydrotreated bio-oils, differencing mostly by TAN, viscosity and oxygen content; these are named HDT-bio-oil A, B, and C, and are described in Table 4-4.

Table 4-4 HDT-bio-oil produced for the CSC co-upgrading process exploration.

HDT Temperature, ºC	300	310	320
HDT WHSV, h^{-1}	0.25	0.20	0.20
HDT Pressure, psig	900	1400	1400
Property	**HDT-bio-oil "A"**	**HDT-bio-oil "B"**	**HDT-bio-oil "C"**
Viscosity at 40ºC, cP	17500	9010	3200
TAN, mg KOH/g	21.3	11.6	< 1.0
Water content, wt.%	< 1	< 1	< 1
Oxygen content, wt.%	8.5	7.5	5.1
H/C ratio	1.38	1.43	1.47
O/C ratio	0.08	0.06	0.05
HHV^{+}, MJ kg^{-1}	40.2	40.9	42.3
Distillation Cuts, wt.%			
Naphtha, (IBP-190 °C)	ND	3.1	4.4
Kerosene (190-260 °C)	ND	7.7	9.3
Diesel (260-343 °C)	ND	14.9	22.3
VGO (343-550 °C)	ND	20.5	16.5
Residue (550+ °C)	ND	53.8	47.5

[+] HHV calculated by the Dulong formula, with the CHN values determined by Elemental Analysis, assuming a 0% sulfur content

The above described HDT-bio-oils were produced in quantities large enough to be carried forward as feedstocks for the co-upgrading CSC investigation presented in Section 4.2.

4.2. Catalytic Steam Cracking (CSC) Process

The Catalytic Steam Cracking (CSC) process is considered to be a first-of-a-kind upgrading investigation for lignocellulosic biomass derived bio-crudes, given that the process has not been applied to such crudes by any other research group. Accordingly, the steam processing stage is original, not proposed by others for this type of feedstock processing; that implies that the catalytic formulation for this specific application is deemed to be original with the combination of steam splitting and steam cracking-hydrogenating functionalities synthesized by and provided for this investigation by Dr. G. Vitale. Further details on the catalyst are not disclosed to secure patentability of the formulas.

Therefore, this thesis investigates CSC for the upgrading of a previously hydrotreated bio-crude oil. The reasoning behind the requirement for the CSC feedstock to be previously hydrotreated arose upon the testing of the original bio-crude, as provided by Steeper Energy, under CSC conditions without any previous treatment. Appendix II presents an overview of the test. Findings indicated that under CSC conditions and without a previous HDT, the bio-crude was significantly affected by polymerization of the highly oxygenated components, resulting in the considerable increase of viscosity and residue contents. Consequently, the idea of CSC as a single upgrading process was deemed not viable, and thus the prerequisite for the HDT process was demonstrated.

The pilot plant, procedure, and sample characterization methodologies described in Chapter 3 of this thesis have been implemented for the CSC upgrading process investigation of hydrotreated bio-crude feedstock (i.e. HDT-bio-oil). The dependence of the CSC process on the feedstock properties is evaluated by the use of three different HDT-bio-oil feedstocks, which are different in terms of oxygen content, viscosity, and TAN. Furthermore, different operating conditions were

evaluated to determine those favorable the most for CSC capable of producing the highest quality bio-oil during stable operation.

The HDT-bio-oils are a complex mixture of hydrocarbons, thus a very complex system of reactions takes place when temperature, pressure, and other reactants are contacted with the feedstock. Some of the reactions that are expected to take place thermally or catalytically in the reactor were reviewed in Section 2.4.2.1. The reactions expected to occur throughout this CSC process include hydrocarbon steam reforming (Eq. 4-6), water splitting (Eq. 4-7), and steam cracking (Eq. 4-8).

$$C_nH_x + 2n\,H_2O \rightarrow n\,CO_2 + \left(2n + \frac{x}{2}\right)H_2 \qquad \text{Equation 4-6.}$$

$$2H_2O \rightarrow 2H^{\bullet} + 2OH^{\bullet} \qquad \text{Equation 4-7.}$$

$$R - CH_2 - R_n + 2H_2O \rightarrow RH + CO_2 + 2H_2 + R_nH \qquad \text{Equation 4-8.}$$

Additionally, partial steam cracking (Equation 4-9), incomplete partial steam cracking (Equation 4-10), thermal dehydrogenation (Equation 4-11), catalytic hydrogenation (Equation 4-12), and steam decarboxylation (Equation 4-13) are also part of the set of reactions that are expected to occur.

$$R - CH_3 + 2H_2O \rightarrow RH + CO_2 + 3H_2 \qquad \text{Equation 4-9.}$$

$$R - CH_3 + H_2O \rightarrow RH + CO + 2H_2 \qquad \text{Equation 4-10.}$$

$$R_1 - CH_2 - CH_2 - R_2 \rightarrow R_1 - CH = CH - R_2 + H_2 \qquad \text{Equation 4-11.}$$

$$R_1 - CH = CH - R_2 + H_2 \rightarrow R_1 - CH_2 - CH_2 - R_2 \qquad \text{Equation 4-12.}$$

$$R - CH_2 - COOH + 2H_2O \rightarrow RH + 2CO_2 + 3H_2 \qquad \text{Equation 4-13.}$$

Furthermore, the preceding reactions do not include the totality of those expected to that take place. For instance, if the saturation of organic free radicals by hydrogen free radicals is not predominant,

in the case of lower hydrogen availability, the free radicals formed by thermal cracking reactions participate in undesirable polymerization and condensation reactions.

4.2.1. Experimental Results.

In this section, the CSC results are presented and discussed. Depending on the operating HDT variables, different HDT-bio-oils are produced as explored in Section 4.1. Therefore, the CSC process of bio-oils previously hydrotreated to different extents provides a starting point for the evaluation of the CSC process and its dependence on the feedstock. A very significant difference between the produced HDT-bio-oils relies on the DOD and thus the TAN of the oil, which is an indication of the unfavourable acidity pertaining the remaining oxygen composition which actively participates in undesirable corrosion and polymerization reactions. For complex mixtures of hydrocarbons, desirable reactions are hard to specify and track, thus physical and chemical properties of the products are used to understand the effectiveness of a reaction.

4.2.1.1. Feedstock Dependence.

The dependence on the TAN of the feedstock is herein investigated to evaluate the effect on the catalyst as the CSC reaction progresses.

Figure 4-11 presents the TAN reduction over time for the CSC of two different feedstocks, HDT-bio-oil "A" (HBO-A) and HDT-bio-oil "B" (HBO-B); each of these HDT-bio-oil feedstocks is described in Section 4.1.2. The TANs for HBO-A and HBO-B prior to the CSC process are 21.3 and 11.6 mg $_{KOH}$/g $_{oil}$, respectively.

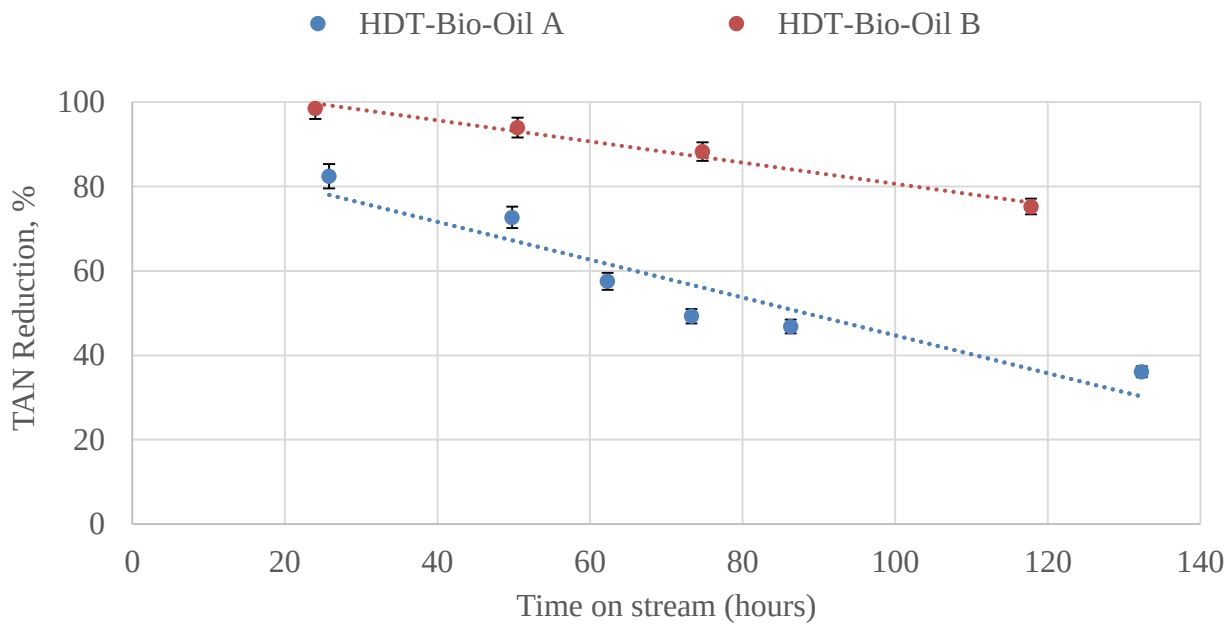

Figure 4-11 TAN Reduction under similar CSC operating conditions for two different HDT-bio-oil feedstocks. HDT-bio-oil-A (in blue; TAN_i 21.3 mg $_{KOH}$/g $_{oil}$) and HDT-bio-oil-B (in red; TAN_i 11.6 mg $_{KOH}$/g $_{oil}$)

Figure 4-11 shows that a difference of almost doubled initial TAN (TAN_i) signifies a substantial difference in the deactivation of the CSC catalyst over time. HBO-B with a TAN_i of 11.6 mg $_{KOH}$/g $_{oil}$ achieves a maximum TAN reduction of > 98 % within the first 24 hours of the reaction; however, HBO-A with a TAN_i of 21.3 mg $_{KOH}$/g $_{oil}$ achieves a maximum TAN reduction of 82 % within the first 24 hours. Nevertheless, both result in the rapid decrease in TAN reduction capacity where the catalyst deactivation is to be accounted for. The trend for the curve depicts the HBO-B results in a reduced slope, as oppose to that for the higher TAN feedstock HBO-A; this is evidence of a slower catalyst deactivation when exposed to a lower TAN feedstock. However, both tests indicate the undesired catalyst deactivation within the first 50 hours of continuous operation. Consequently, a deeper HDT of the bio-crude at more severe operating conditions produced an HDT-bio-oil with a lower TAN (i.e. HDT-bio-oil "C" TAN < 1 mg $_{KOH}$/g $_{oil}$). This allowed for an

alternative to preserve the life of the catalyst over an increased period of time – presented in Section 4.2.1.2. For that reason, the overall stability of the CSC process appears to depend on the TAN of the feedstock, given that a lower TAN feedstock allows for preventing drastic changes in the CSC process activity. Therefore, catalyst deactivation throughout the CSC process is evident, and thus the reasoning behind it becomes relevant.

The catalyst used for the CSC reaction of higher TAN HBO-A, that was the most rapidly deactivated catalyst between the two studied reactions shown in Figure 4-11, was recovered for further investigation. TGA-DTA of the spent catalyst, free of oil residue, is presented in Figure 4-12.

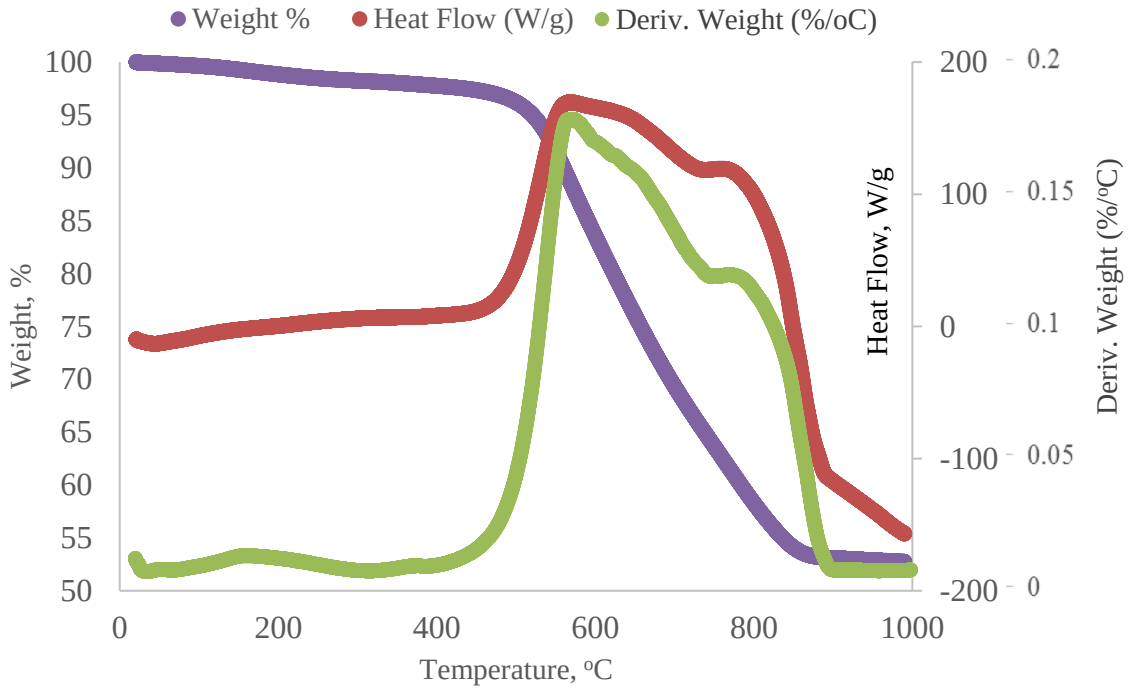

Figure 4-12 TGA-DTA of spent, deactivated CSC catalyst.

In Figure 4-12, two different kinds of coke are observed, the first being a low temperature range coke (> 600 ^{o}C) herein described as amorphous coke, and the second is a higher temperature range coke (> 800 ^{o}C) herein referred to as graphitic coke. Guisnet & Magnoux (2001) describe the lower temperature range coke formation to consist mainly of condensation and rearrangement steps; whereas the higher temperature coke is generally polyaromatics and their formation involves hydrogen transfer and dehydrogenation steps in addition to condensation and rearrangement steps on the surface of the catalyst. The retention of the coke molecules on the catalyst is mainly due to their low solubility (liquid-phase reactions) (Guisnet & Magnoux, 2001). Therefore, such results suggest carbonaceous deposits (i.e. coke) to be the main cause of catalyst deactivation.

With the understanding of the rapid CSC catalyst deactivation being due to coke formation, the comparison with a third HDT-bio-oil feedstock became imperative to further explore the CSC process. Said third HDT-bio-oil is HBO-C, which TAN is < 1 mg $_{KOH}$/g $_{oil}$ was achieved by a deep HDT process at the most severe conditions explored throughout Section 4.1. This is further evidence of the inevitable requirement for an HDT process able to eradicate the bio-crude acidity to at least a TAN of 1 mg $_{KOH}$/g $_{oil}$ with corresponding DOD close to 60%, prior to the CSC co-upgrading stage of the investigation. Furthermore, by introducing such a low acidity oil to the CSC process, catalyst activity remains stable for a prolonged period of time, thus allowing for a screening of operating conditions – as presented in Section 4.2.1.2.

4.2.1.2. Screening of Operating Conditions.

A CSC evaluation for the HBO-C as feedstock under two different reaction temperatures and two WHSV, was investigated throughout a continuous reaction (325 hours), where catalyst deactivation was avoided due to the low TAN feedstock. The water-to-oil ratio was maintained constant throughout the study, at 5 wt. % water. The exploration of different reaction conditions

allows for an understanding of the effect that temperature and WHSV have on the CSC process of the previously hydrotreated bio-oil. Furthermore, gas products concentrations and liquid products quality were evaluated and herein discussed.

Gas composition is an important property to be tracked since it gives an indication of the reactions that are taking place and their extents. Figure 4-13 presents the composition of the product gases at different CSC operating conditions evaluated over time.

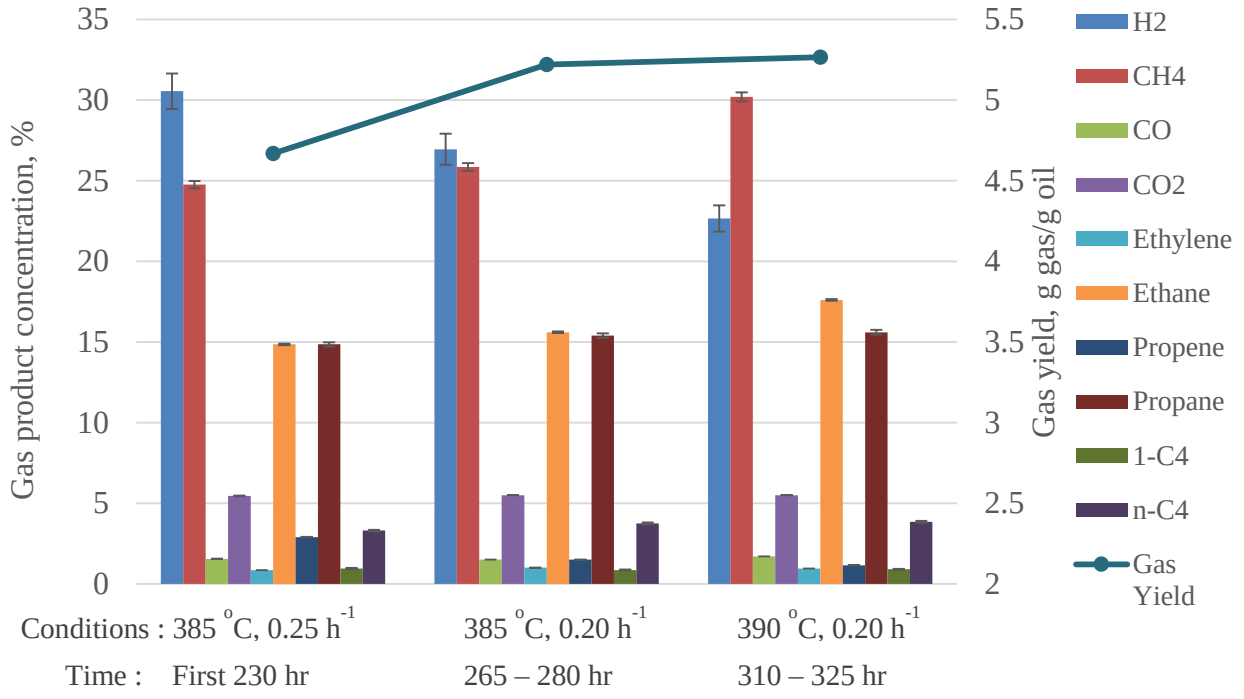

Figure 4-13 Gas products composition for CSC reactions of HBO-C at different operating conditions, increasing in severity, and over time.

An indication of the catalyst continuous activity throughout the reaction is the constant carbon dioxide production. An increment in carbon dioxide production would result from the production of carbonaceous deposits, which appears to have been avoided. Figure 4-13 shows no change in carbon dioxide production as the CSC reaction conditions increase in severity over time.

Furthermore, the most severe reaction conditions favour the rate of formation of light hydrocarbons, as the concentrations of ethane, and propane product gases are observed to increase in Figure 4-13. Thus, the material is being cracked further. The gas product yield also shows a slight increase from 4.7 to 5.2%.

The hydrogen concentration is observed to decrease with the increase in reaction severity, while propene concentration is observed to decrease. This is indicative of the partial consumptions of the formed hydrogen by the saturation of olefins in the cracked material. This is further evidence of the continuous activity of the CSC catalyst, unaffected by the low TAN HBO-C feedstock. Lastly, Figure 4-13 shows the evident increment in methane production as the process temperature increases from 385 to 390 ^{o}C. Cracking and methanation reactions are favoured at higher temperatures, and the increase in methanation of carbon dioxide is further evidenced by the higher CH_4/CO_2 ratio, as presented in Figure 4-14 below.

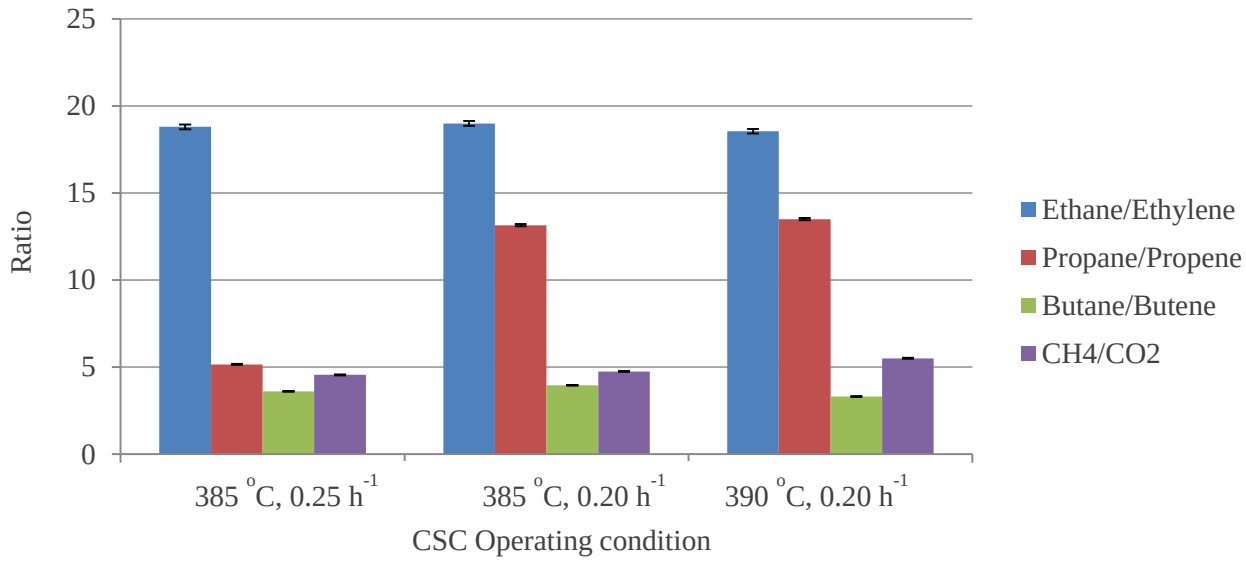

Figure 4-14 Paraffin-to-oil ratios and methane-to-carbon dioxide ratios for different CSC operating conditions

Figure 4-14 presents the paraffin-to-oil ratio for the hydrocarbon gas products and the methane-to-carbon dioxide ratio at each CSC condition investigated. For all the tested conditions, the paraffin-to-olefin does not decrease with time on stream as the continuous reaction proceeds with an increase in severity. Instead, the paraffin-to-olefin ratios are observed to increase with the increasing severity of reaction conditions. Olefins result from thermal cracking, as well as polymerization reactions in the absence of an active catalyst. Therefore, such high paraffin-to-olefin ratios indicate that the catalyst remained active during the complete length of the CSC reaction (325 hours) performed under different operating conditions, varying temperature and then WHSV.

These results confirm that the main cause of deactivation of the catalyst, as observed in the previous Section 4.2.1.1, relate to a remaining high acidity of the HDT-bio-oil in feedstocks HBO-A and HBO-B, as well as the presence of other reactive oxygenated components such as ketones. Thus, by performing a deeper hydrogenation of the feedstock, and achieving a TAN < 1 mg KOH/g in HBO-C, a reduction of the coke deposition on the surface of the CSC catalyst was accomplished, allowing for a continuous CSC operation of 325 hours.

On the other hand, regarding the quality of the CSC-bio-oil produced, the residue conversion achieved at each CSC condition evaluated was determined by TGA. Figure 4-15 presents the sample weight loss % as a function of temperature obtained by heating each sample at a rate of 10 ^{o}C/min in the presence of nitrogen via the TGA.

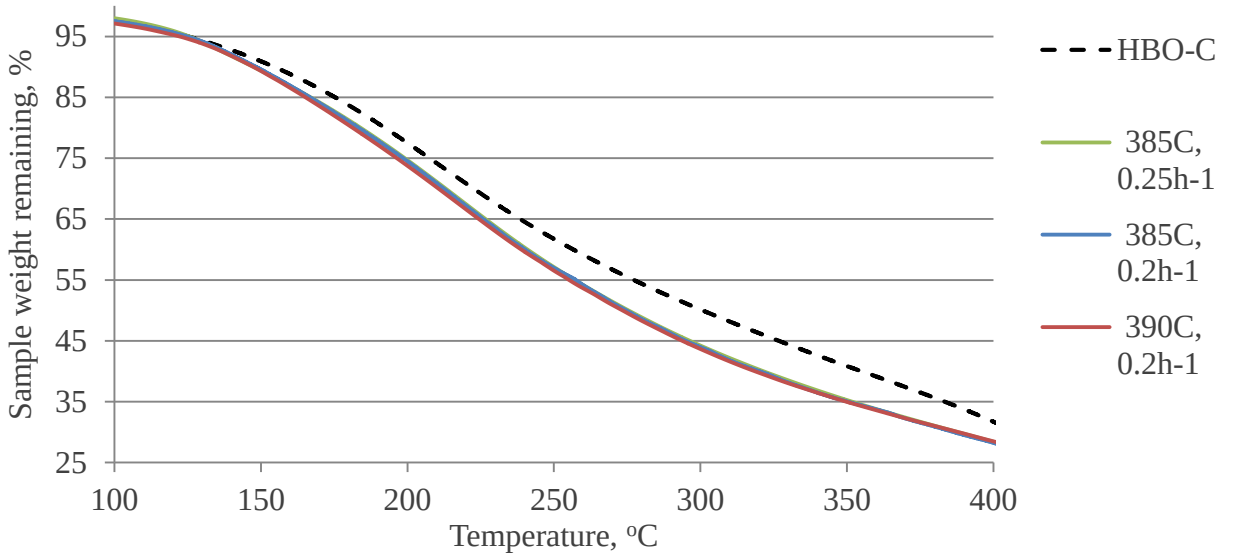

Figure 4-15 TGA for HBO-C (in black) and CSC-bio-oils produced at different operating conditions; 385 ºC and 0.25 h^{-1} (in green), 385 ºC and 0.20 h^{-1} (in blue), and 390 ºC and 0.20 h^{-1} (in red).

TGA in Figure 4-15 shows the curves for the CSC-bio-oil produced under varying reaction conditions to be very different from that of the HDT-bio-oil feedstock (HBO-C). That observation alone remarks conversion of the oil via CSC. However, the residue conversion requires a detailed evaluation. According to Carbognani *et al*. in his work submitted to ACS books, accounting for an existing thermal cracking phenomena observed in TGA instruments, the conversion of TGA data for any oil material into an HTSD calculated result can be corrected by Equation 4-14. Percent relative errors derived from such conversion were determined to span the ± 10 range.

$$HTSD = 1.36\,TGA + 90 \qquad \text{Equation 4-14.}$$

Therefore, for an HTSD residue conversion at 550 ^{o}C, the corresponding TGA temperature is calculated by Eq. 4-14 to be 338 ^{o}C. And thus, by referring to Figure 4-15, the residue conversion of the HBO-C under different CSC operating conditions can be determined as presented in Table 4-5 below.

Table 4-5 Residue conversion for produced CSC-bio-oils under different reaction conditions

CSC condition	385 ^{o}C, 0.25 h^{-1}	385 ^{o}C, 0.20 h^{-1}	390 ^{o}C, 0.20 h^{-1}
+550 ^{o}C HTSD Residue equivalent conversion, %	13.4 ± 1.3	14.3 ± 1.4	14.4 ± 1.4

Per the corrected TGA residue determination, Table 4-5 presents the +550 ^{o}C HTSD equivalent residue conversion resulting at different CSC operating conditions. The two most severe reactions at 0.20 h^{-1}, and 385 and 390 ^{o}C, result in the highest liquid fraction residue conversion at 14.3 and 14.4 %, respectively. Although the three determined conversion values show no difference within the error. Nevertheless, such conversion results are in accordance with the gas products analysis previously discussed, where the higher severity of reaction achieved enhanced catalytic steam cracking of the oil. Furthermore, each liquid product cut may be additionally determined by HTSD. The results are presented in Figure 4-16.

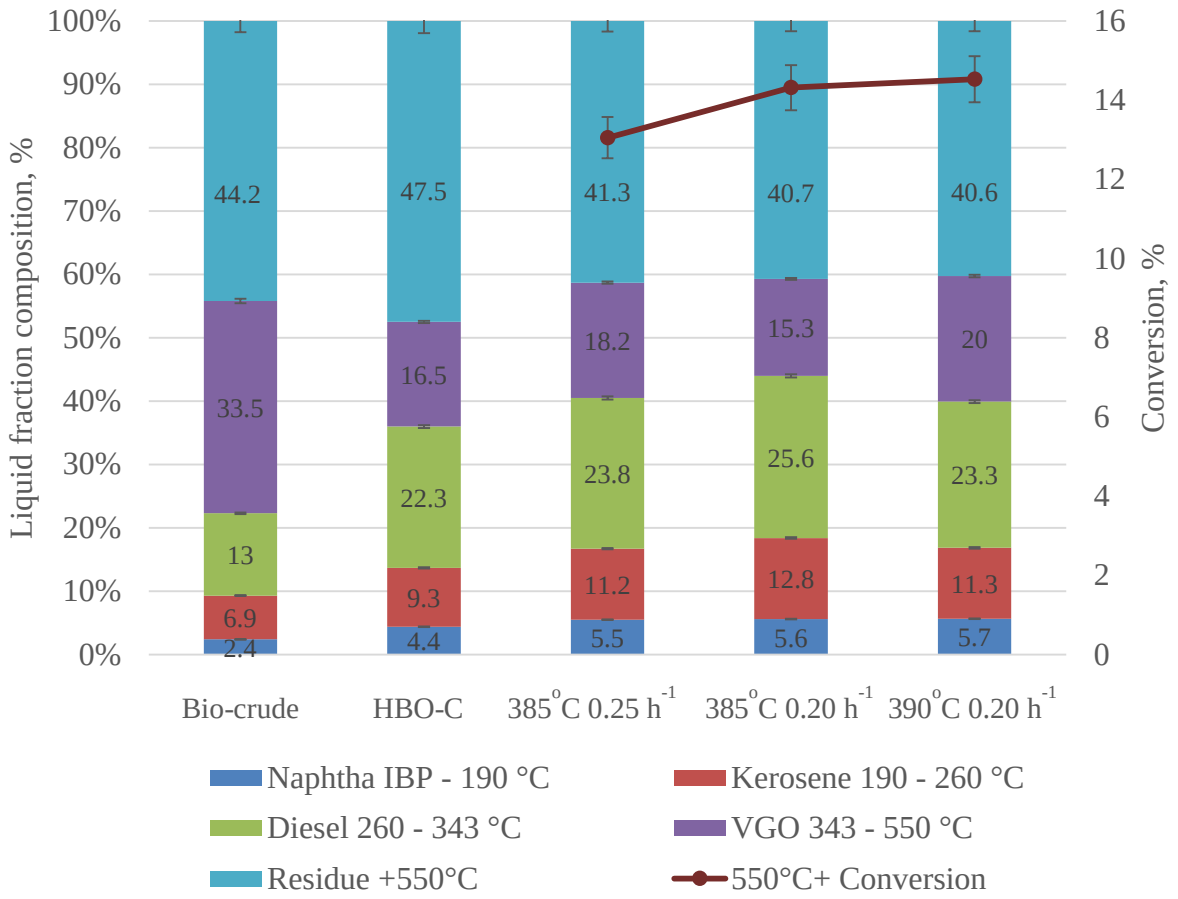

Figure 4-16 HTSD for liquid product distribution of CSC-bio-oil at different operating conditions.

HTSD for the Bio-Crude, HTD-bio-oil (HBO-C) and the different CSC-bio-oils is presented in Figure 4-16. It shows that CSC, as secondary process, completed conversion to petroleum equivalents reaching values of 5.6% Naphtha (IBP-190ºC), 12.8% Jet-fuel (190-260ºC) and 25.6% Diesel (260-343ºC) range hydrocarbon. The proportion of light distillates boiling below 260 ºC increases with increasing severity of CSC reaction conditions. The diesel fraction (260 – 343 ºC) also increases, but it is mostly produced under CSC at 385 ºC and 0.20 h^{-1}, a further increase in severity by increasing the temperature to 390 ºC results in the increment of the VGO fraction and a reduction in the diesel fraction. Given that the desired fraction disclosed by Steeper Energy is diesel, the CSC operations are to be further optimized for the increased production of diesel.

Furthermore, regarding the residue conversion, HTSD results correspond to those calculated from the TGA. Residue conversion with respect to the HDT-bio-oil is found to increase with CSC reaction's severity, however, there is no significant difference between the 385 and 390 ºC tests (at 0.20 h^{-1}). Additionally, a consistent decrease in viscosity by 68 ± 3 % was measured for all the CSC-bio-oils; this further confirms the catalytic cracking of the HBO-C, supporting the residue conversion to lighter distillates.

Finally, elemental analysis allows for the determination of the hydrogen-to-carbon and oxygen-to-carbon ratios of the produced CSC-bio-oil. Results are presented in Figure 4-17.

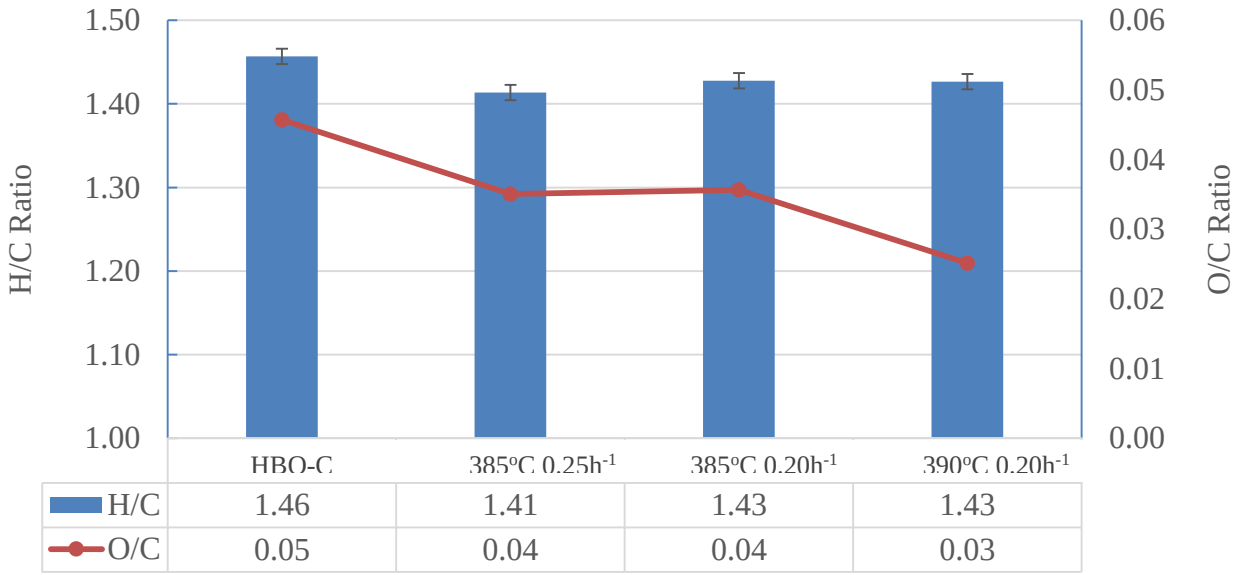

Figure 4-17 Hydrogen-to-carbon and oxygen-to-carbon ratios for each CSC-bio-oil produced under different reaction conditions.

A decrease in the oxygen-to-carbon (O/C) ratio is evidence of further deoxygenation reactions occurring throughout the CSC reactions. This is also evidence that TAN does not account for the presence of other oxygen containing acids, such as phenolic acids. The DOD for the CSC reactions investigated follows the same trend as the O/C ratio presented in Figure 4-17, where the most

severe condition tested (i.e. 390 ^{o}C, 0.20 h^{-1}) resulted in the lowest O/C achieving a DOD of 43.7 % with respect to the oxygen content in the HBO-C feedstock. Regarding the hydrogen-to-carbon (H/C) ratio, this is found to decrease slightly with respect to that of the HBO-C feedstock. The most severe condition has an H/C ratio slightly higher than the least severe condition. Poor saturation of the hydrocarbon radicals formed during CSC by hydrogen radicals results in the reduction of the H/C ratio for the liquid product.

Additional characterization of the CSC-bio-oil includes a further investigation of the different chemical functionalities. Some were found to be troublesome species present in the oil; these being the oxygenated components in the form of phenols and carboxylic acids. Characterization of the produced CSC-bio-oil and its comparison with the original Steeper Energy Hydrofaction^{TM} Renewable Crude Oil, and the HDT-bio-oil was carried out via FTIR. Results are discussed in Section 4.2.2.

4.2.2. Characterization of Chemical Functionalities.

Further investigation regarding the highly oxygenated components in the bio-oil is required to understand the effectiveness of the HDT-CSC bio-crude upgrading process, and its effect on the bio-crude to produce petroleum equivalents. FTIR spectroscopy was carried out to investigate the distinguishable bands for the oxygenated components such as hydroxyls, carbonyls, and ethers. Also, the aromatics and alkyls can be observed. The comparison between the original bio-crude, and the bio-oil's evolution over the HDT and then CSC processes is presented.

4.2.2.1. FTIR study.

The FTIR spectra for the original bio-crude feedstock, the most hydrotreated oil HBO-C carried forward as feedstock for the CSC investigation, and the three CSC-bio-oils produced under different operating conditions are presented in Figure 4-18.

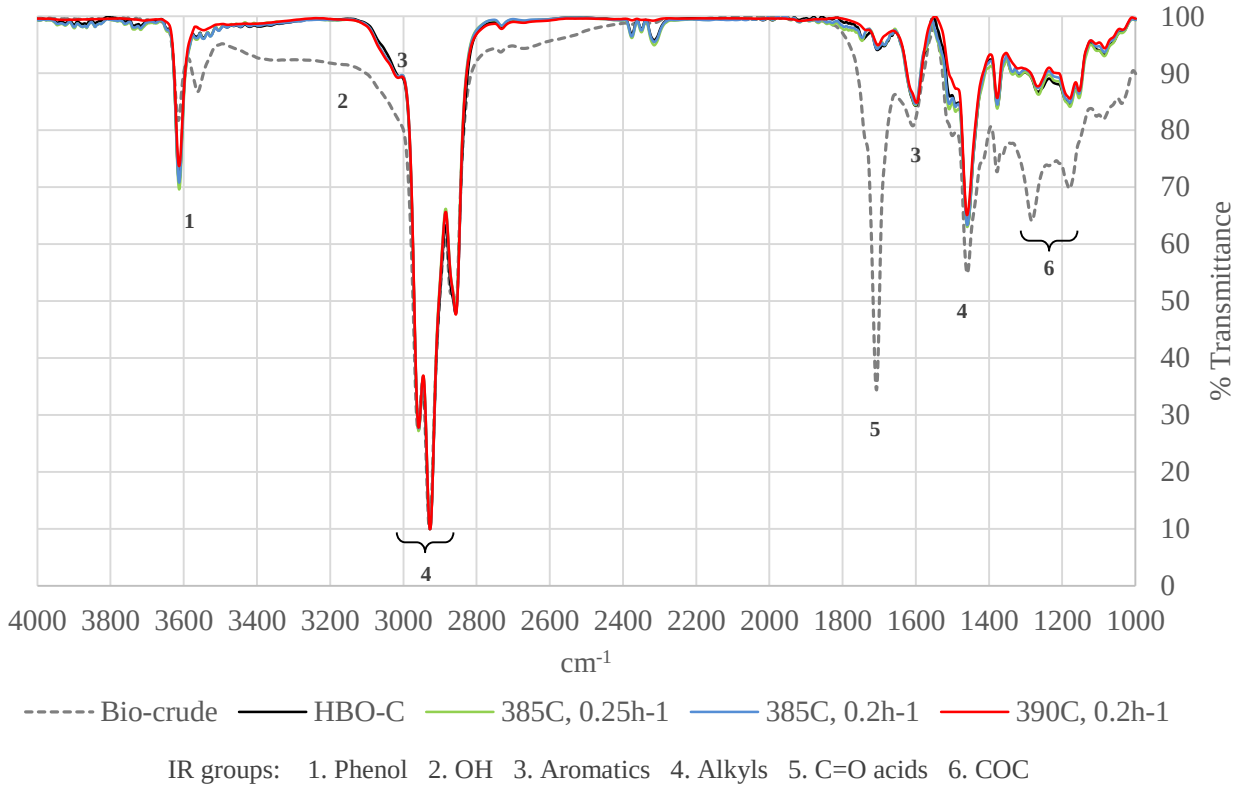

Figure 4-18 FTIR spectra for bio-crude, HDT-bio-oil and CSC-bio-oils produced.

General FTIR band assignment is based on well-known monographs (Silverstein, et al., 2005). The identification of the different bands observed in Figure 4-18 allows for the understanding of the behavior of compounds of interest, and how these evolve throughout the HDT-CSC upgrading process herein explored. Starting at the left-most region, two intense bands depict stretching vibrations of phenol O-H groups: the first band, near 3600 cm^{-1}, depicts phenols with no intermolecular hydrogen bonding (i.e. free phenols), and the second band, near 3550 cm^{-1},

corresponds to vibrations for phenol O-H groups forming intermolecular hydrogen bonds (i.e. bonded phenols). Then, the broad band spanning the 3500 to 2500 cm^{-1} portrays the hydrogen bonded OH, likely present as carboxylic acid OHs; first is the free OH band close to 3400 – 3300 cm^{-1} and then the bonded OH band spanning down to 2500 cm^{-1}. The aromatics are represented by the two stretching bands at 3000 cm^{-1} and at 1600 cm^{-1}. Alkyls appear in the strong stretching bands occurring between 2850 and 2950 cm^{-1} and the bending bands appearing at 1450 and 1370 cm^{-1}. The stretch between 1750 and 1650 cm^{-1} represents esters and carbonyls, and inter-molecularly bonded carbonyls in acids appear at 1710 cm^{-1}. Lastly, ethers are observed as the stretches between 1350 and 1150 cm^{-1}. Outside the peaks of interested pertaining the sample, possible detectability of CO_2 from the laboratory air environment results in the stretch between 2300 – 2400 cm^{-1}, these may be disregarded.

By analyzing the resulting spectra presented in Figure 4-18 with the preceding FTIR band assignments, a clear comparison between the original bio-crude, the HDT-bio-oil, and the CSC-bio-oils is possible. Figure 4-19 presents in greater detail the comparison between the bio-crude and HBO-C (i.e. TAN < 1 mg KOH/g, HDT-bio-oil produced under 320 ^{o}C, 1400 psig, and 0.20 h^{-1} hydrotreating process).

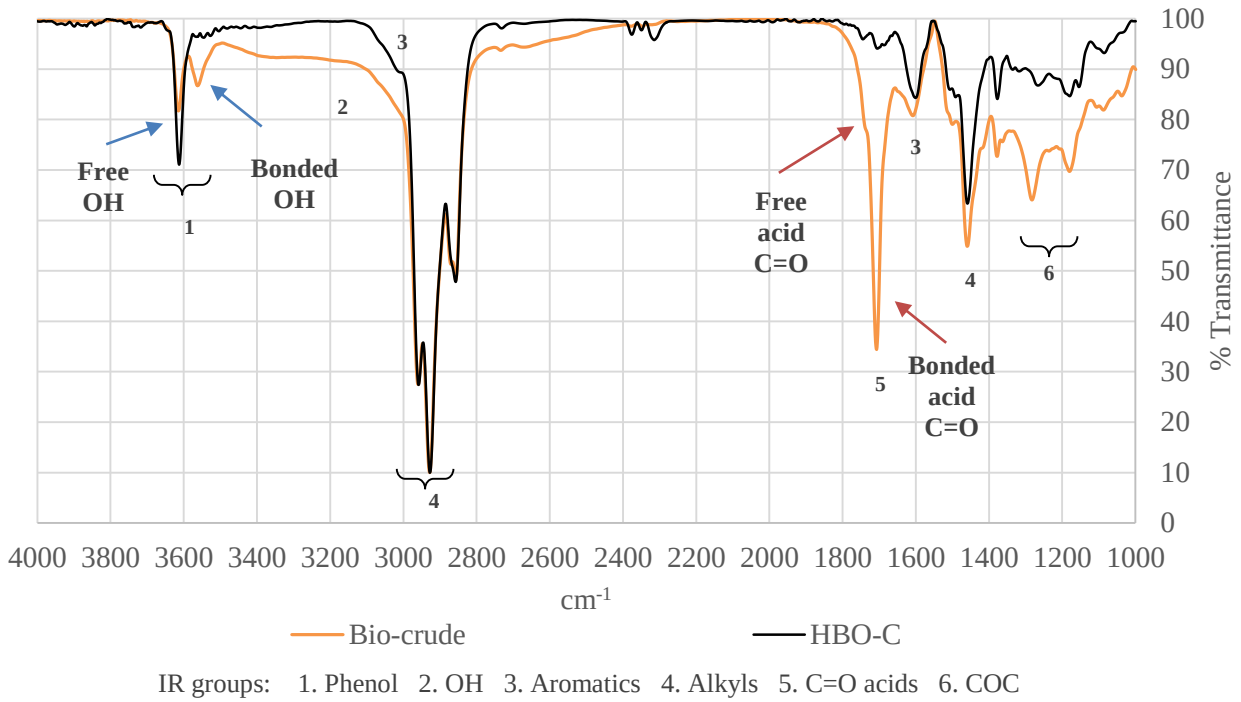

Figure 4-19 FTIR spectra for bio-crude and HDT-bio-oil product HBO-C (i.e. TAN < 1 mg KOH/g, produced at 320 ^{o}C, 1400 psig, and 0.20 h^{-1}).

Comparing the bio-crude and HBO-C in Figure 4-19, some reduction of the aromatics is observed for the hydrotreated oil, as the stretch at 1600 cm^{-1} and the band at 3000 cm^{-1} are slightly shortened. This is in agreement with the effect on the viscosity discussed in Section 4.1.1.2.

The reduction of the TAN in the hydrotreated product HBO-C (i.e. < 1 mg $_{KOH}$ / g $_{oil}$) results in a significant reduction of the inter-molecularly bonded acid carbonyls' stretch at 1710 cm^{-1}. This indicates that most of the acids were converted by hydro-decarboxylation reactions. The small stretch may be associated with the presence of protected carboxylic groups as well as possible ketones remaining in the hydrotreated oil.

The free and bonded phenols are clearly distinguished in the bio-crude, at 3600 and 3550 cm^{-1}, respectively. By reducing the TAN to < 1 mg $_{KOH}$ / g $_{oil}$ the bonded phenols in the hydrotreated oil are reduced, resulting in an increased single band at 3600 cm^{-1}. This is evidence of the

intermolecular and intra-molecular hydrogen bond associations being destroyed by the removal of carboxylic acids, resulting in a significant portion of phenols existing as the monomeric non-aggregated form. This complements the observation that the standard method for TAN measured the acidity caused by carboxylic acids, and phenolic acidity was not accounted for. Further evidence regarding the TAN's detectability for carboxylic acids, and not for phenolic acids is presented in Figure 4-20-a and 4-20-b.

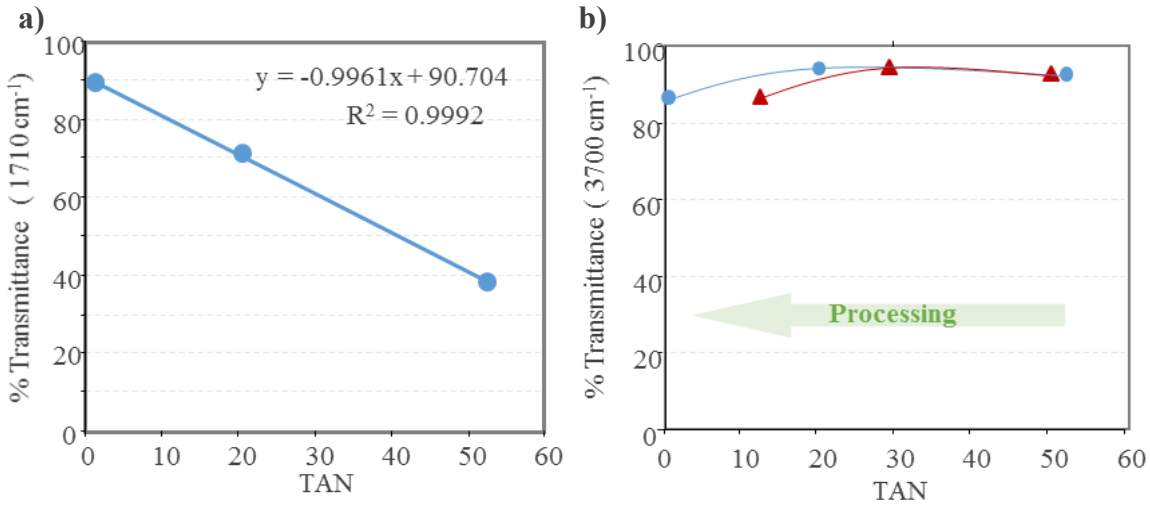

Figure 4-20 FTIR resulting transmittance with respect to the sample's TAN for the bands corresponding to a) carbonyl acids, and b) phenolic acids.

The TAN measurements for different oil samples (i.e. bio-crude, HDT-bio-oil, and CSC-bio-oil) are presented with respect to the transmittance corresponding to carboxylic C=O shown in Figure 4-20-a and phenols in Figure 4-20-b. Regarding the carboxyl C=O (i.e. carboxylic acids), Figure 4-20-a shows a linear correlation between the TAN and the carboxylic acid transmittance of the FTIR spectra. However, no correlation is observed for the phenolic acids (i.e. –OH bands) as seen in Figure 4-20-b. Therefore, the preceding indicates that the reduced TAN pertains exclusively to carboxylics, and thus phenols have no correlation with TAN determined by ASTM D664 used thoughout this study.

With respect to the FTIR for the produced CSC-bio-oils, recalling Figure 4-18, these are depicted in Figure 4-21 for further evaluation.

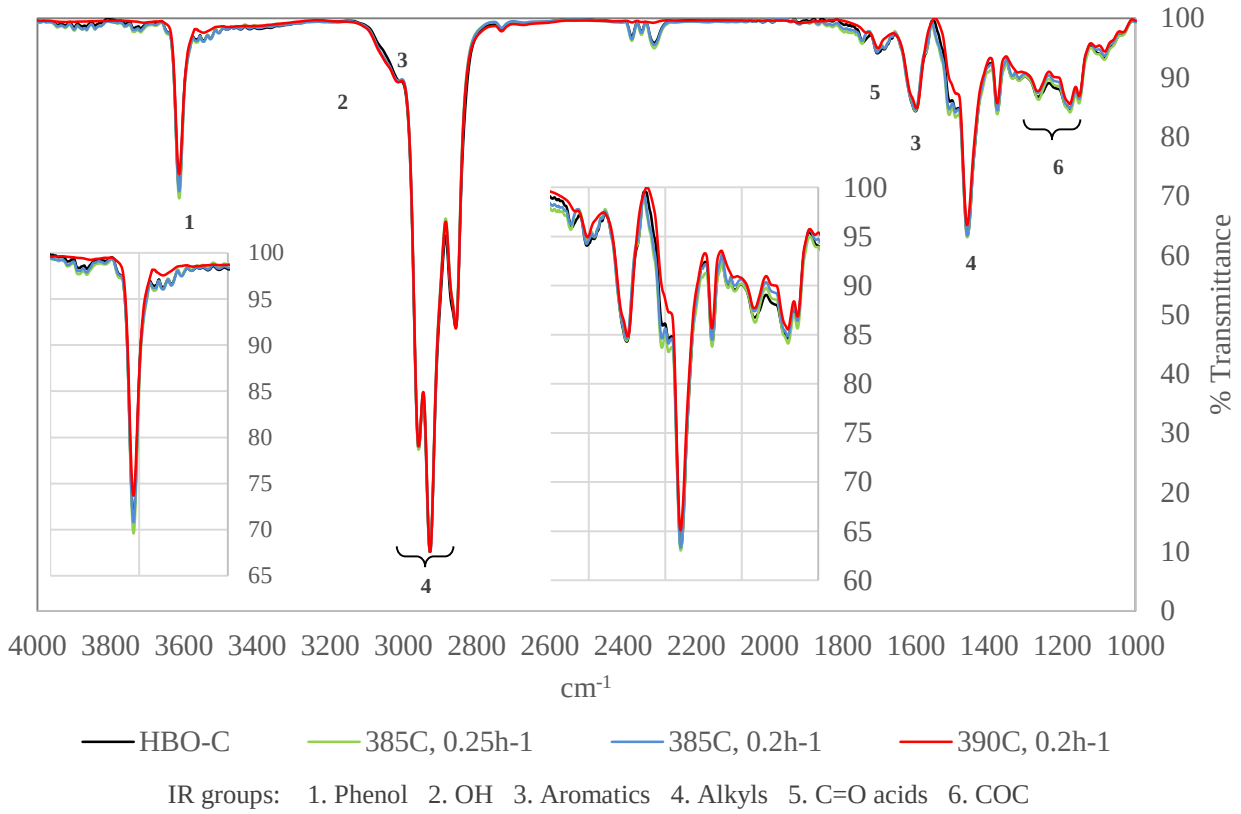

Figure 4-21 FTIR spectra for HBO-C and the CSC-bio-oils produced under different operating conditions.

The resulting spectra for the CSC-bio-oils produced indicate little or no change of phenols, thus evidencing that the CSC catalyst had a minor effect for phenol reduction under the tested conditions. This may be due to the inability of the catalyst to hydrogenate the aromatic phenolic rings, as observed throughout the HDT investigation. Other differences are observed in the ether groups region, where a slight reduction at the most severe CSC condition (i.e. 390 ^{o}C, 0.2 h^{-1}) is shown. This supports the results pertaining the oxygen content removal resulting in the decreased O/C ratio previously discussed in Section 4.2.1.2.

Further investigation to assess a wider range of CSC operating conditions would provide more information regarding the fate of troublesome species present in the bio-crude, and their evolution throughout the upgrading processes herein evaluated.

Chapter Five: Global Mass Balance in Hydrogen

The final exploratory stage of this thesis lies on the recycle of the produced and unconsumed hydrogen from the CSC process, back to the HDT process. This is the novelty of the proposed bio-crude upgrading process herein investigated, given that otherwise recycled, a fresh make up of hydrogen would be required for the HDT stage of the bio-crude upgrading process. The amount of hydrogen consumed (i.e. grams of hydrogen consumed per grams of processed bio-crude) in HTD to produce HBO-C (i.e. lowest TAN, and deepest HDT-bio-oil) was calculated, and it is reported in Section 5.1. Then, the amount of excess hydrogen (i.e. grams of hydrogen produced and unconsumed in the CSC process) was quantified, and it is reported in Section 5.2. Furthermore, the theoretical hydrogen production considering a Catalytic Steam Reforming (CSR) stage to treat the CSC product gases is calculated and presented in section 5.2.1. Consequently, a global mass balance in hydrogen determines the ability of this bio-crude upgrading process to recycle back the unconsumed hydrogen, avoiding the requirements for significant make-up of hydrogen.

5.1. HDT Hydrogen Consumption

Depending on the severity of the HDT process, different hydrogen consumptions were observed. These were reported in Section 4.1.1.6 of this thesis. The more severe HDT conditions in terms of operating temperature, pressure, and WHSV, were found to achieve the highest DOD by HDO reactions, resulting in the highest consumption of hydrogen. To portray a consistent overview of the combined HDT-CSC bio-crude upgrading process, the hydrogen consumption specific to the HDT-bio-oil carried forward as feedstock for the continuously active CSC process is herein presented. That is, the hydrogen consumption required to produce HBO-C.

The atomic balance in hydrogen for the HDT process under 1400 psig, 320 ºC, and 0.20 h^{-1}, in the presence of a HDT catalyst is carried out based on the diagram presented in Figure 5-1.

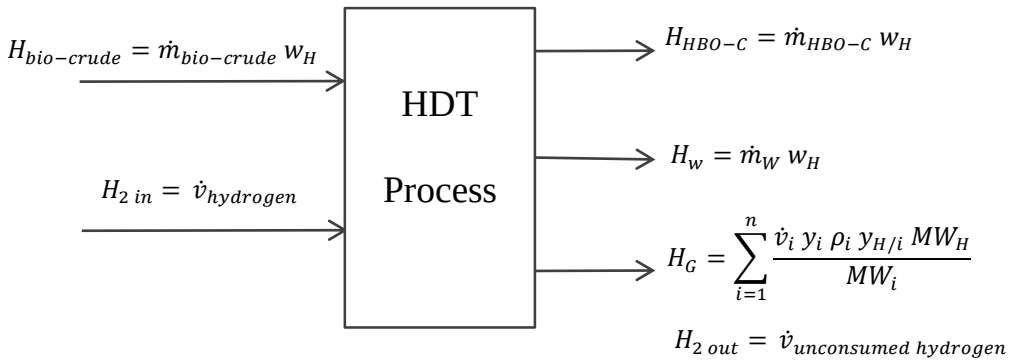

Figure 5-1 Atomic hydrogen balance for the HDT process.

Figure 5-1 illustrates the hydrogen balance for the HDT process, where the mass flow-rate ($\dot{m}$) of hydrogen goes *in* as the hydrogen present in the bio-crude feedstock ($H_{bio-crude}$), and the hydrogen gas reactant; the hydrogen *out* the process (H_{out}) is in the form of hydrogen present in the HDT-bio-oil (H_{HBO-C}), in the water produced by the HDO reactions (H_W), and in the hydrocarbon gaseous products (H_G).

Equation 5-1 presents the overall consumption of atomic hydrogen. The hydrogen present in the bio-crude fed into the process is based on the hydrogen mass fraction (w_H) determined by elemental analysis of the oil, and it is calculated by Equation 5-2. Equation 5-3 describes the overall atomic hydrogen *out* the process.

$$Consumption\ of\ atomic\ H = H_{out} - H_{bio-crude} \qquad \text{Equation } 5-1$$

$$H_{bio-crude} = \dot{m}_{bio-crude}\, w_H \qquad \text{Equation } 5-2$$

$$H_{out} = H_{HBO-C} + H_W + H_G \qquad \text{Equation } 5-3$$

The atomic hydrogen present in the produced HBO-C, in the produced water, and in the hydrocarbon gaseous products is calculated by Equations 5-4, 5-5, and 5-6, respectively.

$$H_{HBO-C} = \dot{m}_{HBO-C}\, w_H \qquad \text{Equation } 5-4$$

$$H_w = \dot{m}_W\, w_H \qquad \text{Equation } 5-5$$

$$H_G = \sum_{i=1}^{n} \frac{\dot{v}_i\, y_i\, \rho_i\, y_{H/i}\, MW_H}{MW_i} \qquad \text{Equation } 5-6$$

The hydrocarbon gaseous products observed during the HDT process and their corresponding mole fractions (y_i) are presented in Table 5-1.

Table 5-1 Hydrocarbon gaseous products observed during the production of HBO-C.

Component *i*	y_i, mol i/mol gas
Methane	0.006
Ethane	0.004
Propane	0.002
Butylene	0.001
Butane	0.016

Finally, the yield of consumed hydrogen presented as grams of consumed hydrogen per grams of bio-crude feedstock in the HDT process is calculated by Equation 5-7, and the result is presented in Table 5-2.

$$yield_{\ hydrogen\ consumed} = \frac{(H_{out} - H_{bio-crude})\ MW_{H_2}}{MW_H\, y_{H/H_2}} \qquad \text{Equation } 5-7$$

Table 5-2 HDT process operation description, including the hydrogen consumption to produce HBO-C.

Pressure, psig	Temperature, ºC	WHSV, h^{-1}	TAN, mg $_{KOH}$ / g $_{oil}$	DOD, %	Consumed H_2, mg H_2 / g oil
1400	320	0.20	< 1	58.9 ± 0.2	21

Therefore, to produce a deeply hydrotreated bio-oil from an originally highly oxygenated bio-crude, a hydrogen consumption of 21 mg-H_2 per g-bio-crude was required. The HDT-bio-oil is then carried forward as feedstock for the CSC process, where water is introduced as the source of hydrogen.

The present thesis investigation proposes the recycle of the unconsumed hydrogen produced by the subsequent CSC upgrading process. The results regarding such unconsumed hydrogen are presented in the following Section 5.2.

5.2. CSC Unconsumed Hydrogen

The exploration of the CSC process for the hydrotreated oil HBO-C presented in Section 4.2 evaluated different operating conditions and resulted in the production of different qualities of bio-oil. When using a catalyst able to perform water splitting, hydrogen is produced in the reactor and used to hydrogenate heavy molecules. At the same time, cracking reactions take place. Consequently, hydrogen was produced throughout the CSC process, where some of the produced hydrogen was consumed by the saturation of organic free radicals, and the remainder-unconsumed hydrogen could be quantified.

The yield of unconsumed hydrogen presented as grams of hydrogen per grams of HDT-bio-oil (i.e. HBO-C) feedstock in the CSC process is calculated by Equation 5-8, and the results are presented in Figure 5-2.

$$yield_{\ hydrogen\ unconsumed} = \frac{\left(\dot{v}_g - \dot{v}_{N_2}\right) y_{H_2}\ \rho_{H_2}}{\dot{v}_{HBO-C}\ \ \rho_{HBO-C}} \qquad \text{Equation } 5-8$$

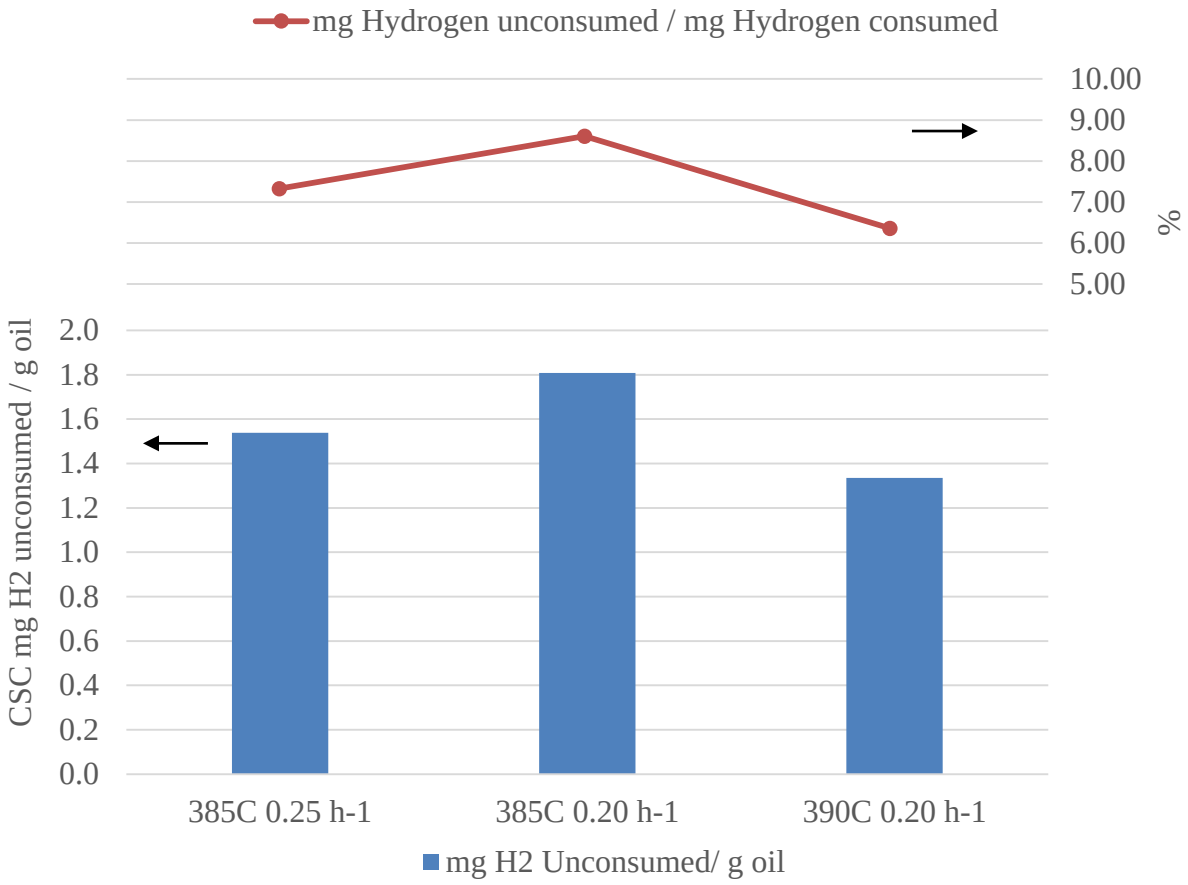

Figure 5-2 CSC unconsumed hydrogen yield (i.e. grams of unconsumed hydrogen over grams of HBO-C feedstock), and the percentage of hydrogen available to meet recycle requirement for HDT process.

Figure 5-2 presents the yield of unconsumed hydrogen, as grams of unconsumed hydrogen per grams of HDT-bio-oil, quantified from the CSC gaseous products stream. The yield of unconsumed hydrogen varies depending on the CSC operating condition. The highest yield of unconsumed hydrogen was observed for 385 ^{o}C, and 0.20 h^{-1}, meeting 8.6 % of the hydrogen required for the HDT process. Therefore, and in order to improve the recycle of hydrogen back into the HDT process to meet the high hydrogen demand, the catalytic steam reforming of the light

hydrocarbons produced is investigated. The theoretical approach is presented in the following Section 5.2.1.

5.2.1. Catalytic Steam Reforming (CSR).

Steam reforming is an industrial technology that produces hydrogen gas from methane or higher molecular weight alkanes. The general chemical reaction for complete steam reforming is given by Equation 5-9 (Duprez, 1992)

$$C_nH_x + 2n\ H_2O \leftrightarrow n\ CO_2 + \left(2n + \frac{x}{2}\right) H_2 \qquad \text{Equation 5-9}$$

If n=1 and x=4, Equation 5-9 becomes the methane steam reforming reaction. Since the maximum value of x is 2n+2 for alkanes, the maximum hydrogen yield is 3n+1 for a production of n molecules of CO_2. Then, the ratio H_2:CO_2 is maximized for methane and it is 4:1. For other alkanes, this ratio varies from 3:1 to 4:1 (Duprez, 1992).

Therefore, upon treatment of the gaseous stream containing light hydrocarbons such as methane, ethane, propane, and butane, the resulting products are carbon dioxide and hydrogen. The modified hydrogen recovery process envisages the installation of hydrogen permeation membranes in the reformer tube, thus permitting direct production of high-purity hydrogen in the reformer. In addition, gaseous hydrocarbon conversion is increased as the removal of hydrogen displaces the chemical equilibrium towards the product side (Oertel, et al., 1987).

The theoretical determination of the production of hydrogen from the CSR of the CSC gaseous products stream was herein performed. This allowed for evaluating the efficiency of the CSR process, and the feasibility of producing the required hydrogen to be recycled back to the HDT process as illustrated in Figure 1-1. The combination of the unconsumed hydrogen resulting from

the CSC process, and the hydrogen recovered from the CSR process were calculated and are presented in Figure 5-3.

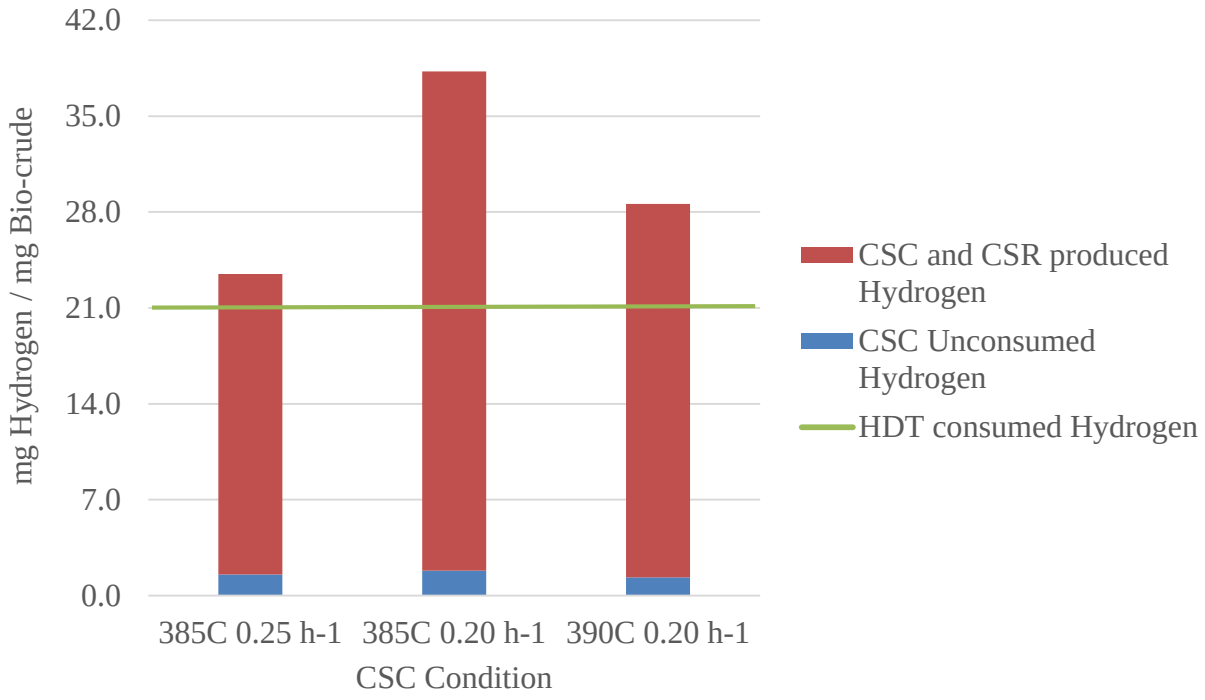

Figure 5-3 Hydrogen yield overview for different CSC operating conditions and the contribution of the theoretical hydrogen yield by CSR.

Calculations show that, the CSC unconsumed hydrogen in addition to the CSR of the CSC gaseous stream, as observed in Figure 5-3, surpasses the hydrogen requirements for the bio-crude HDT producing HBO-C. These results are promising given that the CSC catalyst is in essence a steam reforming catalyst, and all the hydrocarbon gases of the sequential processes can be recycled to the CSC or the beds in a multi-reactor configuration needed for the purpose of regeneration, and thus can be alternatively used for CSC and CSR. This would allow for the overall hydrogen recycle process to be deemed possible for the HDT-CSC upgrading of lignocellulose derived bio-crude. Nevertheless, this remains at a theoretical stage and require further exploration as part of future developments of this pioneer bio-crude upgrading investigation.

Chapter Six: Final Remarks and Recommended Future Work

This final chapter presents the conclusions of the work done to assess the viability of processing Steeper Energy Hydrofaction™ Renewable Crude Oil (bio-crude) as part of a proposed pioneer upgrading scheme with Hydrotreating followed by Catalytic Steam Cracking, both evaluated separately in fixed-bed reactors as conversion units. The exploration of different variables and their effect on the produced oil was investigated for each process. The objective of HDT is to hydrogenate oxygenates present, and thus reduce the acidity of the bio-crude; then, the CSC process improves the quality of the bio-oil through the conversion of the oil via thermal cracking and hydrogen addition from catalytic steam dissociation reactions. Therefore, general goal of the present research project was to explore the overall upgrading process for lignocellulose derived bio-crude, and whether the required hydrogen make-up level may be reduced by the hydrogen recycle proposed in the catalytic upgrading scheme. The conclusions reached are herein presented.

HDT process

A thorough screening of different operating variables for the HDT process was performed to evaluate the effect that each operating condition had on the HDO reactions desired for the highly oxygenated bio-crude feedstock. The parameters evaluated were Temperature, Weight Hourly Space Velocity (WHSP), Hydrogen-to-oil (HTO) ratio, and Pressure. Each variable had a different effect on the quality of the produced oil. This was monitored in terms of degree of hydro-deoxygenation (DOD) monitored by water production, total acid number (TAN) reduction by hydro-decarboxylation and carbon dioxide production, effects on viscosity and micro carbon residue (MCR). The HDT process operating at the highest tested pressure (1400 psig) secured a higher solubility of hydrogen in the oil and thereby a higher availability of hydrogen in the vicinity

of the catalyst, resulting in a deeper HDT process. A combination of high severity conditions including the highest pressure used (1400 psig), a longer residence time with a WHSV of 0.20 h^{-1}, a temperature of 320 ^{o}C, and an improved catalyst with a higher hydrogenating agent composition resulted in the production of the most hydrotreated bio-oil (HBO-C). The lowest TAN was achieved by the preceding most severe HDT operation, resulting in a TAN < 1 mg $_{KOH}$/g (DOD 59 %), with a remaining oxygen content of 5.1 %. Such results indicated the inability of the HDT process to treat phenolic acidity under the tested conditions, as evidenced by the FTIR results presented in Section 4.2.2. Regarding the carboxyl C=O (i.e. carboxylic acids), a linear correlation between the TAN and the carboxylixc acid transmittance of the FTIR spectra was observed. However, no correlation was observed for the phenolic acids (i.e. –OH bands). Therefore, the preceding indicates that the reduced TAN pertains exclusively to carboxylics, and thus phenols have no correlation with TAN determined by ASTM D664 used thoughout this study.

CSC process

Three HDT-bio-oils were produced and tested as feedstock for the CSC process, each with a different TAN. The HDT-bio-oils with TAN > 11 mg $_{KOH}$/g caused the rapid deactivation of the CSC catalyst. TGA and GC results evidenced that the main cause of deactivation of the catalyst, as observed in Section 4.2.1, related to a remaining high acidity of the HDT-bio-oil in feedstocks HBO-A (TAN 21.3 mg $_{KOH}$/g) and HBO-B (TAN 11.6 mg $_{KOH}$/g). Thus, by performing a deeper hydrogenation of the feedstock, and achieving a TAN < 1 mg $_{KOH}$/g in HBO-C, a reduction of the coke deposition on the surface of the CSC catalyst was accomplished, allowing for a continuous CSC operation of 325 hours.

Also, different operating conditions were evaluated for the HBO-C as feedstock under two different reaction temperatures, and two WHSVs. Regarding the quality of the CSC-bio-oil produced, the residue conversion achieved at each CSC condition evaluated was determined by TGA and compared to HTSD results. Regarding the residue conversion, HTSD results were found to correspond to those calculated from the TGA. Residue conversion was found to increase with CSC operating condition severity, however there was no significant difference between the 385 and 390 ^{o}C tests at a WHSV of 0.20 h^{-1}. Furthermore, Catalytic Steam Cracking as secondary process completed desired conversion to petroleum equivalents of 5.6% Naphtha (IBP-190^{o}C), 12.8% Jet-fuel (190-260^{o}C) and 25.6% Diesel (260-343^{o}C) range hydrocarbons. Finally, the CSC operations are to be further optimized for the increased production of diesel.

Global mass balance in hydrogen

The novelty of the proposed scheme relies on the fact that the unconsumed hydrogen produced in CSC may be recycled back to the HDT unit, thus reducing the fresh hydrogen make-up otherwise required for this unit. The amount of hydrogen consumed (i.e. grams of hydrogen consumed per grams of bio-crude) in the HTD process to produce HBO-C (i.e. lowest TAN, and deepest HDT-bio-oil) was calculated to be 21.0 mg of hydrogen consumed per grams of bio-crude, as reported in Section 5.1. The amount of excess hydrogen (i.e. grams of hydrogen produced and unconsumed in the CSC process per grams of bio-oil) was quantified and the highest yield was 1.83 mg of unconsumed hydrogen in the CSC process per grams of bio-crude, as reported in Section 5.2. Therefore, the recycle of the unconsumed hydrogen from the CSC stage would meet 8.6 % of the hydrogen requirement for the HDT stage of the bio-crude upgrading process. Nevertheless, the theoretical hydrogen available for recovery considering a CSR stage to treat the CSC hydrocarbon gaseous stream was calculated, and the yield exceeded the hydrogen requirements for the HDT

stage. These results are promising given that the CSC catalyst is in essence a steam reforming catalyst and all the hydrocarbon gases of the sequential processes can be recycled to the CSC or the beds in a multi-reactor configuration, needed for the purpose of regeneration and thus can be alternatively used for CSC and CSR. However, this remains at a theoretical stage and require further exploration as part of future developments of this pioneer bio-crude upgrading investigation.

Recommended Future Work

The primary objective of this first-of-a-kind bio-crude upgrading investigation was to assess the bio-crude's progression towards a low acid and low oxygen content petroleum like oil. However, some developments remain to be done in the future to better understand the process, its kinetics, and economics. For instance, the optimization of the operating conditions for both HDT and CSC processes is required. The present thesis reports an overview of the complete process, however these were investigated separately. Therefore, the merging of the processes into one single continuous operation must be performed. Also, the experimental exploration of the CSR of the CSC hydrocarbon gaseous stream to determine the experimental hydrogen yields for the recycle stage require testing. Also, the development of a kinetic model is an important factor to have a better understanding of the process and be able to predict product quality at different operating conditions. Furthermore, the economic aspect of the process must be investigated, to assess the feasibility of the HDT-CSC and CSR stages required. The proposed upgrading scheme was designed based on successfully recycling the unconsumed hydrogen, but the reliability of this assumption is key to the economics of the process. Although this is a costly and time-consuming investigation, efforts must be made in the future in order to really understand the potential of this application.

References

Aitani, A. M., 2004. Oil refining and products. In: *Encyclopedia of Energy, ed.*. C. J. Cleveland(New Yourk): Elsevier, pp. 715-729.

Akhtar, J. & Amin, N., 2011. A Review on Process Conditions for Optimum Bio-Oil Yield in Hydrothermal Liquiefaction of Biomass. *Renew. Sustain. Energy Rev.,* Volume 15, pp. 1615-1624.

Alfke, G., Irion, W. & Neuwirth, O., 2008. Energy Sources for Transportation. In: *Handbook of Fuels.* Weinheim: Wiley-VCH.

Antal Jr., M. J. et al., 1987. Heterolysis and homolysis in supercritical water. *Supercritical Fluids*, p. 77–86.

Antal, M. J., Mok, W. S. L. & Richards, G. N., 1990. *Carbohydr. Res. ,* Volume 199, p. 91.

ASTM-D2892, 2011. Standard Test Method for Distillation of Petroleum (15-theoretical plates column).

ASTM-D5236, 2011. Standard Test Method for Distillation of Heavy Hydrocarbon Mixtures (Vacuum Pot Still Method).

ASTM-D664, 2011. Standard Test Method for Acid Number of Petroleum Products by Potentiometric. pp. 1-10.

ASTM-D975, 2015. *Standard Specification for Diesel Fuel Oils.* [Online] Available at: http://www.astm.org/Standards/D975.htm [Accessed January 2018].

Baker, E. & Elliot, D., 1988. Catalytic hydrotreating of biomass-derived oils. In: *Pyrolysis Oils from Biomass.* Washington(DC): American Chemical Society, pp. 228-240.

Balat, M., 2011. *Energy Convers. Manage.,* Volume 52 , p. 858–875.

Bali, G., Meng, X. & Deneff, J., 2015. The effect of alkaline pretreatment methods on cellulose structure and accessibility. *Chem Sus Chem*, 2(8), p. 275–279.

Banerjee, D. K., 2012. *Oil Sands, Heavy Oil & Bitumen From Recovery to Refinery.* Oklahoma: Penn Well Corporation.

Berl, E., 1944. Production of oil from plant material. *Science,* 99(2573), p. 309–312.

Bobleter, O., 1994. Hydrothermal degradation of polymers derived from plants. *Prog. Polym. Sci.,* Issue 19, pp. 797-841.

Boelhouwer, J. W. M., Nederbragt, G. W. & Verberg, G., 1951. Viscosity Data of Organic Liquids. *Appl. Sci. Res.,* Volume 2, pp. 249-268.

Branca, C., Giudicianni, P. & Blasi, C. D., 2003. GC/MS Characterization of Liquids Generated from Low-Temperature Pyrolysis of Wood. *Industrial & Engineering Chemistry Research* , 42(14), pp. 3190-3202.

Bridgwater, A., Toft, A. & Brammer, J., 2002. A techno-economic comparison of power production by biomass fast pyrolysis with gasification and combustion.. *Renew. Sustain. Energy Rev.,* Volume 6, pp. 181-246.

Bridgwater, A. V. & Peacocke, G. V. C., 2000. Fast Pyrolysis Processes for Biomass. *Renewable and Sustainable Energy Reviews,* 4(1), pp. 1-73.

Carbognani, L., Carbognani Arambarri, J., Molero, H. & Pereira-Almao, P., 2013. High Temperature Simulated Distillation of Bitumen Fractions with Open Tubular Capillary Columns Depleted in Silicone/Siloxane Stationary Phases. *Energy & Fuels,* 27(4), pp. 2033-2041.

Carbognani, L. et al., 2014. Reliable Determination of Water Contents of Bitumen and Vacuum Residua via Coulometric Karl Fischer Titration Using Tetrahydrofuran. *Petroleum Science and Technology,* 5(32), pp. 602-609.

Czernik, S. & Bridgwater, T., 2004. Overview of Applications of Biomass Fast Pyrolysis Oil. *Energy*, Volume 18, pp. 590-598.

Daudin, A., Bournay, L. & Chapus, T., 2013. *Method for converting effluents of renewable origin into fuel of excellent quality by using a molybdenum-based catalyst.* US, Patent No. 0163458 .

Deguchi, S., Tsujii, K. & Horikoshi, K., 2006. Cooking cellulose in hot and compressed water. *Chemical Communication*, Issue 31, p. 3293–3295.

Demirbas, A., 2005. Thermochemical Conversion of Biomass to Liquid products in the Aqueous Medium. *Energy Source,* Issue 27, pp. 1235-1243.

Demirbas, A., Gullu, D., Çaglar, A. & Akdeniz, F., 1997. Estimation of calorific values of fuels from lignocellulosics. *Energy Sources,* Volume 19, p. 765–770.

Diebold, J., 2000. A Review of the Chemical and Physical Mechanisms of the Storage Stability of Fast Pyrolysis Bio-Oils; National Renewable Energy Laboratory. *Energy,* 2(1).

Dote, Y. et al., 1994. Recovery of liquid fuel from hydrocarbon-rich microalgae by thermochemical liquefaction. *Fuel,* Issue 73, pp. 1855-1857.

Duprez, D., 1992. Selective steam reforming of aromatic compounds on metal catalysts. *Applied Catalyst A: General,* Volume 82, p. 111–157.

ECN, 2012. *Database for biomass and waste.*. [Online]
Available at: https://www.ecn.nl/phyllis2/
[Accessed January 2017].

Egeberg, R., Michaelsen, N. & Skyum, L., 2009. *Novel hydrotreating technology for production of green diesel,* Lyngby: Haldor Topsøe A/S.

Eisentraut, A., 2010. *Sustainable Production of second-generation biofuels: potential and perspective in major economies and developing countries.,* Paris: International Energy Agency.

Elliott, D., 2007. Historical developments in hydroprocessing bio-oils. *Energy Fuels*, 21(3), pp. 1792-1815.

Elliott, D. C. et al., 1991. Developments in direct thermochemical liquefaction of biomass. *Energy Fuels,* 3(5), pp. 399-410.

Elliott, D. et al., 2009. Catalytic hydroprocessing of biomass fast pyrolysis bio-oil to produce hydrocarbon products. *Environ Prog Sustainable Energy,* 28(3), pp. 441-449.

Elliott, D. & Neuenschwander, G., 1998. Liquid fuels by low-severity hydrotreating of biocrude. Abstr 1998;39:259. *Fuel Energy,* 39(259).

Elliott, D. & NG, G., 1996. *Developments in thermochemical biomass conversion.* 1st Edition ed. London: Kluwer Academic Publishers.

Elliott, D. & Schiefelbein, G., 1989. *Liquid hydrocarbon fuels from biomass.* Richland, Pacific Northwest Laboaratory, pp. 1160-1166.

Flinn, R., Larson, O. & Beuther, H., 1960. The Mechanism of Catalytic Hydrocracking. *Ind. Eng. Chem.*, 52(2), p. 153.

Funazukuri, T., Wakao, N. & Smith, J., 1990. Liquefaction of lignin sulfonate with subcritical and supercritical water. *Fuel,* 3(63), pp. 349-353.

Furimsky, E., 2000. Catalytic hydrodeoxygenation. *Appl. Catal. A: General,* 199(2), pp. 147-190.

Gandarias, I. et al., 2008. From biomass to fuels: hydrotreating of oxygenated compounds. *Int. J. Hydrog Energy,* Issue 33, pp. 3485-3488.

Garcia-Hubner, E. A., 2015. *Catalysts Evaluation for Catalytic Steam Cracking of De-asphalted Oil in a Fixed Bed Reactor*, Calgary: University of Calgary.

Grange, P. et al., 1996. Hydrotreatment of pyrolysis oils from biomass: Reactivity of the various categories of oxygenated compounds and preliminary techno-economical study. *Catal. Today*, 29(1-4), pp. 297-301.

Guisnet, M. & Magnoux, P., 2001. Organic chemistry of coke formation. *Applied Catalysis A: General*, Volume 212, pp. 83-96.

Hassan, A., Carbognani, L. & Pereira-Almao, P., 2008. Development of an alternative setup for the estimation of microcarbon residue for heavy oil and fractions: Effects derived from air presence. *Fuel*, 87(17), pp. 3631-3639.

Huang, H. et al., 1996. Distillation of Liquid Fuels by Thermogravimetry. *Am. Chem. Soc. Prep. Pet. Chem. Div.*, Issue 41, pp. 87-92.

Huber, G., Iborra, S. & Corma, A., 2006. Synthesis of Transportation Fuels from Biomass: Chemistry, Catalysts, and Engineering. *Chem. Rev.*, Issue 106, pp. 4044-4098.

Iversen, S., 2015. *Process and apparatus for producing liquid hydrocarbon.* s.l. Patent No. Patent WO2012/167794.

Jensen, C. et al., 2017. Fundamentals of Hydrofaction™: Renewable crude oil from woody biomass. *Biomass Conv. Bioref.*, 7(4), p. 495–509.

Junming, X., Jianchun, J., Yunjung, S. & Yanju, S., 2008. Bio-oil upgrading by means of ethyl ester production in reactive distillation to remove water and to improve storage and fuel characteristics. *Biomass and Bioenergy*, Volume 32, pp. 106-156.

Karagöz, S., Bhaskar, T., Muto, A. & Sakata, Y., 2005. Comparative studies of oil compositions produced from sawdust, rice husk, lignin and cellulose by hydrothermal treatment. *Fuel,* 7-8(84), pp. 875-884.

Karatzos, S., McMillan, J. & Saddler, J., 2014. *The potential and challenges of drop-in biofuels.* IEA Bioenergy.

Kruse, A. & Gawlik, A., 2003. Biomass Conversion in Water at 330−410 °C and 30−50 MPa. Identification of Key Compounds for Indicating Different Chemical Reaction Pathways. *Ind. Eng. Chem. Res.* , 2(42), p. 267–279.

Kwon, K. et al., 2011. Catalytic Deoxygenation of Liquid Biomass for Hydrocarbon Fuels. *Renew. Energy,* Volume 36, pp. 907-915.

Li, H. et al., 2010. The formation of bio-oil from sludge by deoxy-liquefaction in supercritical ethanol. *Bioresour. Technol.,* Issue 101, pp. 2860-2866.

Lillebø, A. H., Holmen, A., Enger, B. C. & Blekkan, E. A., 2013. Fischer–Tropsch conversion of biomass-derived synthesis gas to liquid fuels. *WIREs Energy amd Environment* , Volume 2, pp. 507-524.

Marzin, R. et al., 1998. New residue process increases conversion, produces stable residue in Curacao refinery. *Oil & Gas Journal,* pp. 79-86.

Mercader, F. d. M. et al., 2010. Production of advanced biofuels: Co-processing of upgraded pyrolysis oil in standard refinery units. *Appl. Catal. B: Environ.,* Volume 96, pp. 57-66.

Mohan, D., Pittman, C. & Steele, P., 2006. Pyrolysis of wood/biomass for bio-oil: A critical review. *Energy Fuels,* Issue 20, p. 848–889.

Mortensen, P. et al., 2011. A review of catalytic upgrading of bio-oil to engine fuels. *Applied Catalysis A: General,* Volume 407, pp. 1-19.

Narayan, R. & Antal Jr., M., 1990. Influence of pressure on the acid catalyzed rate constant for 1-propanol dehydration in supercritical water. *J. Am. Chem. Soc.,* 5(112), p. 1927–1931.

Oertel, M. et al., 1987. Steam Reforming of Natural Gas with Integrated Hydrogen Separation for. *Chem. Eng. Technol.,* Volume 10, pp. 248-255.

Okuda, K., Man, X. & Umetsu, M., 2004. Efficient conversion of lignin into single chemical species by solvothermal reaction in water– p-cresol solvent.. *J. of Physics. Condens. Matter,* Volume 16, p. 1325– 1330.

Pachauri, R. K. et al., 2014. *Climate change 2014: Synthesis report. Contribution of Working Groups I, II and III to the Fifth Assessment Report of the Intergovernmental Panel on Climate Change,* Geneva, Switzerland: IPCC.

Patel, M. & Kumar, A., 2016. Production of renewable diesel through the hydroprocessing. *Renewable and Sustainable Energy Reviews,* Volume 58, pp. 1293-1307.

Paul de Wild, H. R. &. E. H., 2011. Biomass pyrolysis for chemicals. *Biofuels,* 2(2), pp. 185-205.

Pereira-Almao, P. et al., 2013. *Systems and Methods for Catalytic Steam Cracking of Non Asphaltene Containing Heavy Hydrocarbons.* US, Patent No. 20130015100 A1.

Pereira, P. et al., 2001. Aquaconversion technology offers added value to E. Venezuela synthetic crude oil production. *Oil & Gas Journal: International Petroleum News and Technology,* 99(20), pp. 78-85.

Pereira, P. et al., 1999. *Steam Conversion Process and Catalyst.* United States, Patent No. 5885441.

Peterson, A. A. et al., 2008. Thermochemical biofuel production in hydrothermal media: A review of sub- and supercritical water technologies. *Energy & Environmental Science,* Volume 1, pp. 32-65.

Praharso, A., Trimm, D. & Cant, N., 2004. Kinetic Study of iso-Octane Steam Reforming Over a Nickel-Based Catalyst. *Chemical Engineering Journal,* Volume 99, pp. 131-136.

Quitain, A., Sato, N., Daimon, H. & K., F., 2003. Qualitative investigation on hydrothermal treatment of hinoki (Chamaecyparis obtusa) bark for production of useful chemicals. *J. Agric. Food Chem.,* 27(51), pp. 7926-7929.

Ragauskas, A. J. et al., 2006. The path forward for biofuels and biomaterials. *Science,* 311(5760), p. 484–489.

Raia, J., Villalanti, D., Subramanian, M. & Williams, B., 2000. Application of High-Temperature Simulated Distillation to the Residuum Oil Supercritical Extraction Process in Petroleum Refining. *Journal of Chromatographic Science,* Volume 38.

Ramirez, J., Brown, R. J. & Rainey, T. J., 2015. A Review of Hydrothermal Liquiefaction Bio-Crude Properties and Prospects for Upgrading to Transportation Fuels. *Energies,* June, Volume 8, pp. 6765-6794.

Righi, T., 2016. *Evaluation of Catalytic Steam Cracking Process for Total Acid Number Reduction of Heavy Oils,* Calgary: University of Calgary.

Robinson, P. & Dolbear, G., 2007. Hydrotreating and Hydrocracking: Fundamentals.. In: *Practical Advances in Petroleum Processing.* s.l.:Springer, pp. 177-218.

Roedl, A., 2010. Production and energetic utilization of wood from short rotation coppice — A life cycle assessment. *International Journal of Life Cycle Assessment,* 15(6), pp. 567-578.

Saisu, M. et al., 2003. Conversion of lignin with supercritical water-phenol mixtures. *Energy Fuels,* 4(17), pp. 922-928.

Schaschke, C., 2014. *A Dictionary of Chemical Engineering.* Oxford: Oxford University Press.

Schwartz, H., Brownlee, R. G., Boduszinski, M. M. & Su, F., 1987. Simulated Distillation of High-Boiling Petroleum Fractions by Capillary Supercritical Fluid Chromatography and Vacuum Thermal Gravimetric Analysis. *Anal. Chem.,* Issue 59, pp. 1393-1401.

Silverstein, R., Webster, F. & Kiemle, D., 2005. *Identification of Organic Compounds.* Hoboken(NJ): John Wiley and Sons.

Sjöström, E., 1993. *Wood chemistry: fundamentals and applications.* 2nd ed. San Diego: Academic press.

Speight, J. G., 2014. *High Acid Crudes.* United States: Elsevier Inc, Gulf Professional Publishing.

Stangeland, K., Kalai, D., Li, H. & Yu, Z., 2017. CO2 methanation: the effect of catalysts and reaction. *Energy Procedia ,* pp. 2022-2027.

Tang, Z. et al., 2009. One step bio-oil upgrading through hydrotreatment, esterification, and cracking.. *Ind Eng Chem Res,* Volume 48, pp. 6923-6929.

Tews, I. et al., 2014. *Biomass direct liquefaction options: technoeconomic and life cycle assesment.,* Richland: Pacific Northwest National Lab.

Thiel, P. A. & Madey, T. E., 1987. The Interaction of Water With Solid Surfaces: Fundamental Aspects.. *Surface Science Reports,* 7(6-8), pp. 211-385.

Trujillo-Ferrer, G. L., 2008. *Thermal and Catalytic Steam Reactivity Evaluation of Athabasca Vacuum Gasoil,* Calgary: University of Calgary.

United-Nations, 2015. *Framework Convention on Climate Change, Adoption of the Paris Agreement.* Paris, United Nations.

Venderbosch, R. et al., 2010. Stabilization of biomass-derived pyrolysis oils. *J. Chem. Technol. Biotechnol.*, pp. 674-686.

Vitale, G., Frauwallner, M., Scott, C. & Pereira-Almao, P., 2011. Preparation and characterization of low-temperature nano-crystalline cubic molybdenum carbides and insights on their structures. *Applied Catalysis A: General,* Volume 408, pp. 178-186.

Ward, J., 1993. Hydrocracking processes and catalysts. *Fuel Processing Technology*, 35(1), pp. 55-85.

Watanabe, M. et al., 2005. Glucose reactions with acid and base catalysts in hot compressed water at 473 K. *Carbohydr Res.,* 12(340), pp. 1925-1930.

Weisser, O. & Landa, S., 1973. *Sulphide catalysts, properties and applications.* New York: Pergamon Press.

Wildschut, J., Mahfud, F., Venderbosch, R. & Heeres, H., 2009. Hydrotreatment of Fast Pyrolysis Oil Using Heterogeneous Noble-Metal Catalysts. *Industrial and Engineering Chemistry Research,* 48(23), pp. 10324-10334.

Zhang, Q., Chang, J., Wang, T. & Xu, Y., 2007. Review of biomass pyrolysis oil properties and upgrading research. *Energy Convers. Manage.,* Volume 48, pp. 87-92.

Zingjie, L., Liguang, L. & Shui, Y., 2006. Thermogravimetry analysis of fuel film evaporation. *Chinese Science Bulletin,* Issue 51, pp. 2150-2157.

Appendix I: Overview of Pilot Plant Assessment and Modifications

Water Content in the Organic Products

Temperature of the Hot Separator: The temperature of vaporization of the water at 900 and 400 psig, for HDT and CSC, respectively, was determined by using the Clausius –Clapeyron equation. Corresponding boiling material at < 235°C at 400 psig, or < 270°C at 900 psig is named "light organic material".

To achieve a complete separation of the water from the organic liquid product flowing through the hot separator, a screening of temperatures (i.e. 270-290 ^{o}C) was performed. The results obtained indicate that even at 290^{o}C (wall thermocouple temperature) a complete separation of the water was not achieved. Higher temperature conditions were not tested to avoid any potential polymerization of the material. Instead, the residence time of the liquid product in the hot separator was investigated.

Operating the Bang-Bang valve system.

The Bang-Bang valve system is the term herein used to describe the two-valve-system described in Section 3.2. Optimization of the Bang-Bang system is critical to obtain the liquid product samples without significantly affecting the pressure in the system. By adjusting the residence time of the liquid product in the hot separator, it is also possible to improve the separation of the water from the organic product, without significantly altering the quality of the oil.

Four main parameters are involved in the automatic operation of these valves: the time for V-18 (upper valve) to remain open, the delay time between V-18 closing and V-19 (lower valve) opening, the repeat time in which V-19 closes and V-18 opens. Based on practical experience, repeat time and delay time was set at 5 seconds while the time the sample takes to move from the 3 ml accumulator toward the tank (V-19 open) was set to 290 seconds, to favor the complete

transfer of the liquid. However, the time V-18 remained open was calculated depending on the hydrocarbon flowrates, aiming to obtain the complete transfer into the sampling tank. By experience, it was established that at least 10% of the 3 ml accumulator must remain empty to assure the total transfer of any extra oil pumped by malfunction of the pump.

During normal operation, the liquids obtained in the hot separator (S1) are transferred to a 150 ml storage tank (T1) as aliquots flowing through the Bang-Bang controlled with a LabVIEW Program. The programming of the Bang-Bang is determined based on the flow rate used for the oil and the volume in between the two valves of the system. Different residence times of the oil in the hot separator were tested (i.e. 20, 30, 60 and 240 min at T = 190 ^{o}C). Due to a volume limitation of 3 mL between the two valves of the Bang-Bang, and the significant volume of foam produced, the last two conditions (60 and 240 min) required to empty the hot separator manually by discharging several times aliquots of ~ 3mL until the mass balance closed. Our results indicate that a period of ~240 min is needed to efficiently separate the water from the liquid organic product (value obtained by Karl-Fischer < 0.5%). Due to limitations in the available feedstock, further optimization in the range of 60 to 240 minutes could not be done at that moment.

One drawback in opening repeatedly the Bang-Bang system to transfer the whole product from the hot separator to the storage tank is that the pressure in the system significantly decreased, affecting the measurements of the gas flow rate. In order to recover the pressure in reasonable time, some tests to optimize the N_2 flow rate were performed.

N_2 Flow Rate

Nitrogen is fed to the system through the hot separator; this is to improve the gas-liquid phase separation, while recovering the operating pressure after collecting each mass balance. N2 flow rate was tested in the range of 5 to 30 mL/min. As it was expected, a higher flow rate of N2 allows

for a prompt recovery from the pressure drop in the system after collecting a mass balance. However, the higher flow rate seems to favor the production of foam, affecting the closing of the mass balance by light hydrocarbon losses. Furthermore, a high dilution of the gas products in N2 may compromise the quality of the GC results. As a result of the previous findings, the following modifications in the operation of the catalytic set up have to be taken into account for future reactions:

- Increase the residence time of the liquid product in the hot separator to 240 minutes in order to improve the separation of the water and reduce its content to below 1 %.
- Reduce the opening of the valves in the Bang-Bang to minimize pressure drops in the catalytic system; the volume in between the two valves of the Bang-Bang has to be increased to be able to transfer completely the liquid sample and the foam from the hot separator to the storage tank, eliminating the need of opening the Bang-Bang repeatedly to achieve a good closure of the mass balance.
- Use a low flow rate of N_2 (5 mL/min) to reduce the foam formation and light hydrocarbon losses during the process.

Appendix II: Steam Cracking on Untreated Bio-crude

The initial exploration of the effect of steam cracking process on the Steeper Energy Hydrofaction^{TM} Renewable Crude Oil was carried out by testing the bio-crude as provided by Steeper Energy, without any previous treatment (i.e. Hydrotreating). The operating reaction conditions for the herein presented set of reactions is shown in Table II-1.

Table II-1 Operating conditions tested for steam cracking of bio-crude

Steam Cracking	Reactor packing	Temperature, ^{o}C	Pressure, psig	WHSV, h^{-1}	Wt. % H_2O
Catalytic	CSC Catalyst	370	400	0.3	5
Thermal	Carborundum	370	400	0.3	5

For both reactions, the collected product resulted to be a very viscous material (solid at room temperature).

HTSD Analysis: In order to optimize the conditions of analysis of the products by HTSD, two different methodologies were tested. The first method was to analyze separately the light and the heavy products and then integrate the results (using a software), knowing the ratio light/heavy material. For the second method, a blend was prepared of the light and the heavy material. The mixture was homogenized by applying moderate heating and the samples for SimDist analysis were then prepared.

In both cases there were problems with the base line of the chromatograms, making it impossible to obtain reliable results. The injection of the samples into the SimDist chromatograph seems to damage the column. Therefore, the light material from the catalytic reaction was studied separately, performing a single theoretical plate distillation (using a micro distiller).

The results are presented in Figure II-1.

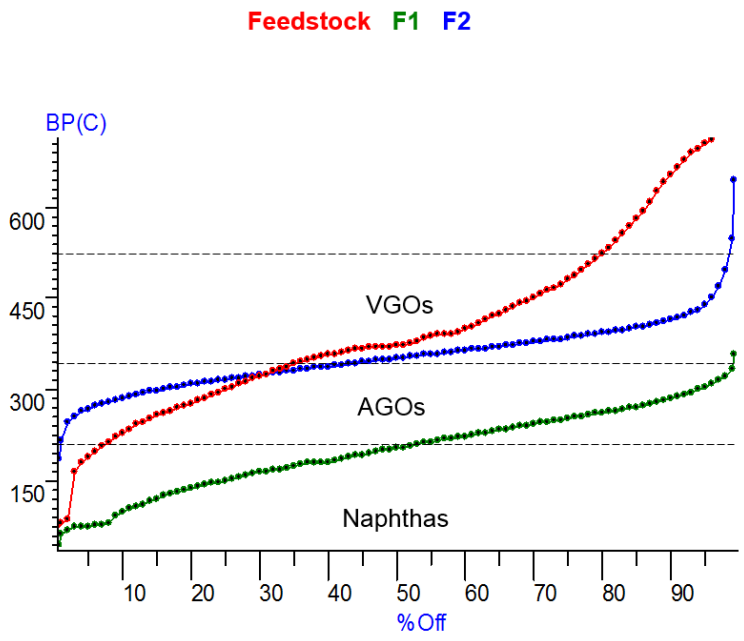

Figure II-1 Light fraction of produced catalytic steam cracking oil, distilled in microdistiller.

The first preparative cut (i.e. F1) was found to be a blend of naphtha/kerosene with a ratio of approximately 1/1. The second preparative cut (i.e. F2) was found to be a blend of kerosene/VGO with a ratio of approximately 45/65. What is called a “light blend” really contains a lot of high boilers (F2 contains 65 wt. % VGO fractions)

Saturates, Aromatics, Resin Analysis (SARA): Figure II-2 shows the SAR analysis results.

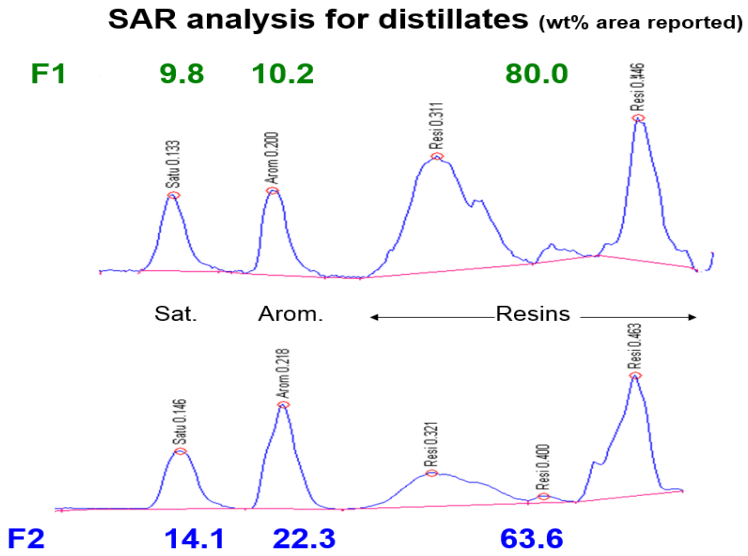

Figure II-2 SARA results for two samples (i.e. F1 and F2) of the light fraction collected under catalytic steam cracking of bio-crude.

The SAR analysis is not necessarily accurate because response factors for oxygenated biomaterials are unknown. At first glance, both products showed abundance of aromatics and particularly polar compounds (i.e. resins), indicating with high probability a low cetane value.

Also, from Figure II-2, the process does not seem to selectively produce abundant paraffins, but a lot of polar components (having strong phenolic aroma).

Thermogravimetric Analysis (TGA): Figure II-3 present a comparison of the TGA of the feedstock, one sample of the catalytic reaction and one sample of the thermal reaction.

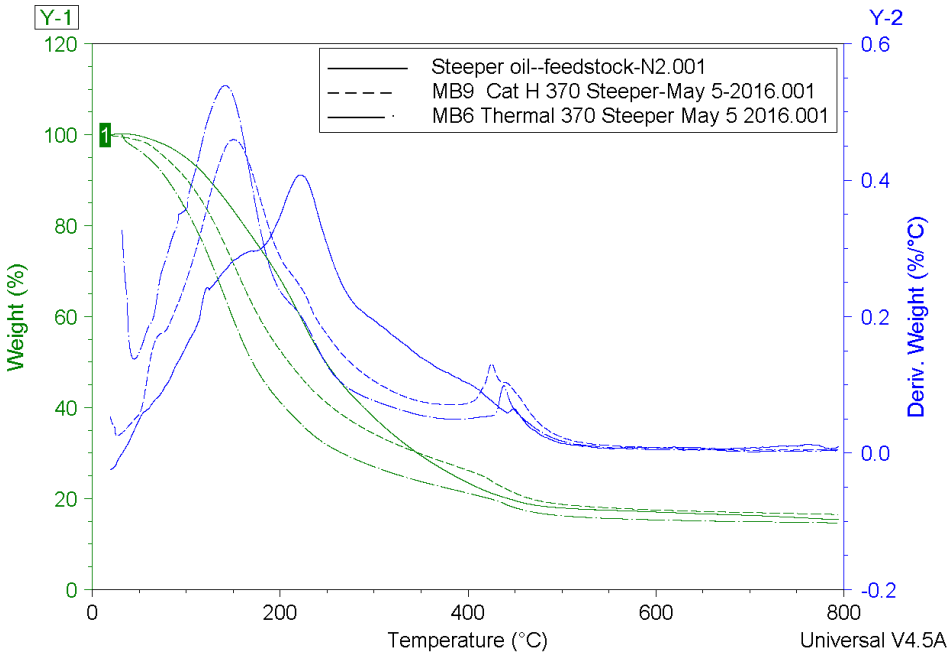

Figure II-3 TGA for bio-crude, and steam cracking products both thermal and catalytic

The material from the thermal reaction seems to be the one converted the most.

Micro Carbon Residue (MCR): In Table II-2 MCR results are reported.

Table II-2 MCR results

Reaction	Sample	MCR
Steeper Energy	1	20.14
Bio-crude	2	20.25
Catalytic Reaction	Mass Balance 4, sample 1	32.85
	Mass Balance 4, sample 2	33.38
	Mass Balance 5, sample 1	28.56
	Mass Balance 5, sample 2	31.00
	Mass Balance 9, sample 1	29.34
	Mass Balance 9, sample 2	30.68
Thermal Reaction	Mass Balance 6, sample 1	27.72
	Mass Balance 6, sample 2	28.09
	Mass Balance 8, sample 1	27.19
	Mass Balance 8, sample 2	25.27

The MCR results presented in Table II-2 strongly suggest the participation of polymerization reactions occurring during the steam cracking process, both catalytic and thermal, as the residue is observed to increase as compared to the bio-crude feedstock.